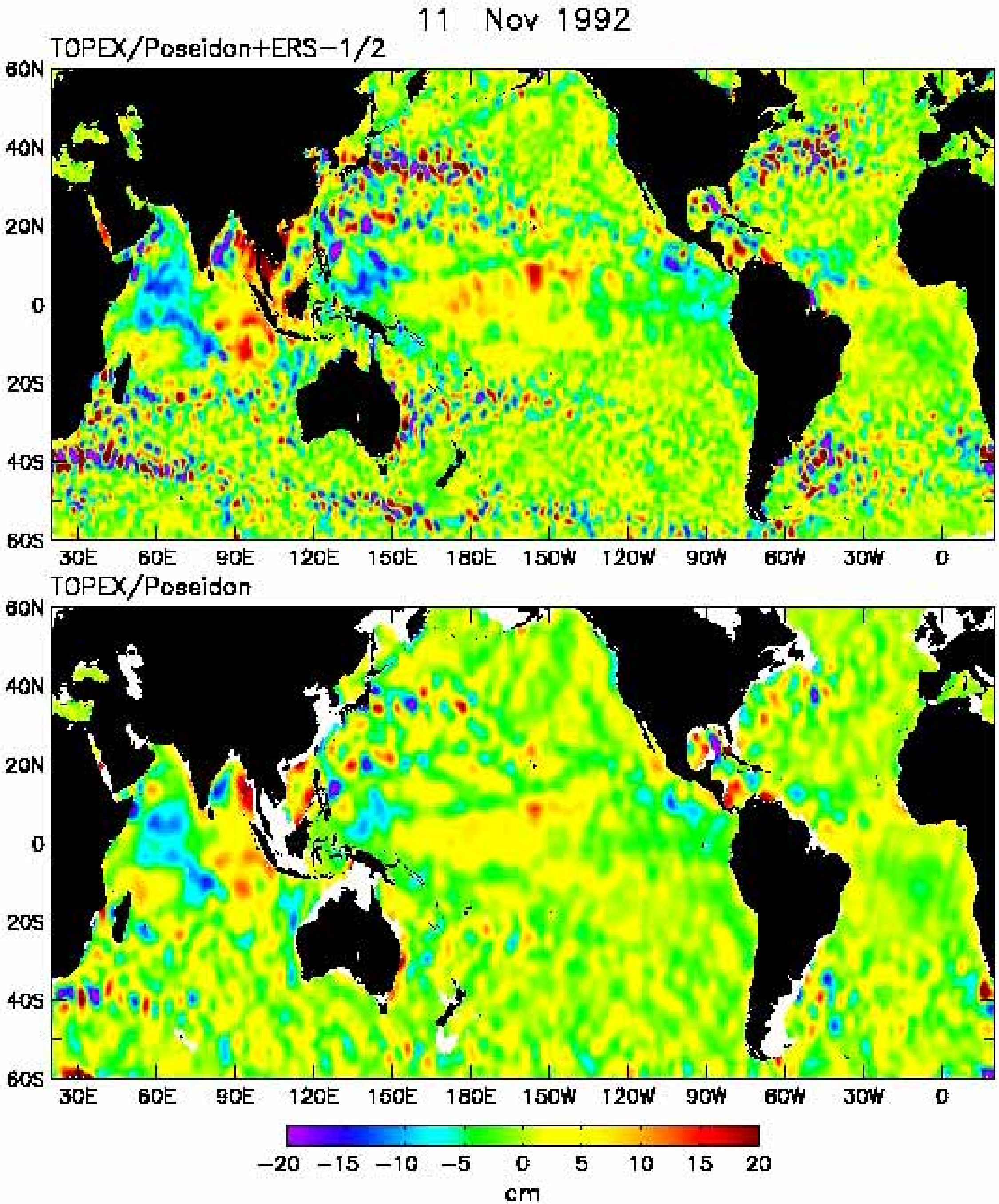

Dudley Chelton video

Satellite altimetry

2 satellites (upper)

1 satellite

Kyoto FDEPS lectures 4-7 xi 2007
Dynamics of oceans and atmospheres

P.B. Rhines

University of Washington

DAY 3

- 1. rotating, stratified fluids: oceans and atmospheres
  - vorticity: a vector-tracer in classical homogeneous fluids
- geostrophic adjustment, thermal wind
- 2. wave dynamics: fundamentals, group velocity, energetics, ray theory
- potential vorticity (PV)
  - vortex stretching, Prandtl's ratio, geography of PV
- 3. Rossby waves
- 4. instability => geostrophic turbulence; subtropical gyres: dynamics, jets and gyres, topography effects
- 5. Case study of topographic effect on atmospheric circulation: Greenland and Atlantic storm track. 7. meridional overturning circulations and the thermohaline circulation
- 6. Teaching young undergraduates about the global environment?
- 7. Seminar: subpolar climate dynamics observed from above and below: altimetry and Seagliders

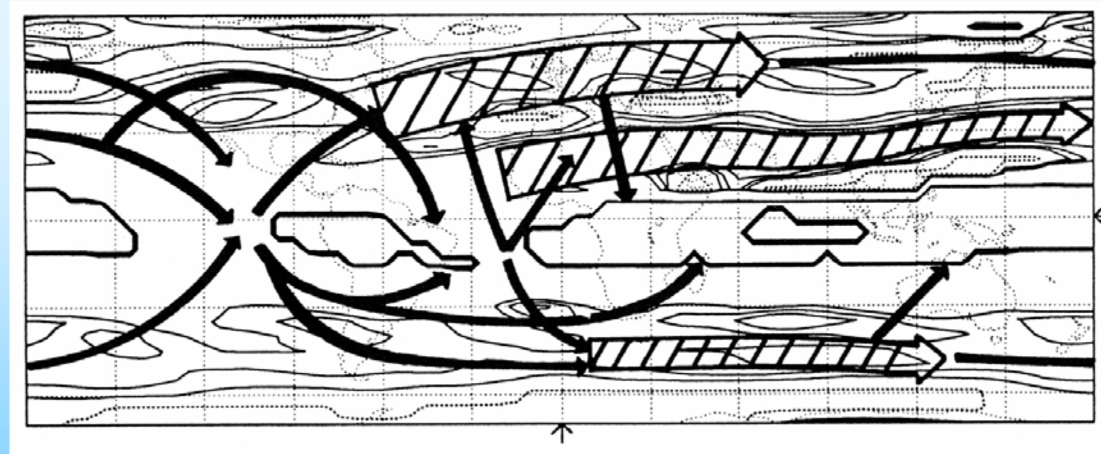

JET STREAM
PV - ROSSBY
WAVEGUIDE

Hoskins+Ambrizzi
JAS 93

0^0

15 July 2002 BRANSTATOR 1899

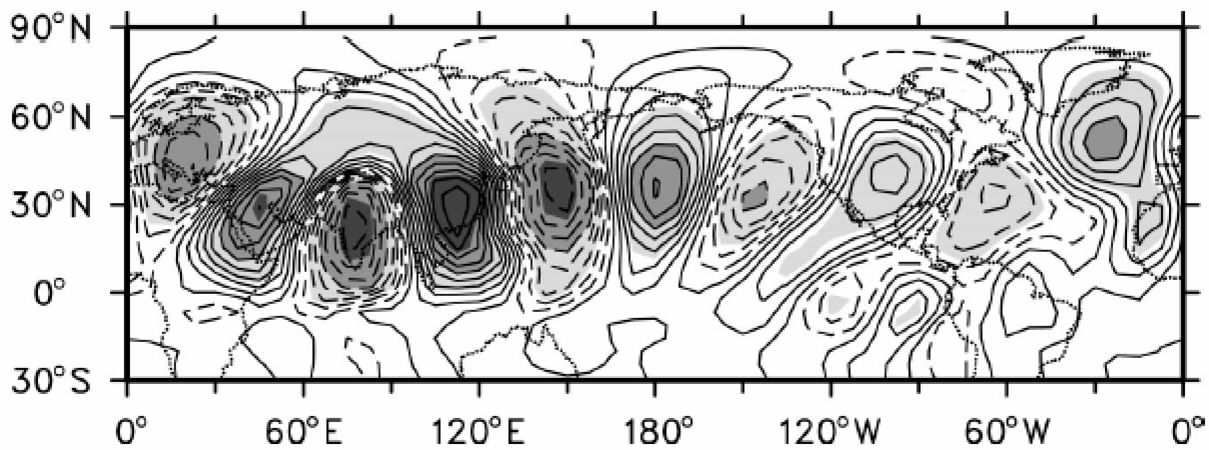

Fig. 4. One-point correlation plot for CCM3 mean Dec–Feb (DJF) 300-mb nondivergent v wind component internal variability for a base point at (28.9°N, 112.5°E). Contour interval is 0.1.

Branstator JClimate 02

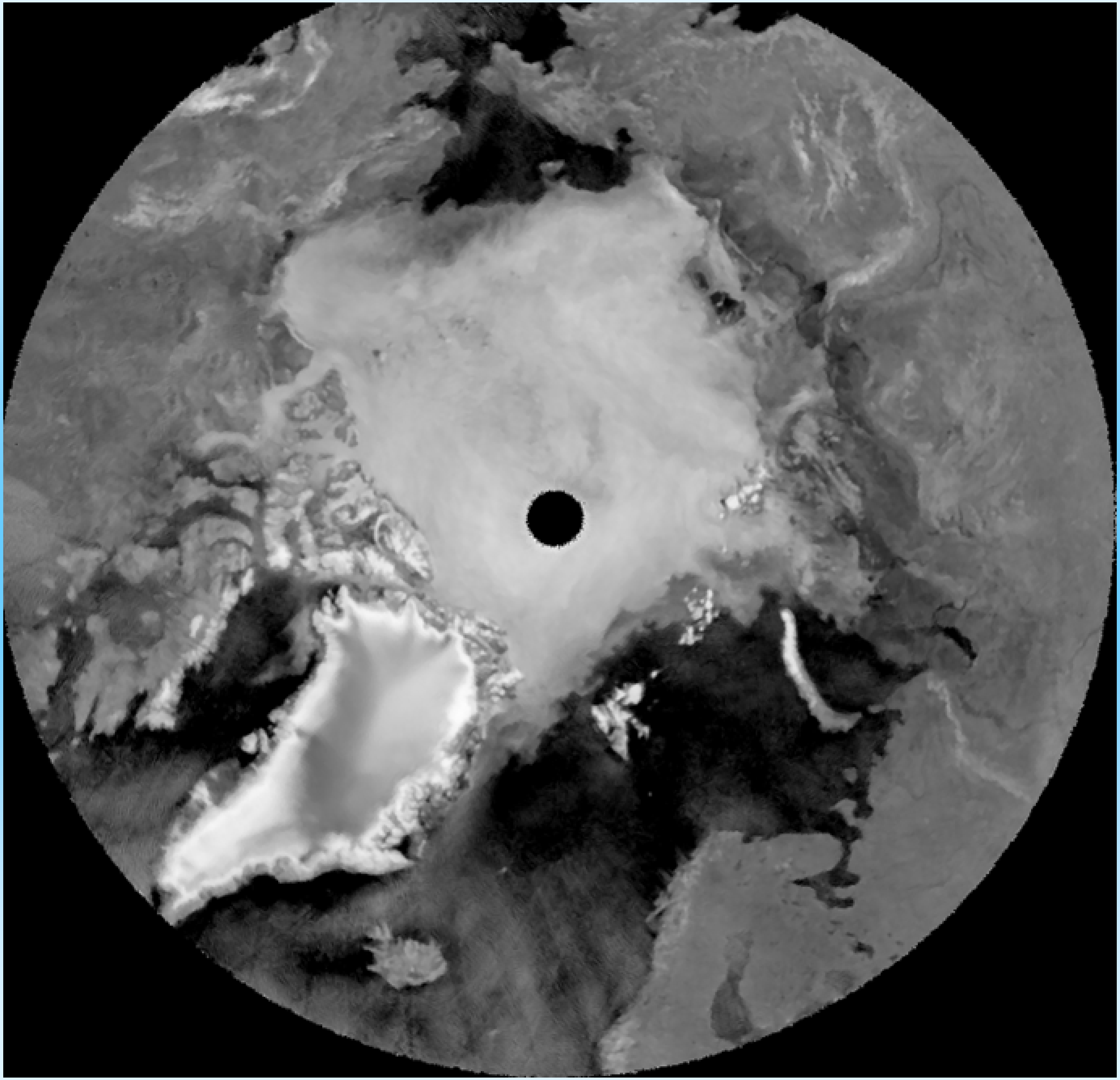

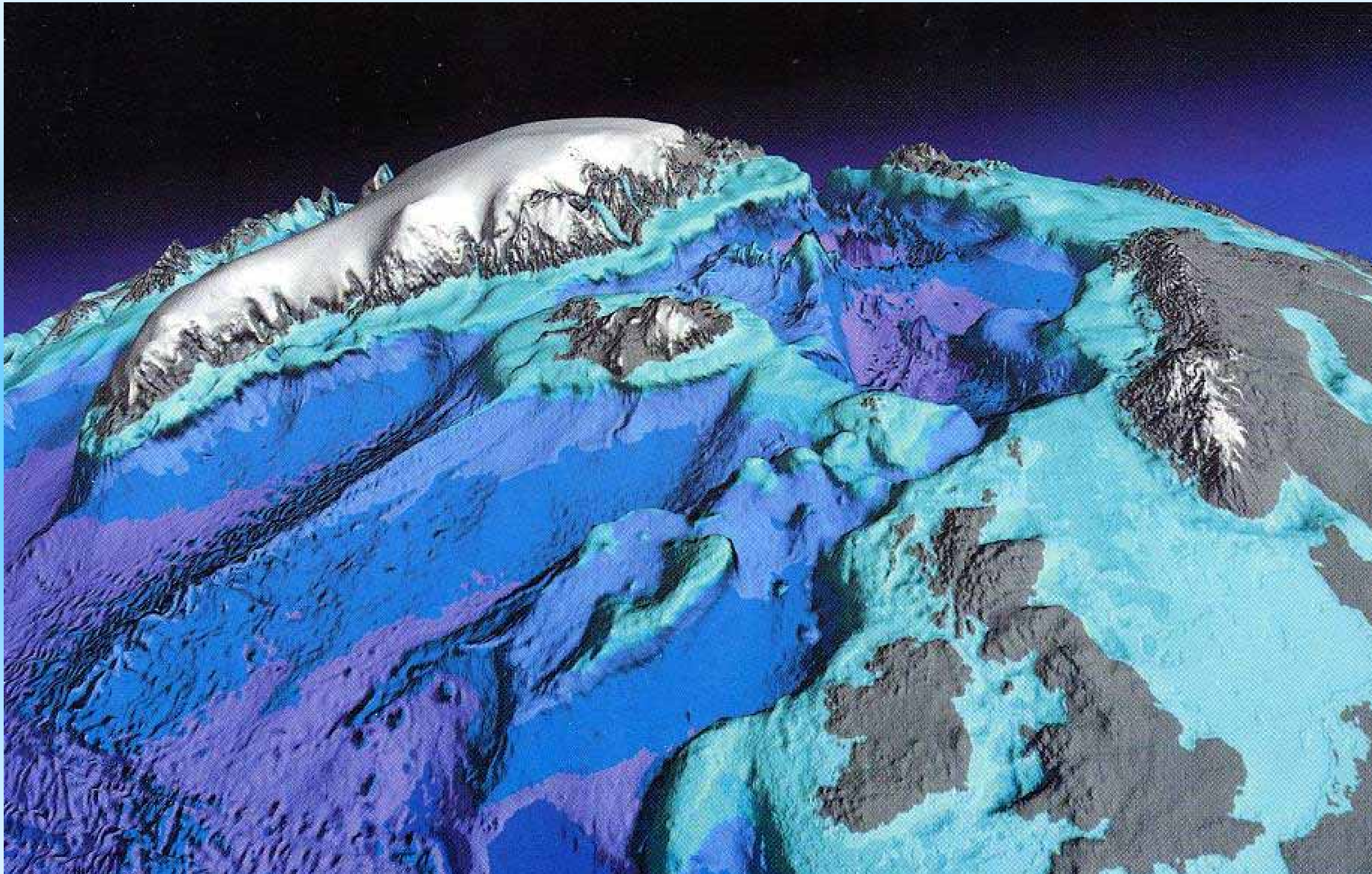

AGU, 2003

zonal wind (m/sec) at 45W with Greenland topography
JFM 1993

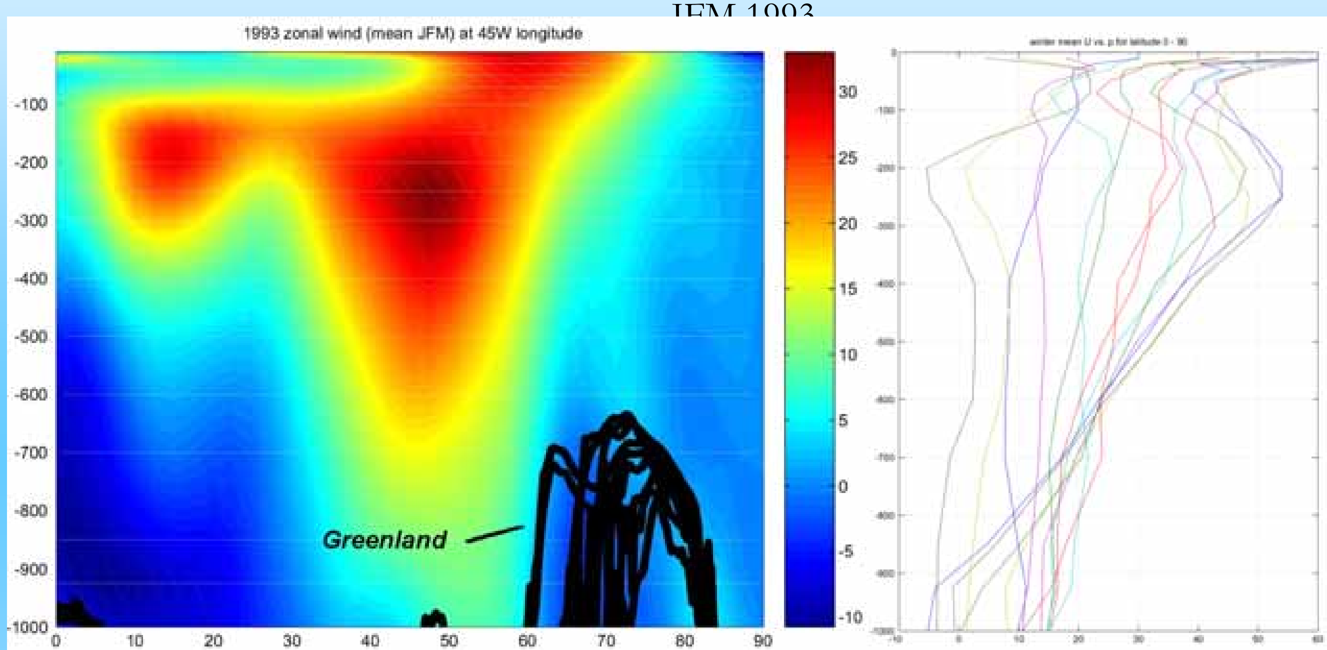

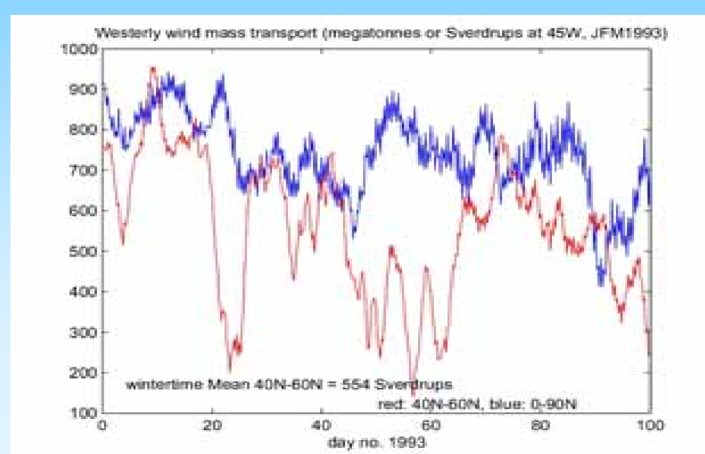

JET STREAM ~ 500 Sv.

"Svairdrups"

1 Sv. = 10^6 tonnes sec^{-1}

KUROSHIO ~ 50-100 Sv

A.C.C. ~ 180 Sv.

Topographic flows: we now introduce the effects of mountainous topography, which owing to the 'vertical stiffness' imparted by rotation, is greatly influential. On an f-plane, the Rossby number, U/fl, topographic height and Froude number Nh/U are key parameters.

(i) 2D stratified flow over bump of height h (buoyancy freq N upstream flow U)

Nh/U (ii) 3D stratified flow …over or around

Nh/U crit ~ 2 *(Schaer+Durran, JAS 1997)*

dispersive lee waves softens the 'sharp' hydraulic effects

(iii) f-plane rotation, unstratified: Taylor column dynamics

flows 'around' if h/H > Ro (Ro = U/fL).

(iv) f-plane rotation weakens blocking (Nh/U crit =>3)Taylor column => Taylor cone Nh/U > 1 again! (independent of Ro)

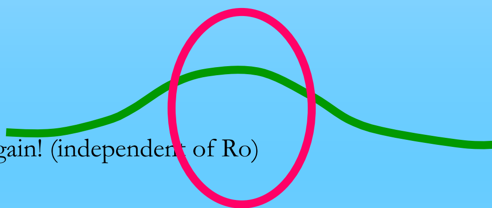

(v) β-plane flows

-large-scale potential vorticity (PV) gradient

-contours of constant background PV (f/h = const)
bend Equatorward over a ridge, locating
a *cyclone* over its crest for very slow flow

-dispersive lee waves, semi-circular wavecrests

-hydraulic structure in some limits (planetary geostrophic)
where the waves are non-dispersive

-strong upstream blocking ('Lighthill mode') for
$\beta L^2/U>1$

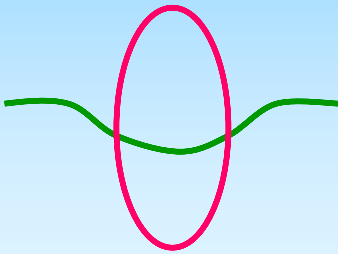

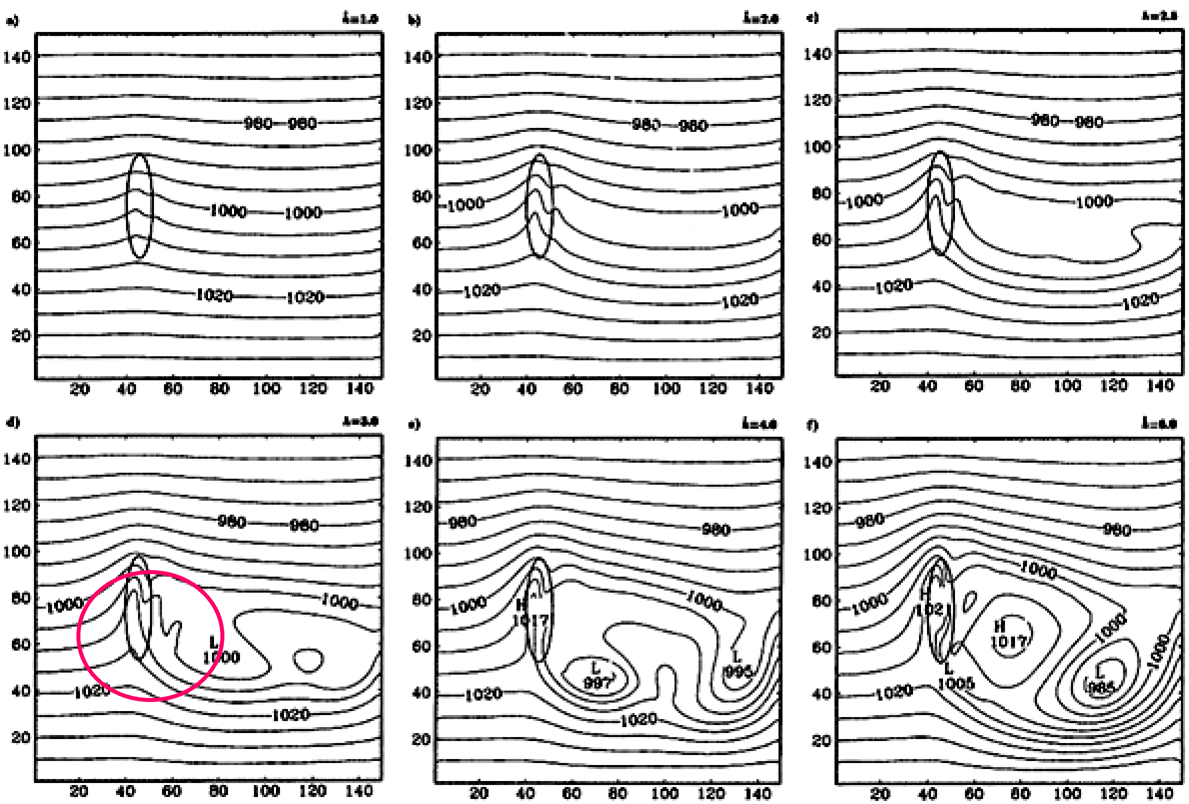

FIG. 2. The sea level pressure (hPa) for different values of $\hat{h}$, with $r = 4$ and Ro = 0.42, at $t^* = 43.2$. (a)–(f) Values of $\hat{h}$ at upper-right corner. Topography at $0.35\hat{h}$.

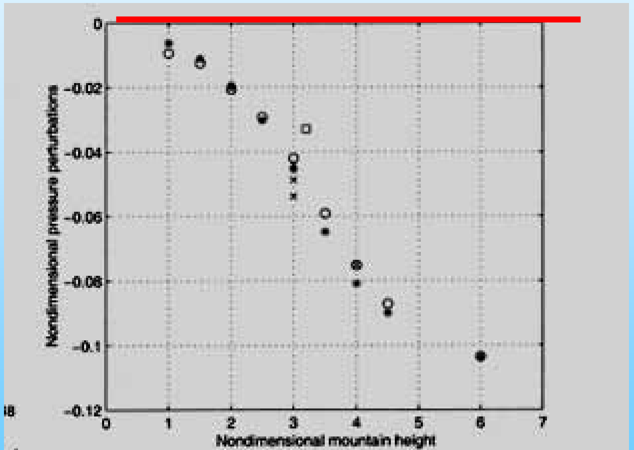

FIG. 5. Nondimensional max sea level pressure deficit downstream of the mountain as a function of $\hat{h}$. The perturbations are normalized by $\rho_o U f L_m$, where $\rho_o = 1.2$ kg m^{-3}. Simulations with $N = 0.01$ s^{-1} and $U = 10$ m s^{-1} (stars), with different combinations of N and h (circles), and where U was varied (crosses) (see Table 1). The exgreen simulation (square).

Nh/U = 1, 2, 2.5, 3, 4, 6

Petersen, Olaffson, Kristjannson JAS2003

pressure drag occurs when the anticyclone shifts *up*stream as wake vorticity is shed, placing the Equatorward flow over the lee downslope

Impulse (the time-integrated force on the solid Earth)

is summed up by meridional PV flux:

<q'v'> which expresses the x-averaged force on the Eulerian fluid along a latitude circle ~ (f/H)<h'v'>

Lee Rossby-waves in the wake of a cylindrical mountain (*McCartney JFM 1976*)

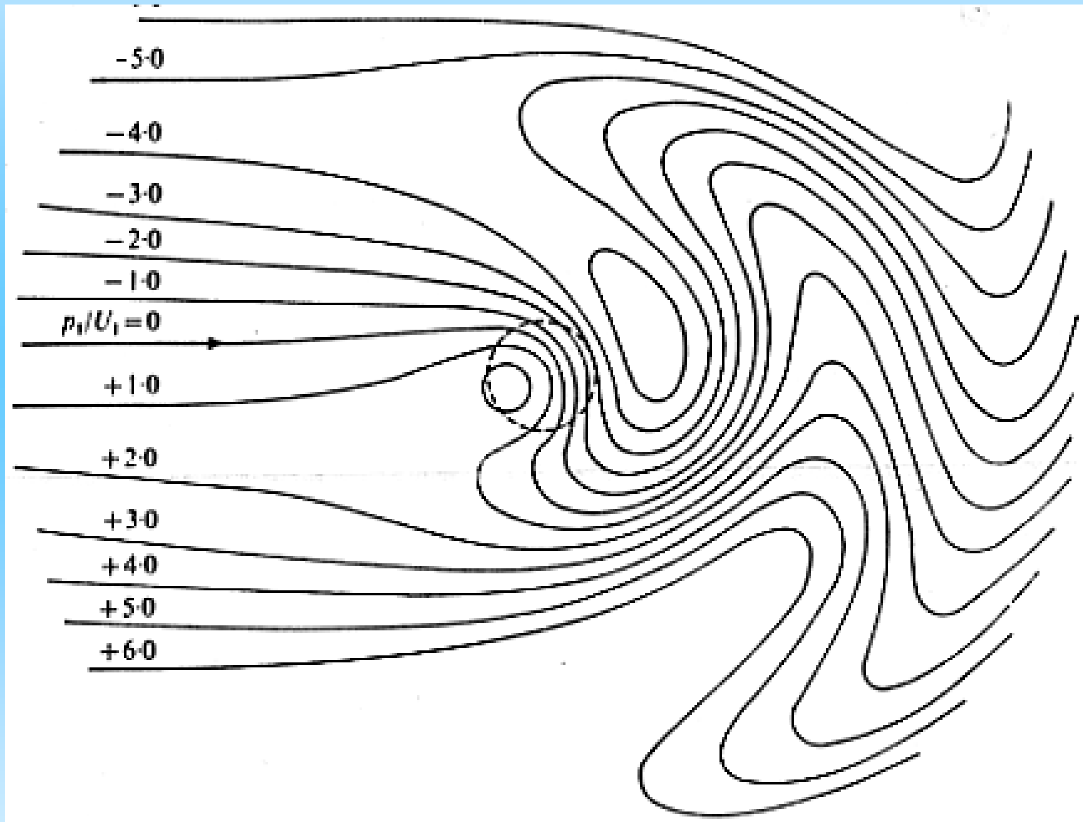

Rossby waves are 'one-way': their phase propagation has a westward component relative to the fluid: thus they exist as lee waves for an *eastward* flow but not a westward flow. Wave drag peaks at:

8.2 δ/ε times the 'naive estimate',

$\rho f U L^2 \delta H$

where δ=h/H is the fractional mountain height, ε the Rossby number, U the mean flow, L the radius and H the total fluid depth

(ASSUMED NO UPSTREAM BLOCKING)

ZONAL ANGULAR MOMENTUM

$\langle v h \rangle \simeq \langle p_x h \rangle$

$\simeq \langle p h_x \rangle$

note strong correlation of meridional velocity and topographic height.....wave drag. Also note the beginnings of jet formation southeast of the mountain, even in the linear theory

wavenumber diagram for Rossby waves in steady zonal westerly flow (U>0)

UNIFORM ZONAL WIND

STATIONARY ROSSBY WAVES

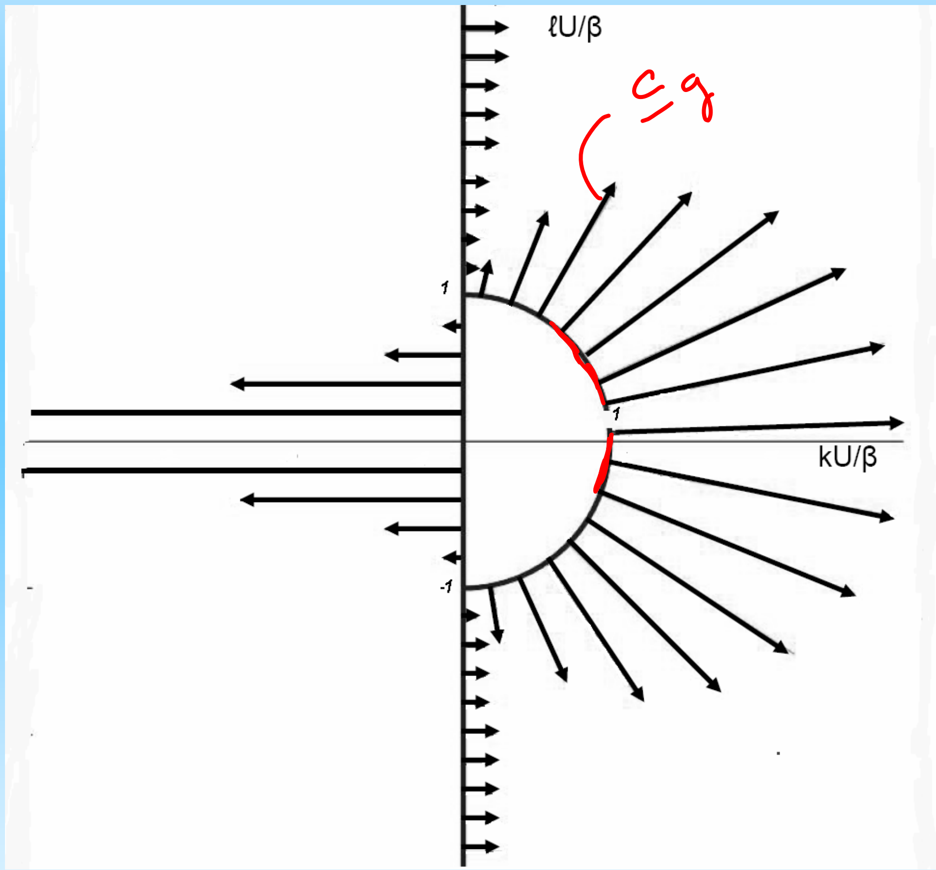

$$\omega - \underline{U}k = -\frac{\beta k}{k^2+l^2}$$

$$\psi = Re(\exp(ikx + ily - i\omega t))$$

$\omega = 0$ STATIONARY WAVES

$$k\left(U = \frac{\beta}{k^2+l^2}\right)$$

$$\begin{cases} k^2 + l^2 = \beta/U \\ k = 0 \end{cases}$$

TWO SOLUTIONS

$\underline{k \doteq \beta/U}$ Rossby wavenumber

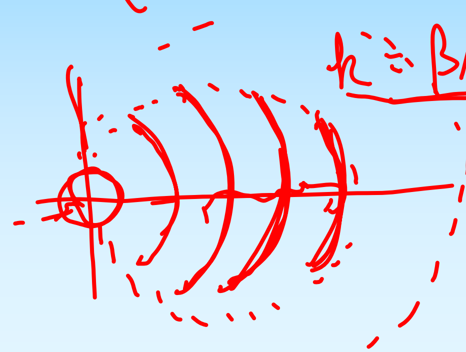

EXTEND DOWNWIND FASTER THAN U ... AT 2xU

PARABOLA

PRESSURE FIELD

POLAR β-PLANE
BAROTROPIC, 1 LAYER

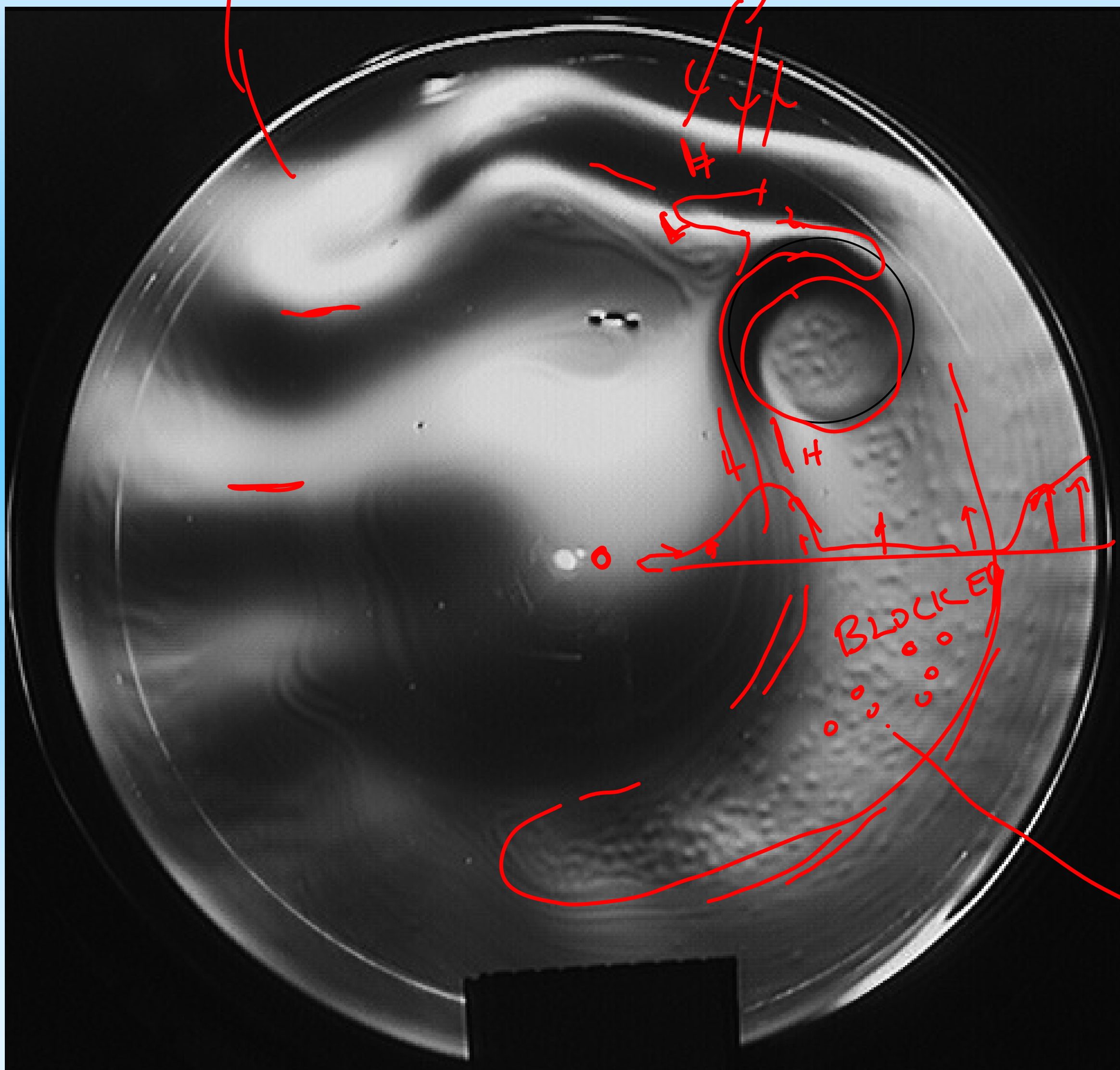

A westerly (prograde, cyclonic) zonal flow encounters a small mountain (at 2 o'clock). Rossby wave dynamics produces standing waves downwind, a convoluted lee cyclone, intense jet structure wrapping round the mountain, and a 'Lighthill block' upstream. This stagnant blocking region is (in linear, yet finite topography, theory, a Rossby wave with vanishing intrinsic frequency and upstream group velocity for merid. wavenumbers < $(\beta/U)^{1/2}$. Note the ruddy pressure features which are fine-scale evaporative convection cells, pillar-like cyclones. The edge of the block is outlined by convective rolls.

Here the controlling parameter $\beta a^2/U > 1$ meaning that the wake is stable; smaller values of this parameter yield unstable wake and transient Rossby waves which ironically fill the hemisphere (they are not simple lee waves). See Polvani, Esler, Plumb JAS 1999 for a numerical study with some of these features.

CONVECTION CELLS

ANALOGOUS TO $\frac{Nh}{U}$

INTERNAL GRAVITY WAVES

LAGRANGIAN PARTICLE TRACKS

Streak image of the same experiment (dots 2 sec apart) showing intensity of jets near mountain, lee Rossby waves and upstream block

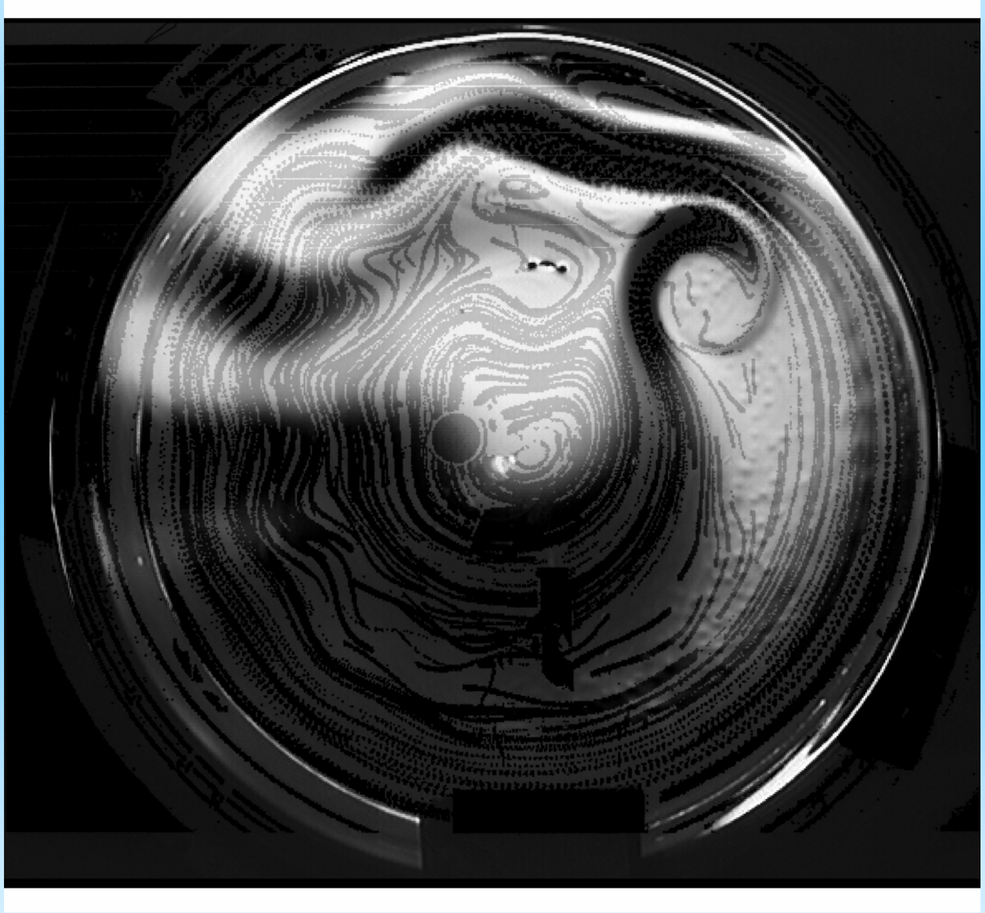

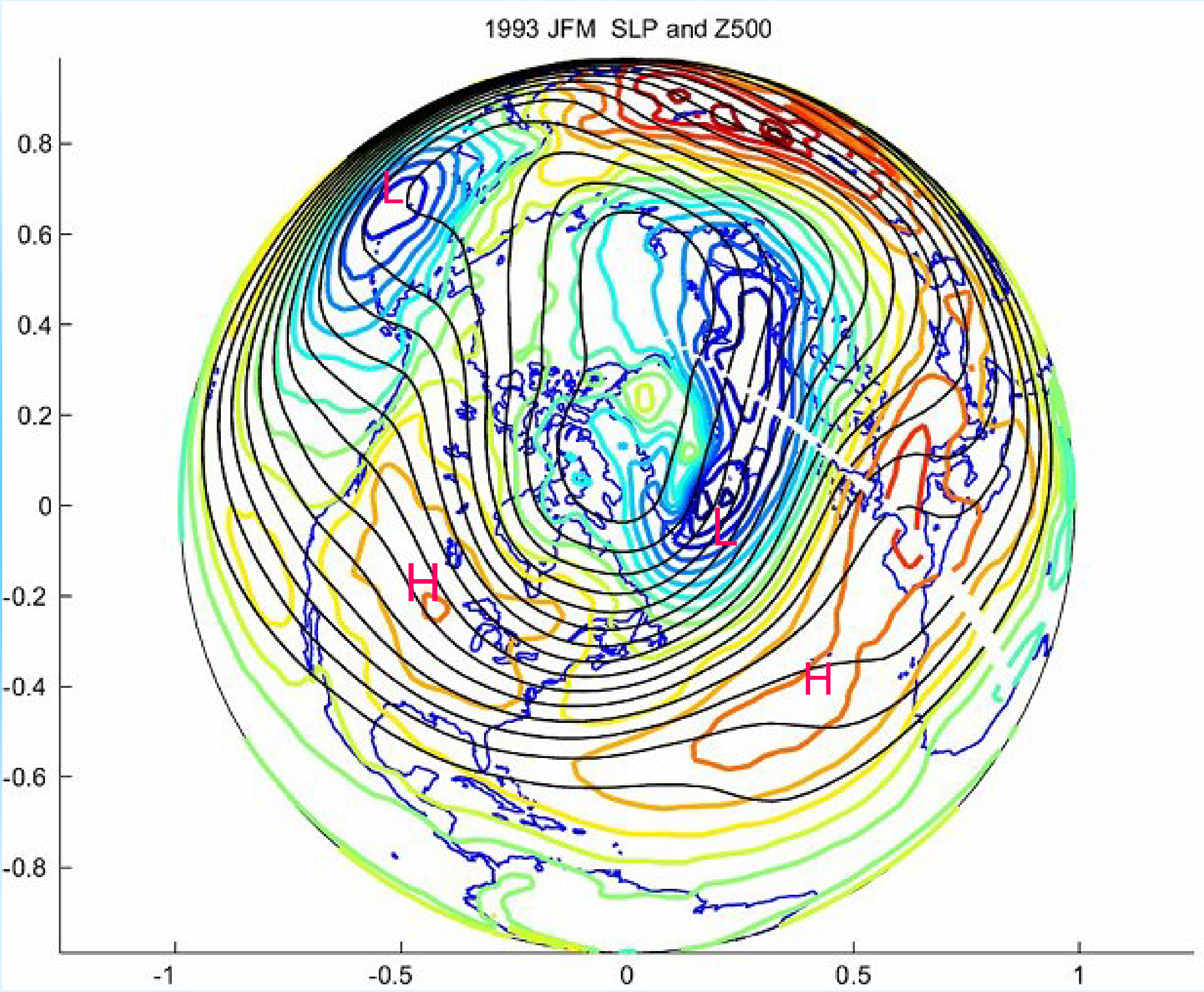

1993 JFM SLP and Z500
0.8
0.6
0.4
0.2
0
-0.2
-0.4
-0.6
-0.8
-1
-0.5
0
0.5
1
L
L
H
H

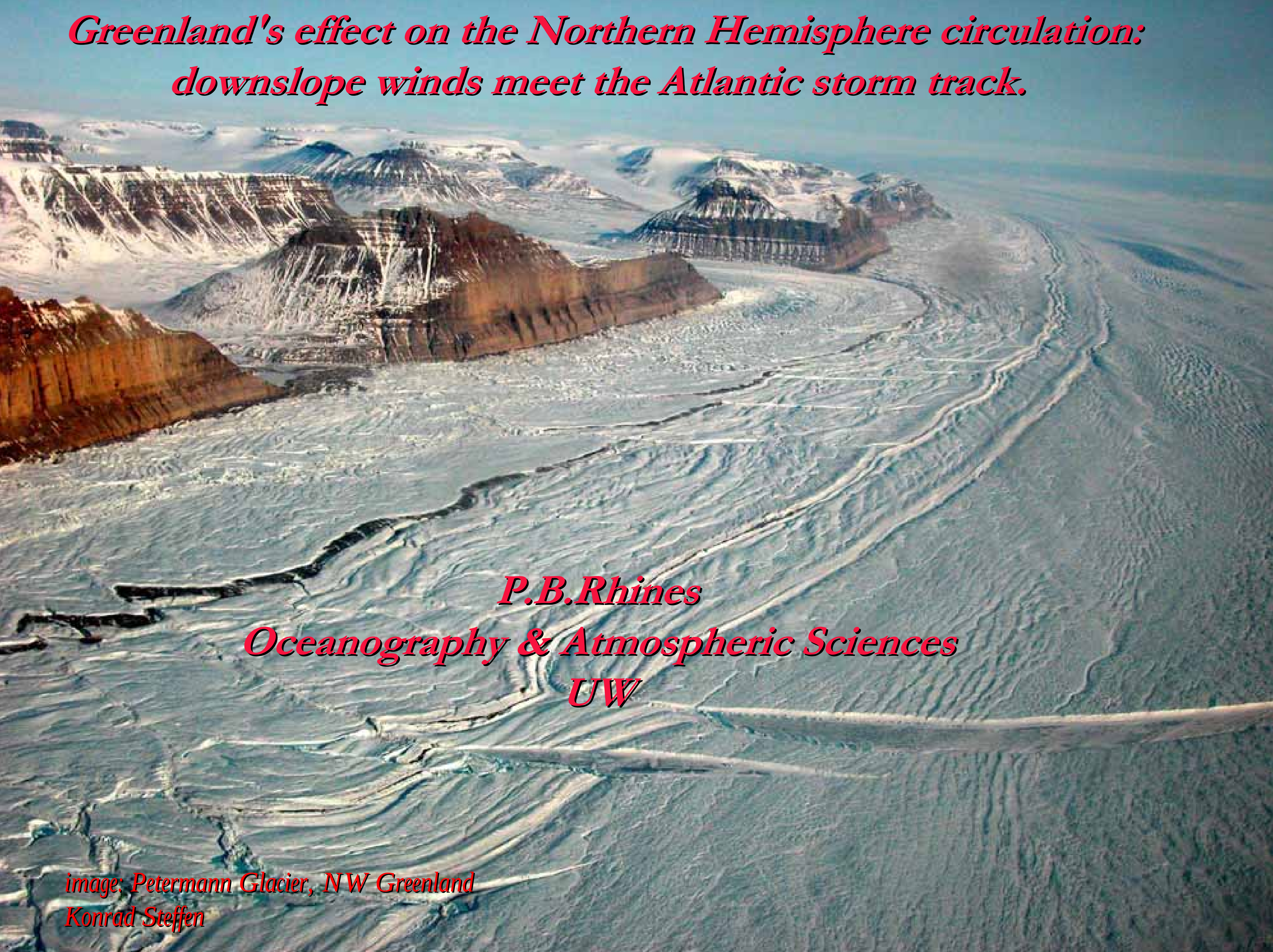

Greenland's effect on the Northern Hemisphere circulation: downslope winds meet the Atlantic storm track.

P.B.Rhines
Oceanography & Atmospheric Sciences
UW

image: Petermann Glacier, NW Greenland
Konrad Steffen

***Let's remove the ice** (only temporarily)*

Konrad Steffen, Univ. of Colo

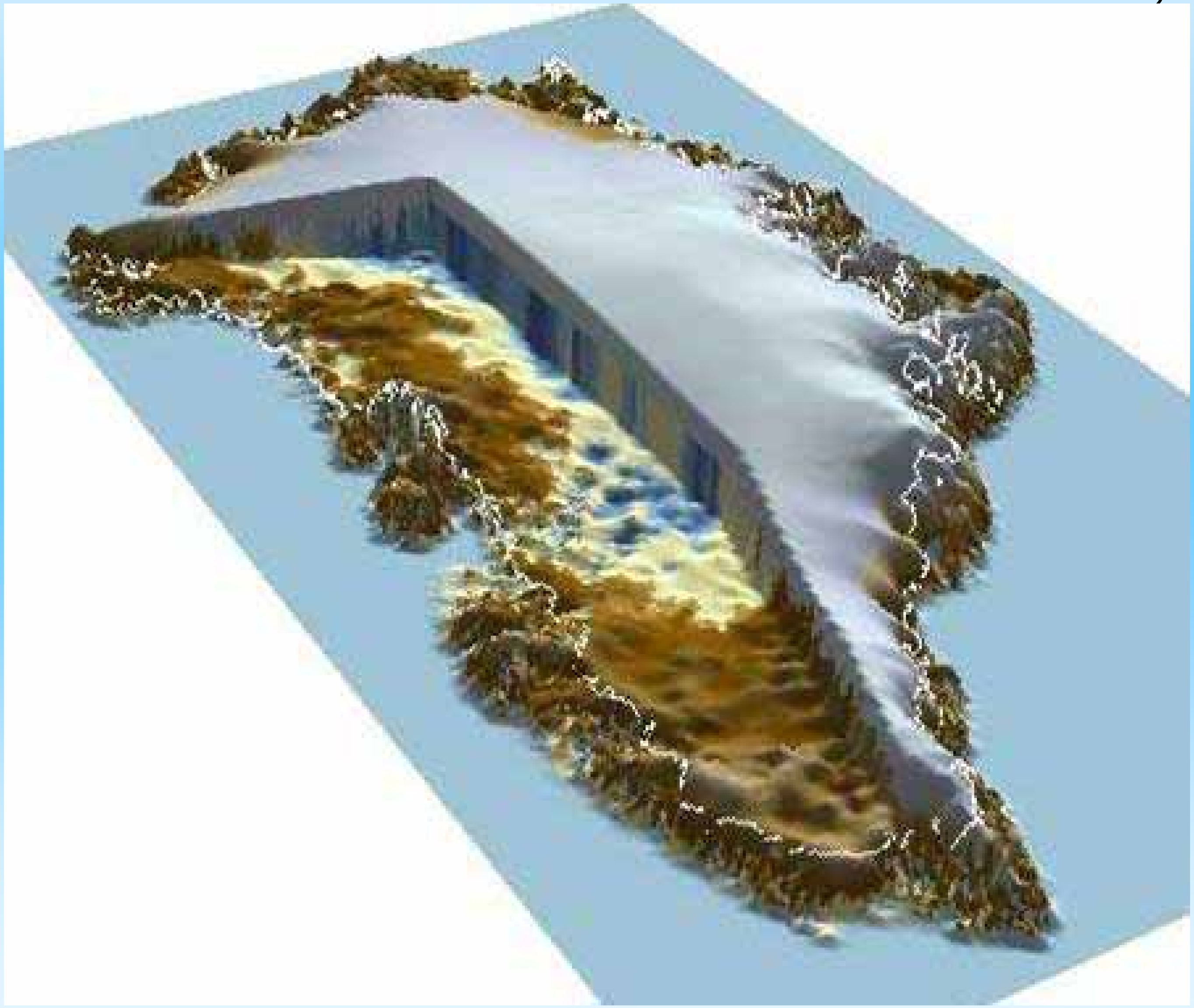

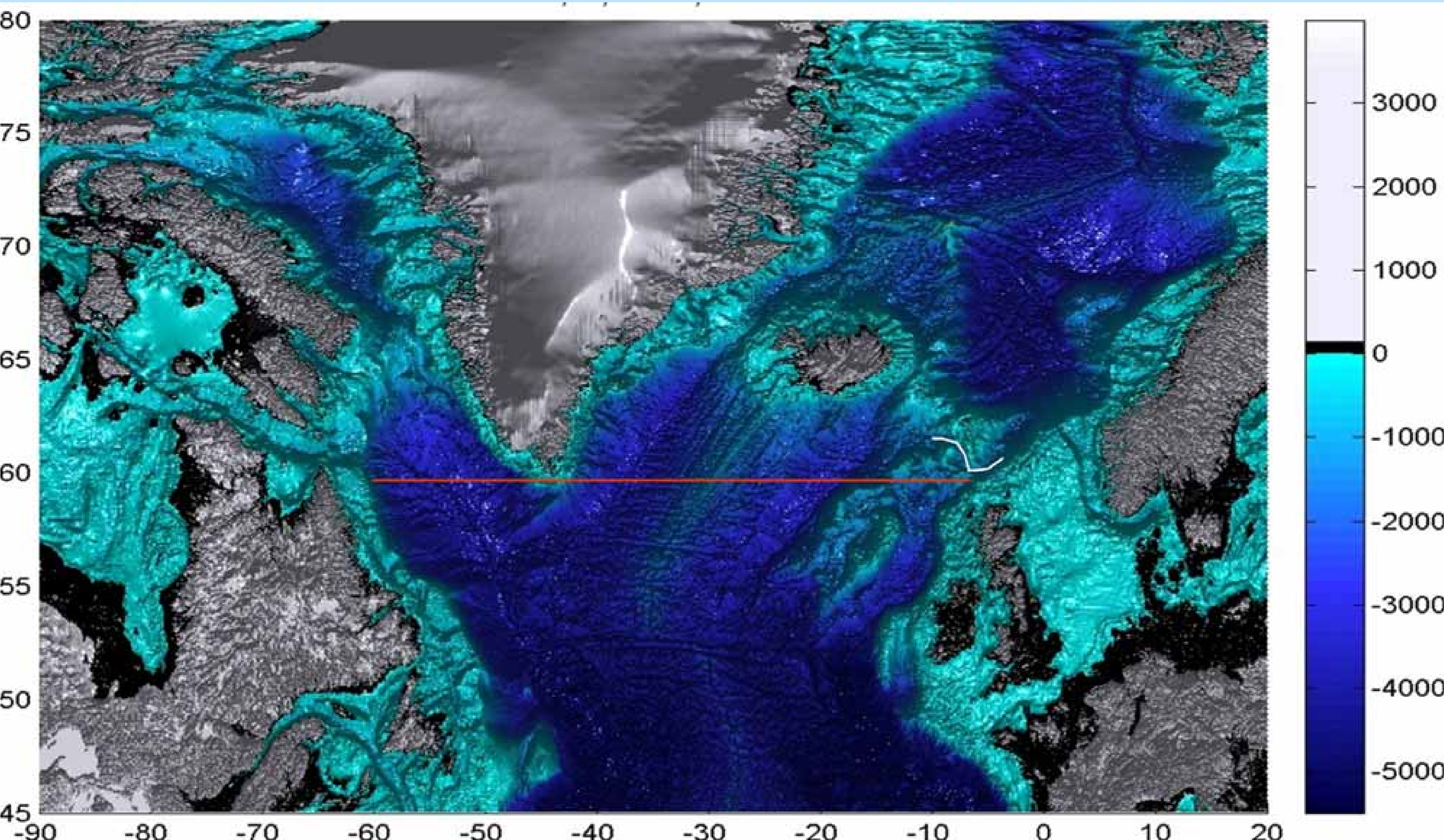
80
75
70
65
60
55
50
45
-90
-80
-70
-60
-50
-40
-30
-20
-10
0
10
20
3000
2000
1000
0
-1000
-2000
-3000
-4000
-5000

R/V Knorr in Labrador Sea. At the time of this research cruise, the first deep ice cores were being drilled on the summit of Greenland. The iceberg likely calved off the Jakobshavn glacier in west Greenland. The strata, faintly visible, record climates back 120,000 years. Air bubbles in the ice accurately give us a whiff of ancient climates, showing the high correlation between Earth's temperature and the amount of carbon dioxide and methane in the air

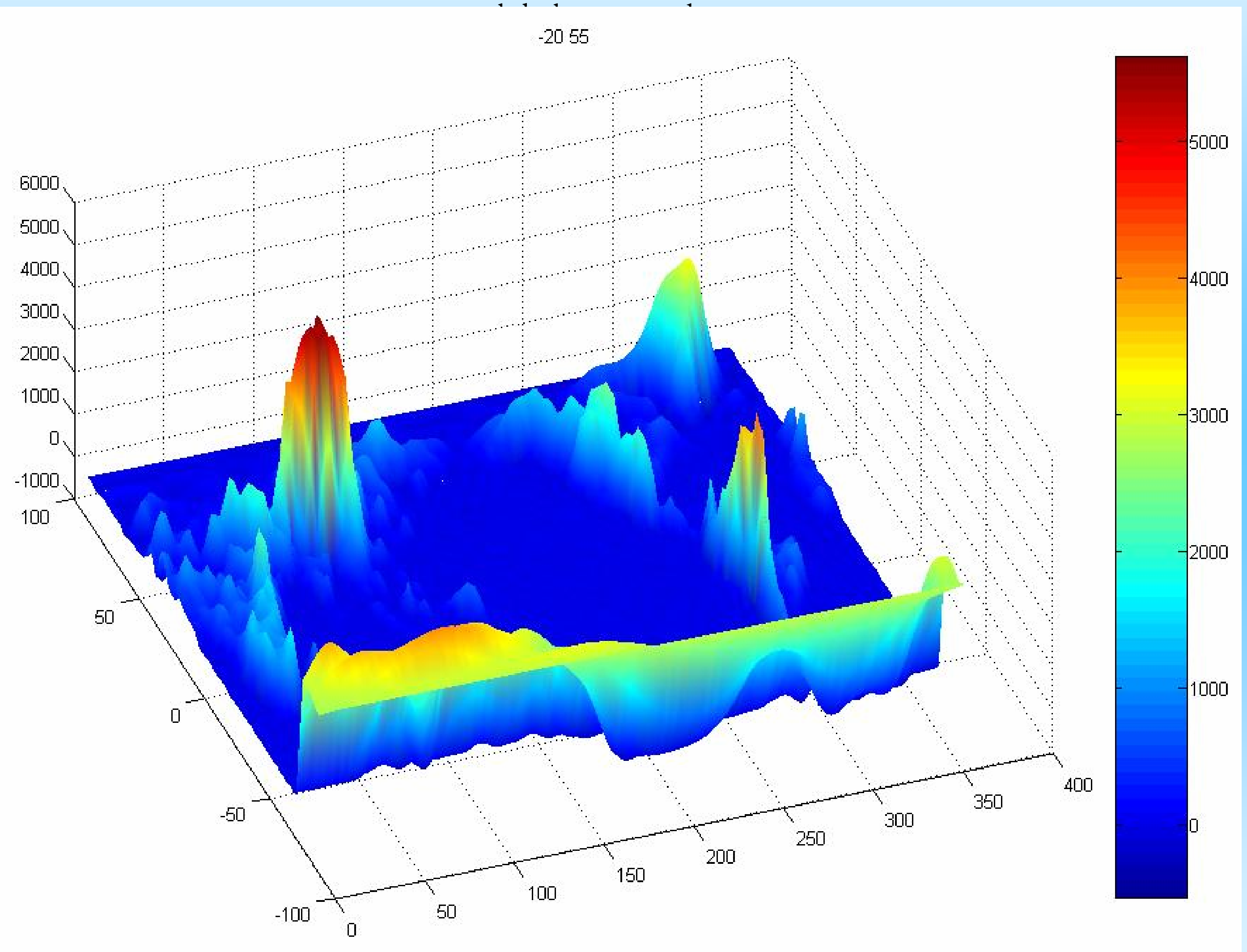

-20 55
6000
5000
4000
3000
2000
1000
0
-1000
100
50
0
-50
-100
0
50
100
150
200
250
300
350
400
5000
4000
3000
2000
1000
0

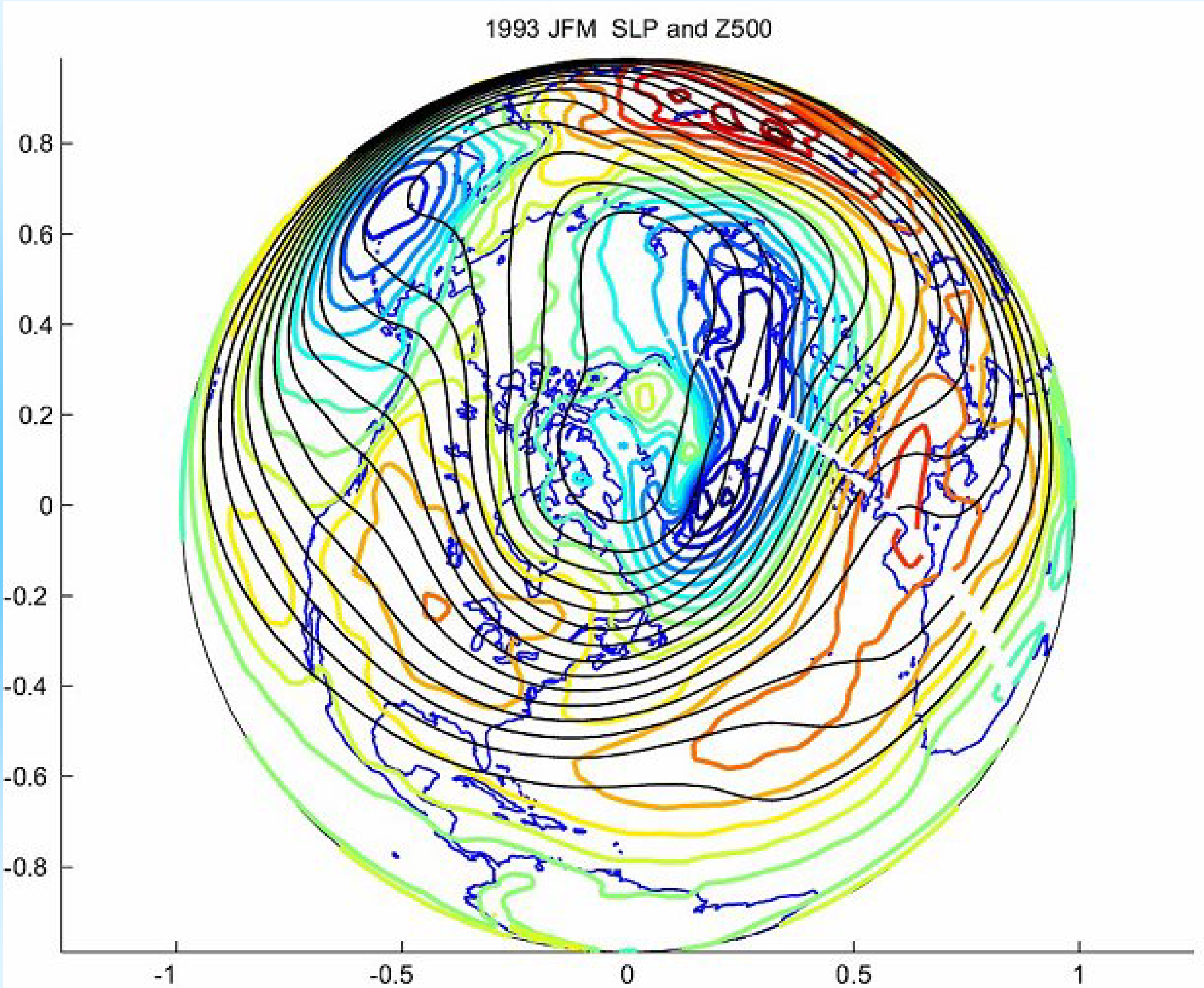
1993 JFM SLP and Z500
0.8
0.6
0.4
0.2
0
-0.2
-0.4
-0.6
-0.8
-1
-0.5
0
0.5
1

Red/blue = high/slow SLP

black contours: Z250

yellow contours Z50

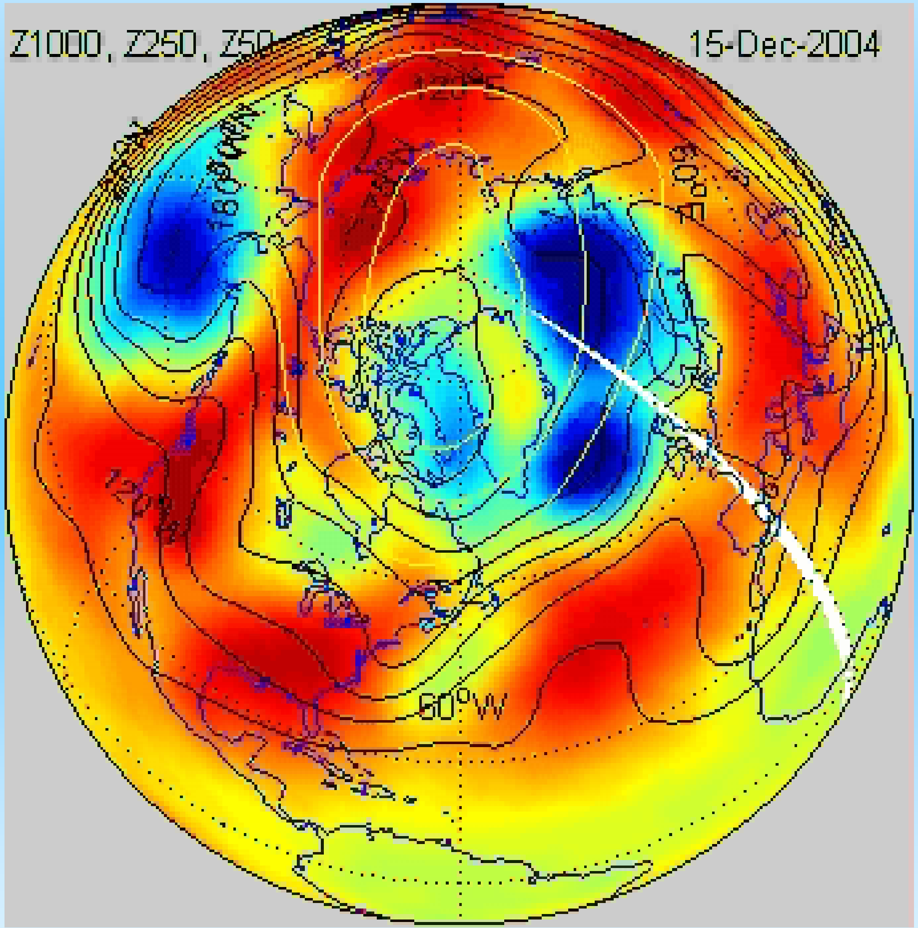

Greenland is near the 'center of action' of the Icelandic low, with extreme activity of jet stream, tropopause folds, storm track, meridional moisture- and heat-flux, stratospheric polar vortex, oceanic global overturning circulation and implicitly the NAM/AO/NAO principal EOF of hemispheric sea-level pressure

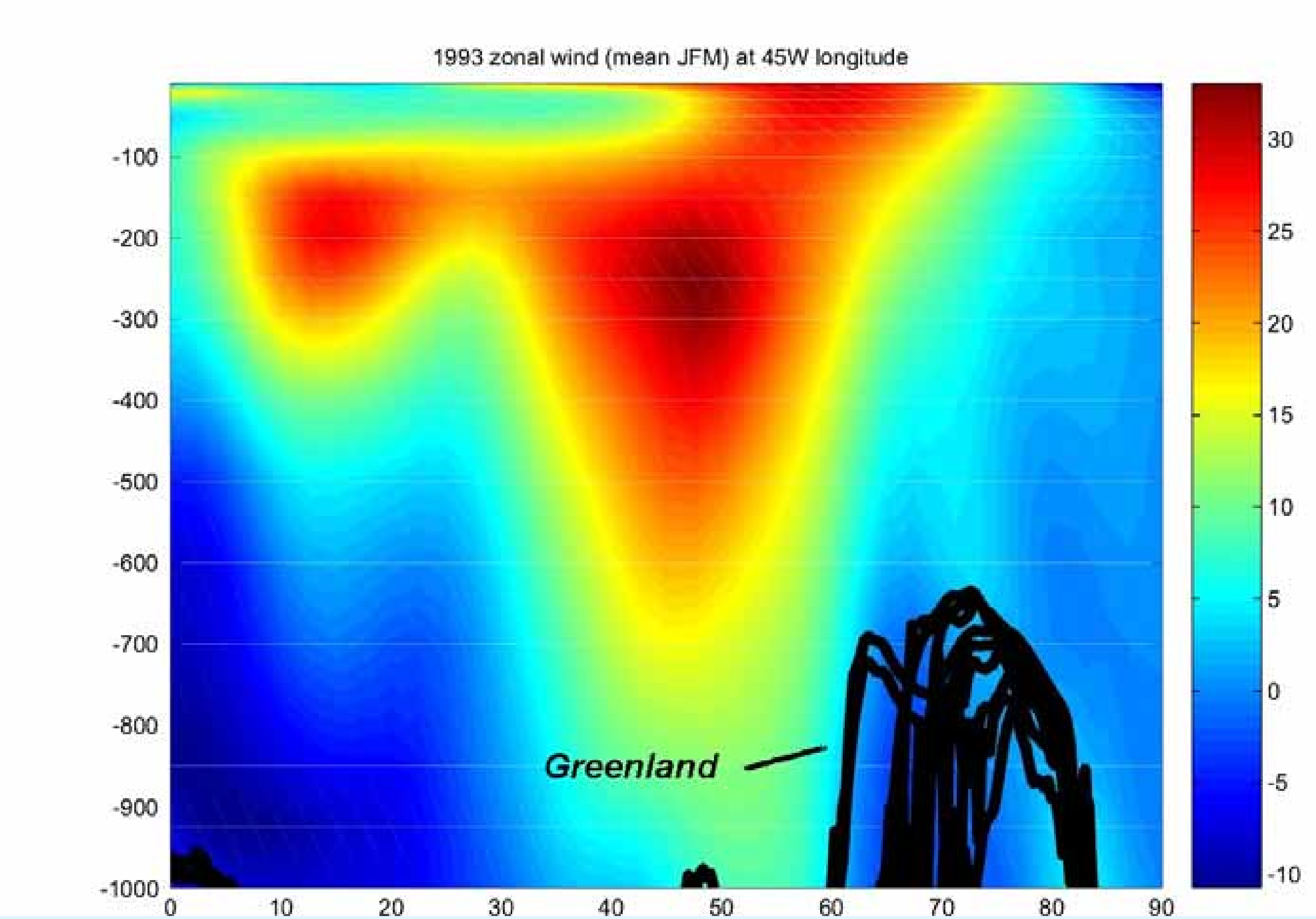

- The next figures are animations of the northern hemisphere circulation for a high-NAO (1989) and low NAO (1996) winter, respectively. They show many things, including strong vertical interaction between clusters of cyclones and the stratospheric polar vortex. Synoptic activity is felt in the stratosphere! A strong sudden warming is seen in 1989.
- The two winters are very different. With low NAO (1996), it seems the storm track is farther south, and does not excite the stratospheric polar vortex overhead as strongly as with high NAO (1989)

1989 JFMA:

NAO index **positive**

colors: 1000 HPa near-surface dynamic height
(blue=low pressure, red=high)
contours:
jet stream level 300 HPa, stratosphere 30 HPa

Synoptic storm tracks are beneath stratospheric polar vortex

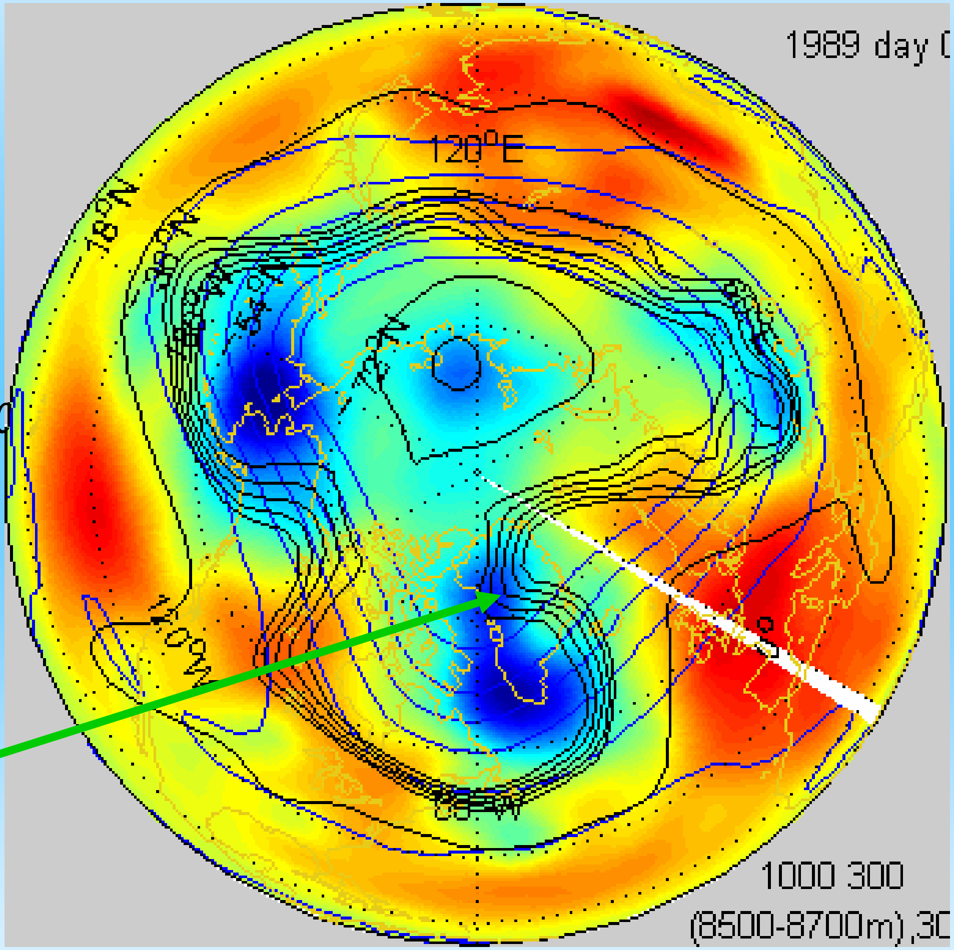

Greenland

1996 JFMA (**NAO** index very **negative**)

colors: 1000 HPa
red contours: 300 HPa
black contours: 30 HPa

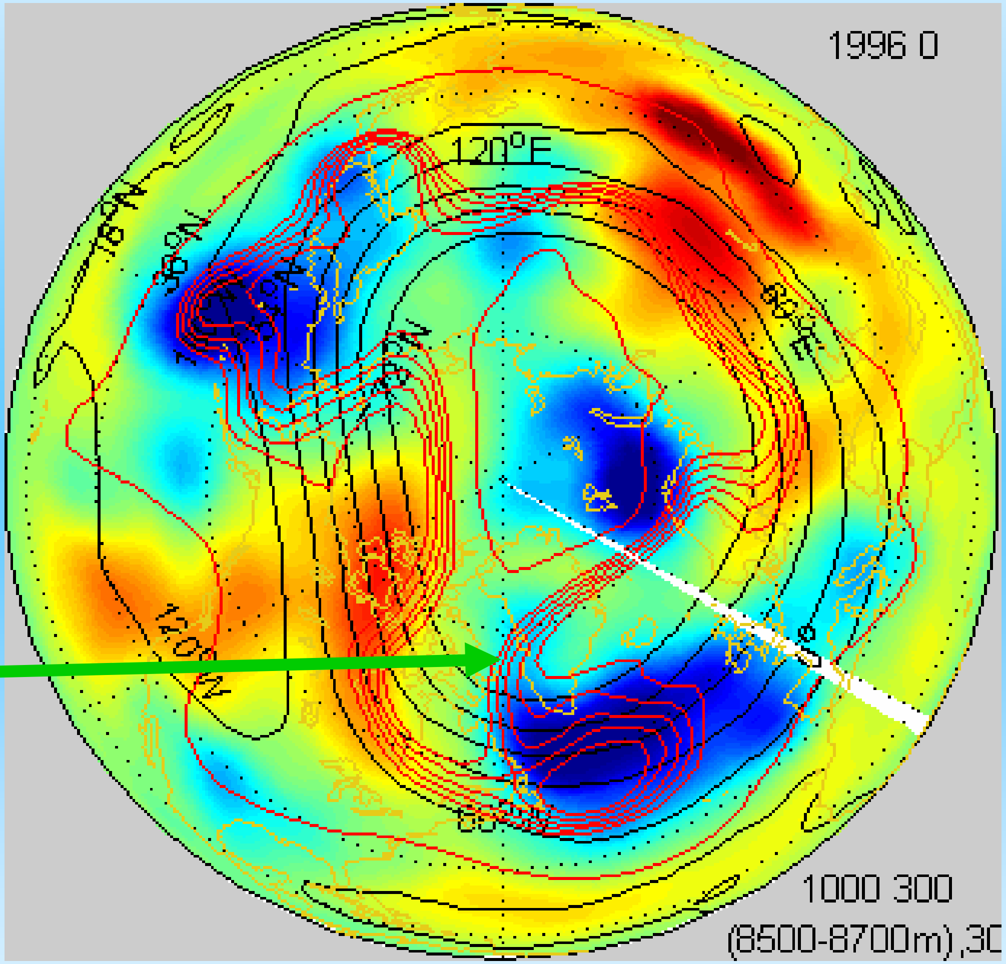

Storm tracks are usually south of stratospheric polar vortex

Greenland

In moderate-resolution simulations, Greenland's topography (but not albedo) actually weakens the Icelandic low: interference pattern with hemispheric standing waves… sea-level pressure is lower to the west and higher to the east of Greenland…model dependent?

SLP *500 hPa* *500-1000 hPa thickness*

DJF no Greenland

contour interval=5 hPa

control minus no Greenland

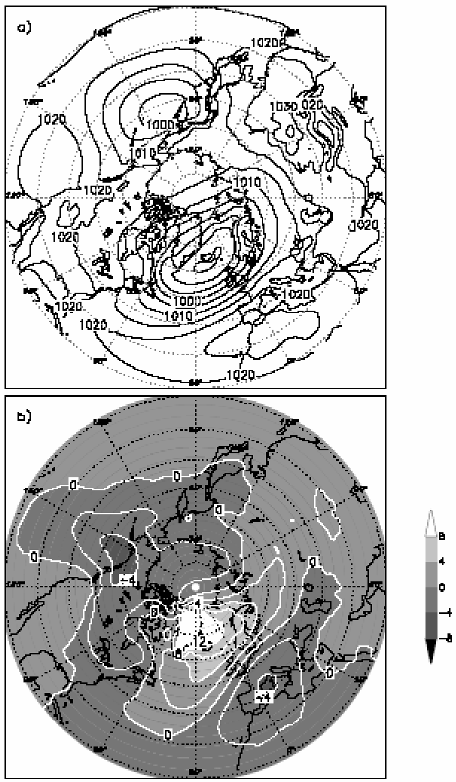

Fig. 4. (a) The mean winter (DJF) sea level pressure (hPa) in the NOGREEN simulation and (b) the mean sea level pressure difference (hPa), CONTROL–NOGREEN. The contour interval is 5 hPa in (a) and 2 hPa in (b). All the major differences in (b) are 95% statistically significant.

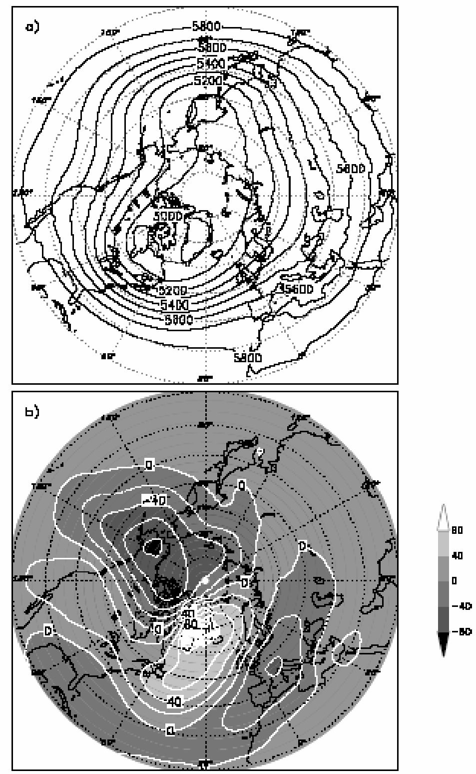

Fig. 5. (a) The mean winter (DJF) 500-hPa geopotential height (gpm) in the NOGREEN simulation and (b) the mean 500-hPa geopotential height difference (gpm), CONTROL–NOGREEN. The contour interval is 100 gpm in (a) and 20 gpm in (b). All the major differences in (b) are 95% statistically significant.

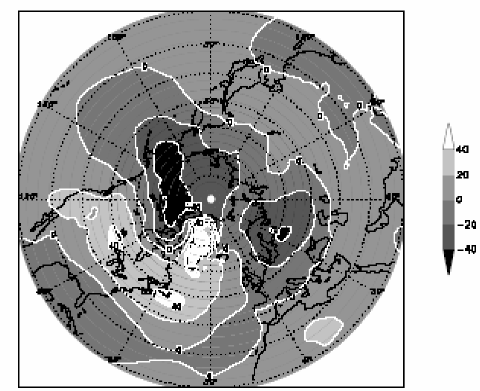

Fig. 6. The mean winter (DJF) 500–1000 hPa thickness (gpm) difference, CONTROL–NOGREEN. The contour interval is 20 gpm and all the major differences are 95% statistically significant.

Petersen, Kristjansson & Jonsson Tellus 04

- Numerical simulations (*Petersen, Kristjansson & Olafsson Tellus 04 T106; Kristjansson &McInness QJRMS 99)* suggest that Greenland topography reduces the strength of cyclonic systems in the Atlantic storm track, blocking cold-air outbreaks from Arctic Canada: Interference pattern with hemispheric standing waves

- Is this model dependent? Paradoxically, tip-jets and gap-jets (downslope winds) are frequently observed there and are very intense. Winds in the Labrador and Greenland Seas can be very strong.

We are not contemplating removing Greenland until it melts

potential vorticity and Θ

(Hoskins, McIntyre & Robertson QJRMS 1985)

GFD-1 HOSKINS ET AL. QJRMS

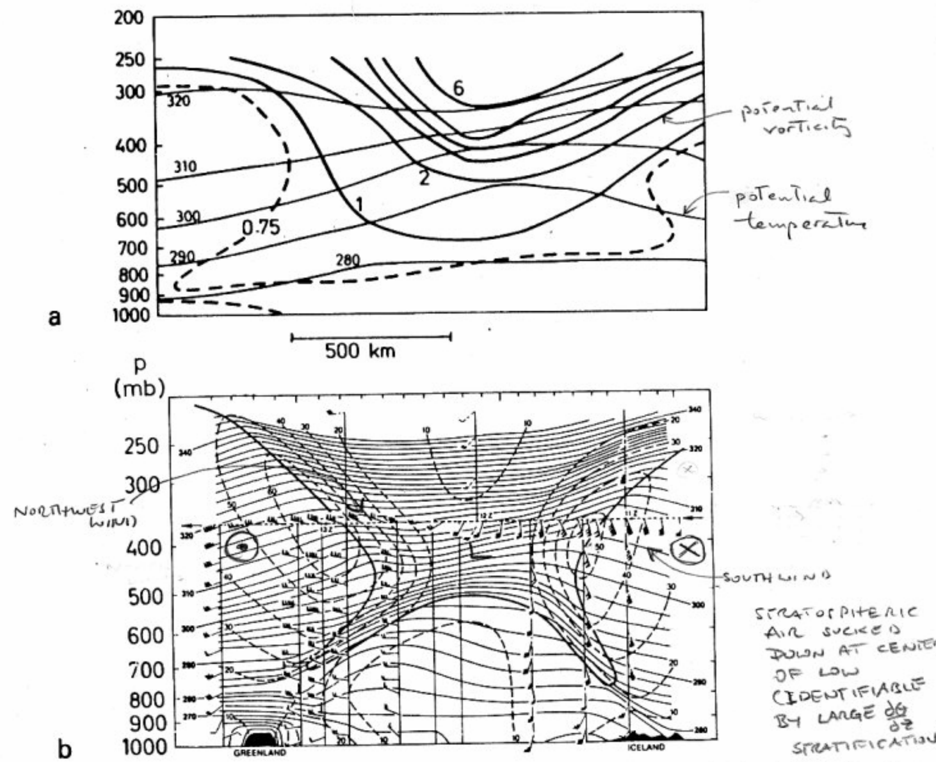

Figure 9. Vertical cross-sections along a SW–NE line through the Icelandic low on 12 April 1983. The first section (a) shows the results obtained by simple finite differences applied to the routine ECMWF analysis at 12 z on that day. The thin lines indicate isentropes at 10 K intervals and the thick lines PV at 1 unit intervals. The 0·75 PV unit contour is shown by a heavy dashed line. The second section (b), from M. A. Shapiro (personal communication), is the result of detailed measurements using aircraft and dropwindsondes. Isentropes every 2 K are indicated by light solid lines, isotachs every 10 m s^{-1} by dashed lines and the estimated tropopause position by a heavy continuous line. The scales and orientation of the two sections are approximately the same.

As far as gross features are concerned, everything is the opposite way round from Figs. 8–10. The tropopause is high, the isentropes in the troposphere bow downwards, and those in the stratosphere bow upwards. The very low potential vorticity just under the ... is particularly striking. Once again we shall see that

- despite this no-Greenland model study, winds are extraordinarily there; pressure drag on Greenland's slopes can propagate upward, block westerly flow, and affect the subpolar (and thus global-) ocean beneath

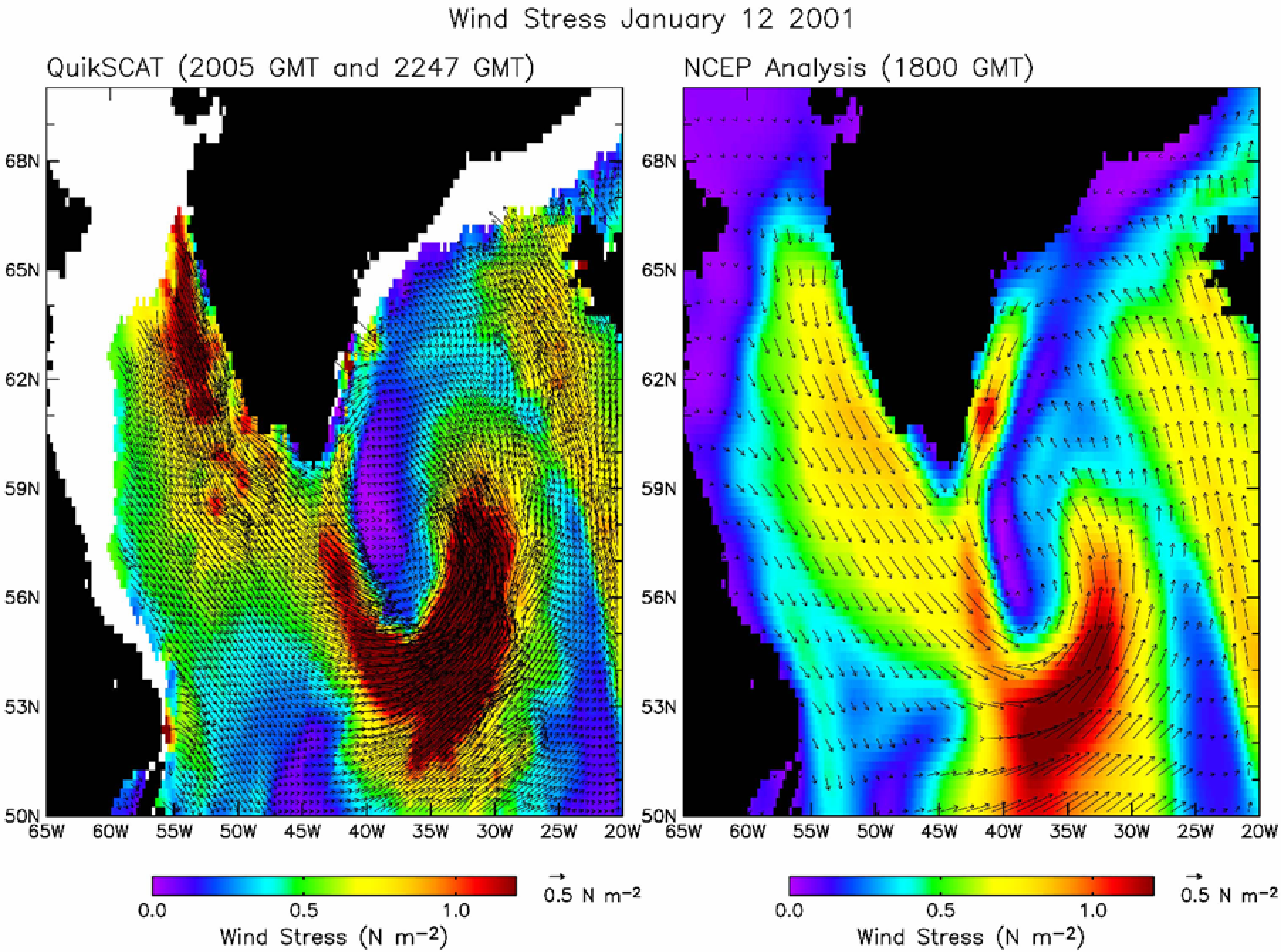

from Dudley Chelton: Greenland tip jet

pressure drag and the length of the day

Hide et al. JGR 1997

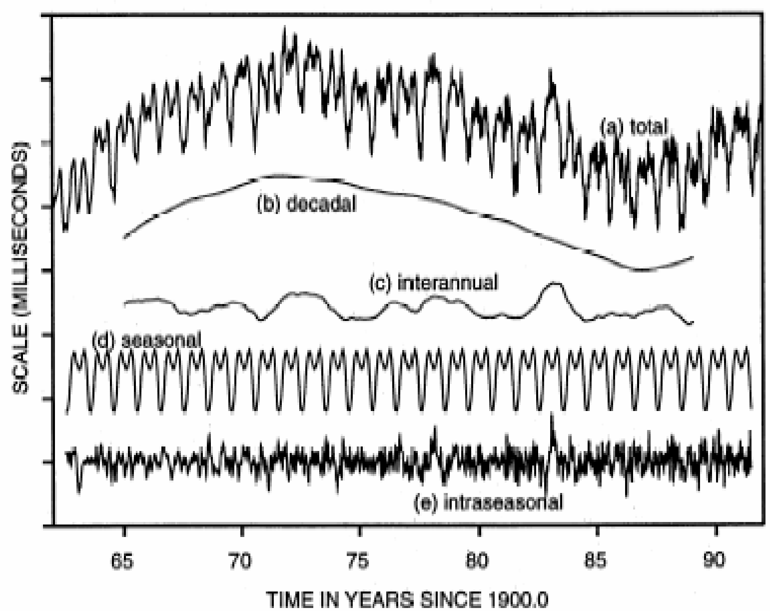

Figure 1. Time series of irregular fluctuations in the length of the day (LOD) from 1963 to 1992 (curve a) and its decadal, interannual, seasonal, and intraseasonal components (curves b, c, d, and e, respectively). The decadal (curve b) component largely reflects angular momentum exchange between the solid Earth and the underlying liquid metallic outer core produced by torques acting at the core-mantle boundary. The other components (curves c, d, and e) largely reflect angular momentum exchange between the atmosphere and the solid Earth, produced by torques (proportional to the time derivative of the LOD time series) acting directly on the solid Earth over continental regions of the Earth's surface and indirectly over oceanic regions (adapted from *Hide and Dickey* [1991]).

$$-\frac{\partial}{\partial t}\left[\int_0^{p_*} m_{\mathrm{r}} \frac{\mathrm{d}p}{g}\right] = \frac{1}{a\cos\phi}\frac{\partial}{\partial\phi}\left(\left[\int_0^{p_*} m_{\mathrm{r}} v\frac{\mathrm{d}p}{g}\right]\cos\phi\right) + \left[p_*\frac{\partial h}{\partial\lambda}\right] + a\cos\phi[\tau_*^{\mathrm{sso}}] + a\cos\phi[\tau_*^{\mathrm{bl}}] - fa\cos\phi\left[\int_0^{p_*} v\frac{\mathrm{d}p}{g}\right].$$

T159 *T511*

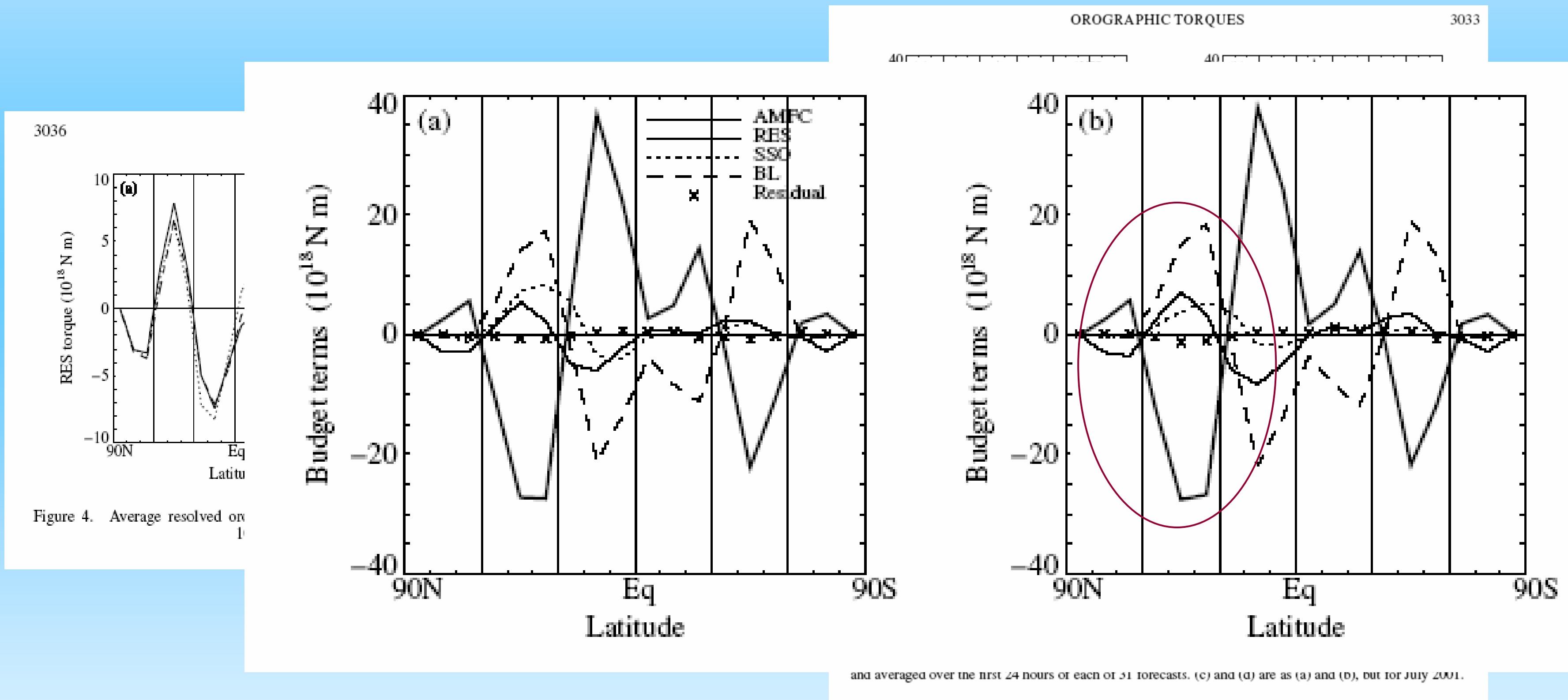

resolved torgue ~ 5 x 10^{18} N m
Brown, QJRMS 2004

6 month ECMWF model integrations at T95-T159 L60 and T255 L40, and case studies

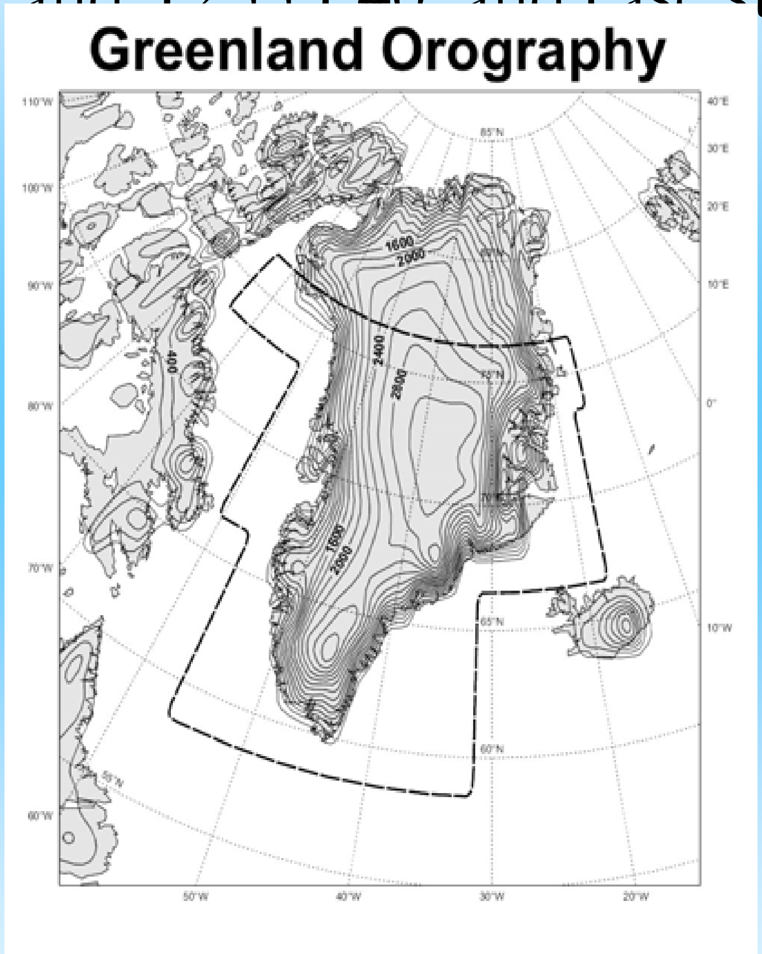

Pressure drag on Greenland (using T511L60 ECMWF model)

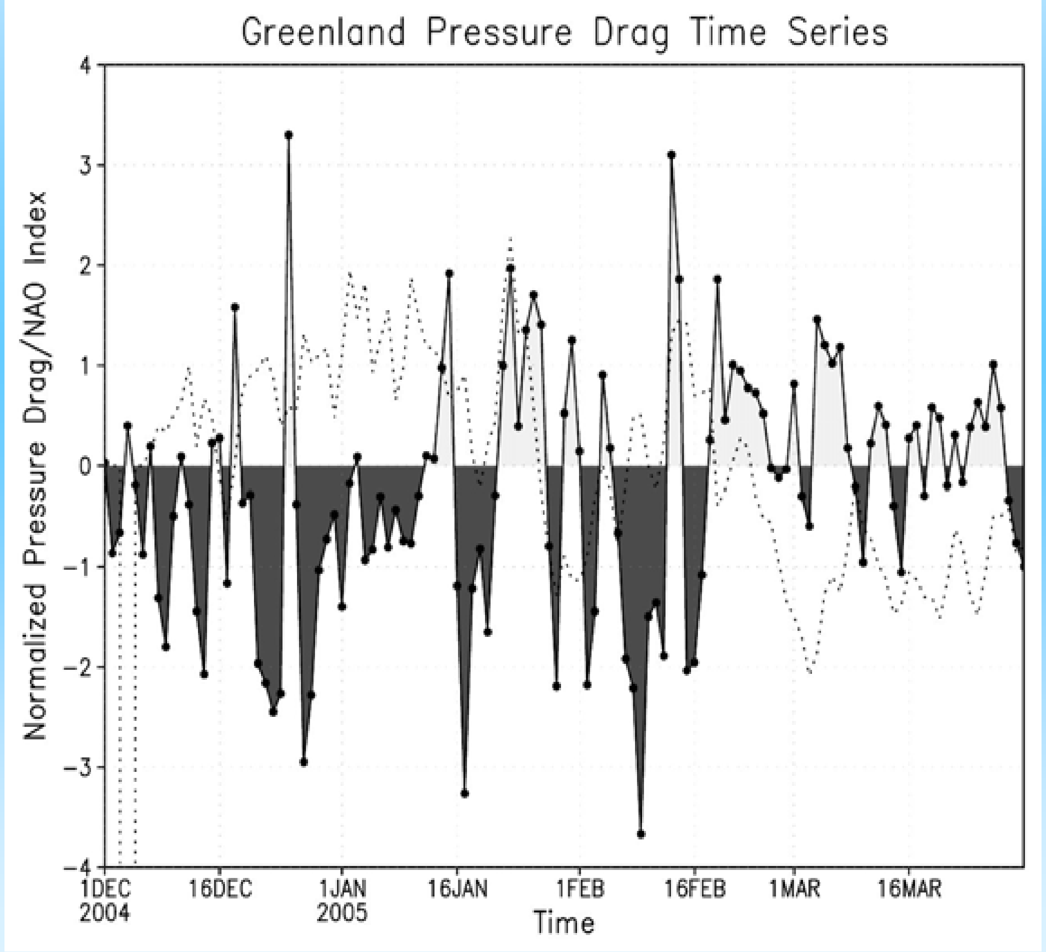

'normal' drag events (Greenland pushes atmosphere westward , low pressure to the east)

1000 hPa fields correlated with high pressure drag events at lags -6 days to + 4days ERA-40 reanalysis data (T159L60) 1982-2001

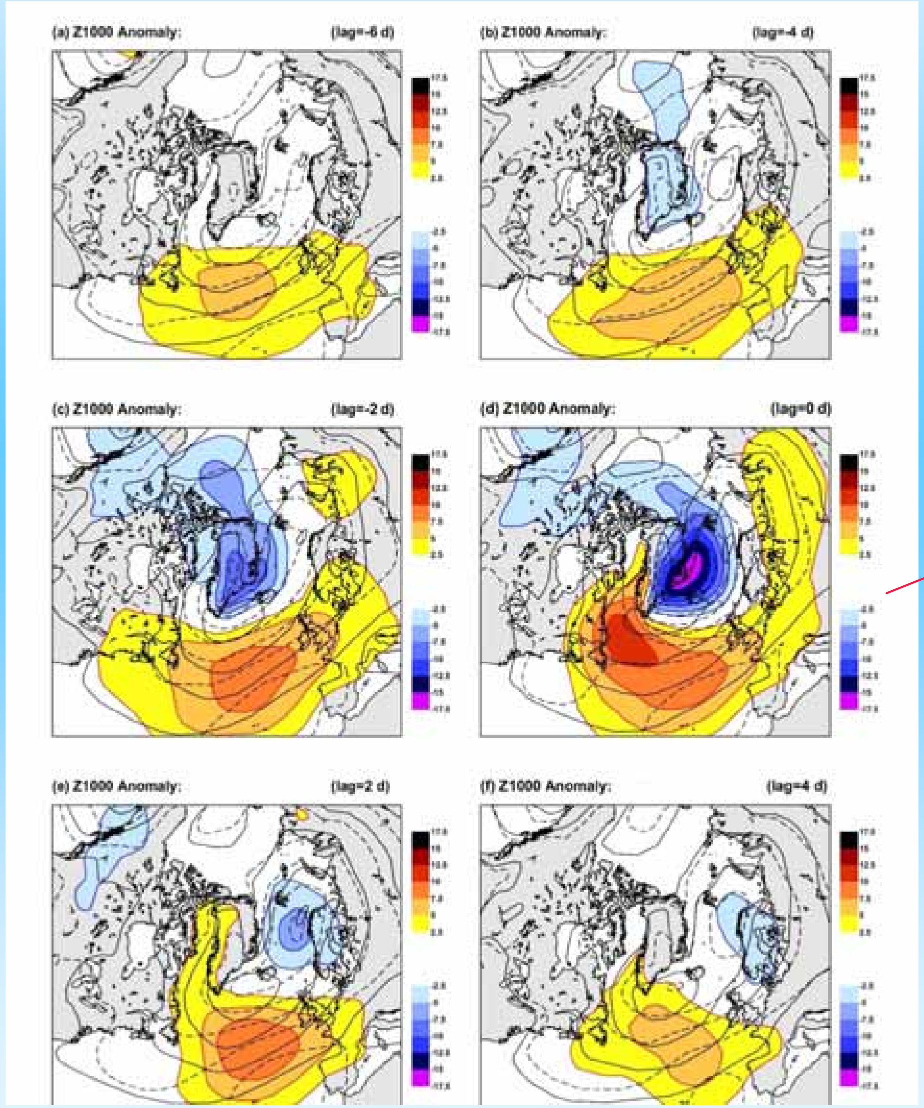

0 lag

250 hP

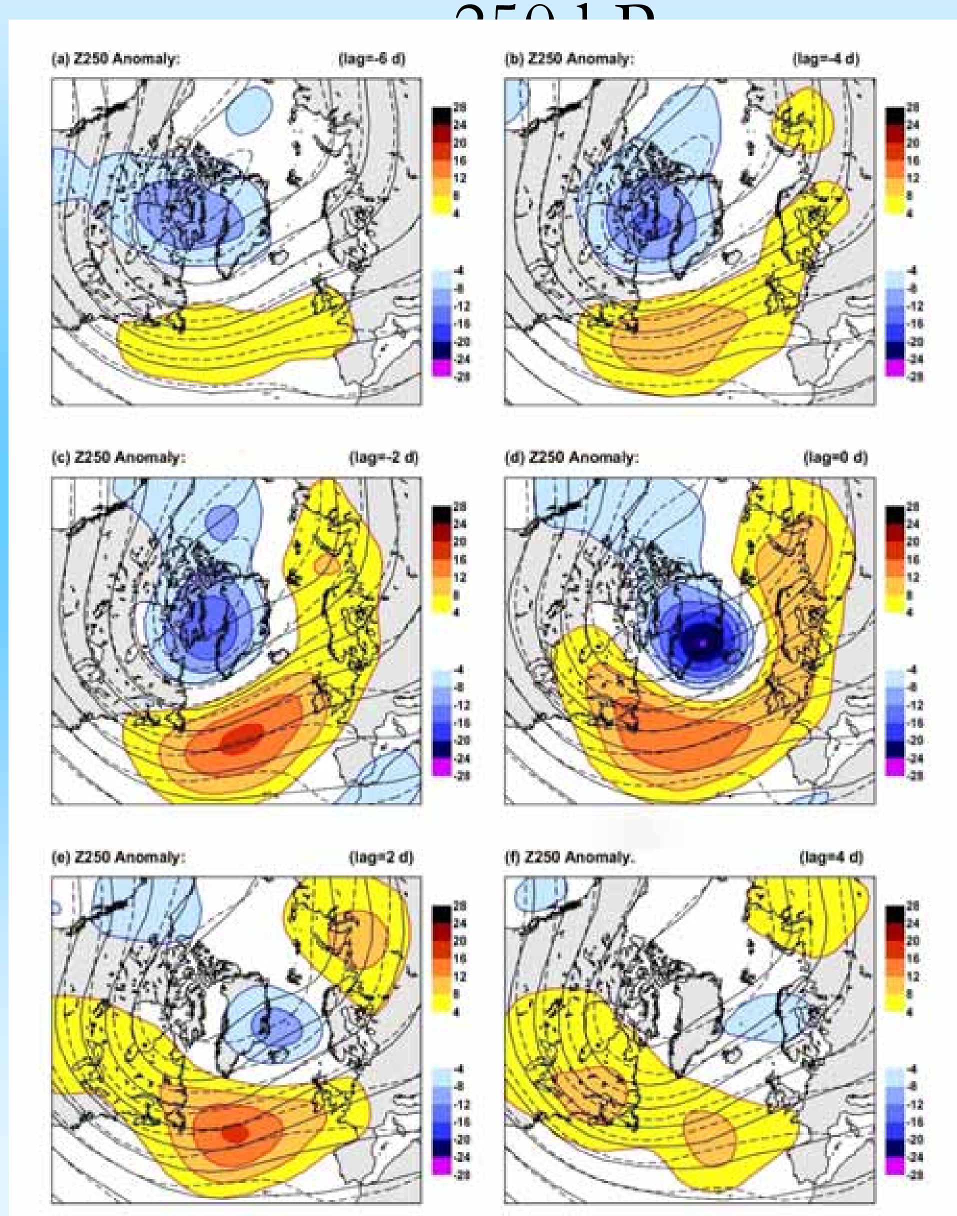

(a) Z250 Anomaly: (lag=-6 d)
(b) Z250 Anomaly: (lag=-4 d)
(c) Z250 Anomaly: (lag=-2 d)
(d) Z250 Anomaly: (lag=0 d)
(e) Z250 Anomaly: (lag=2 d)
(f) Z250 Anomaly: (lag=4 d)
28
24
20
16
12
8
4
-4
-8
-12
-16
-20
-24
-28

50 hPa   hemispheric response with precursor: the SPV is pulled toward Baffin Bay during high normal pressure drag events

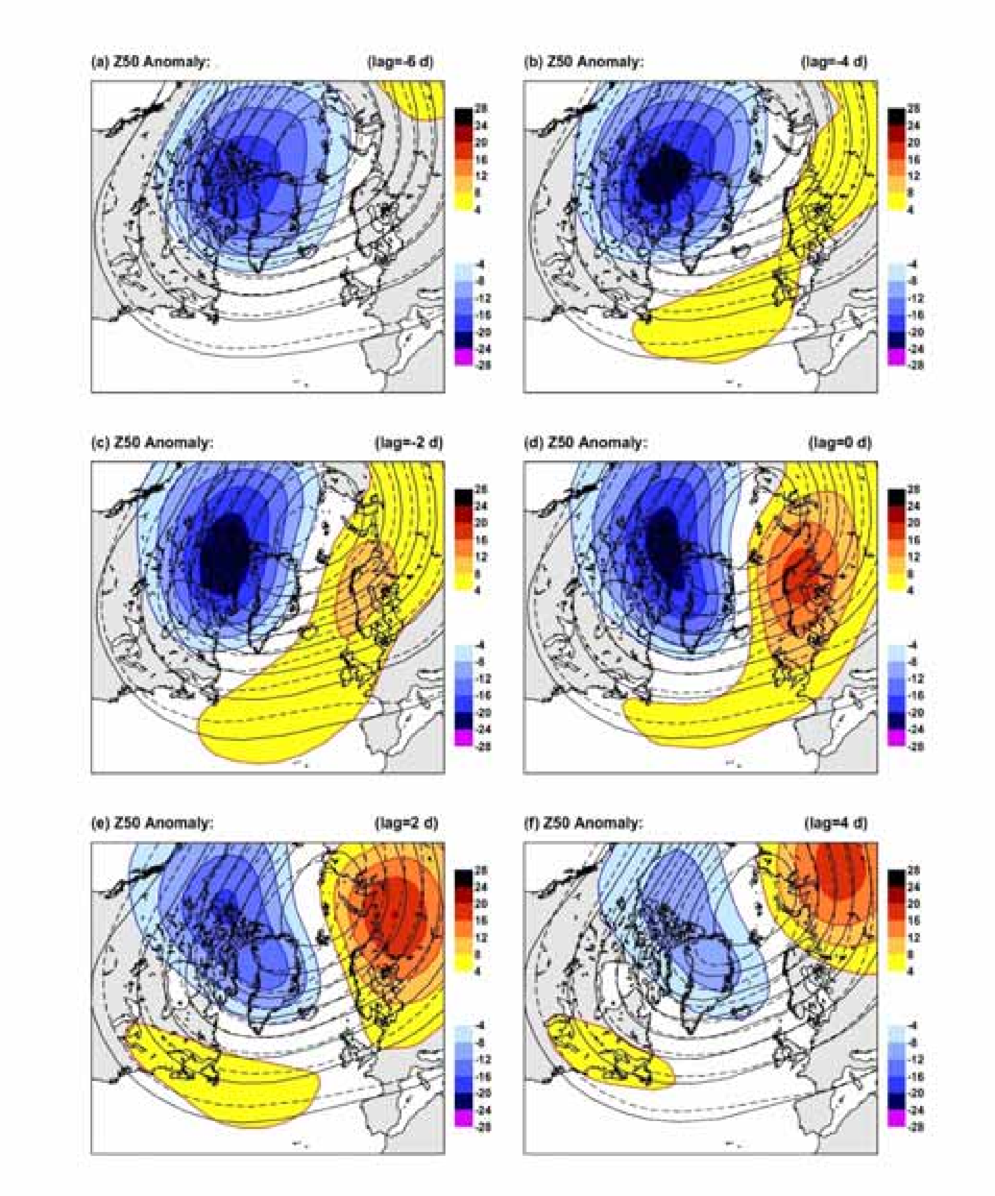

1000 hPa fields correlated with high normal pressure drag across Greenland: high-pass filtered eddies (2-10

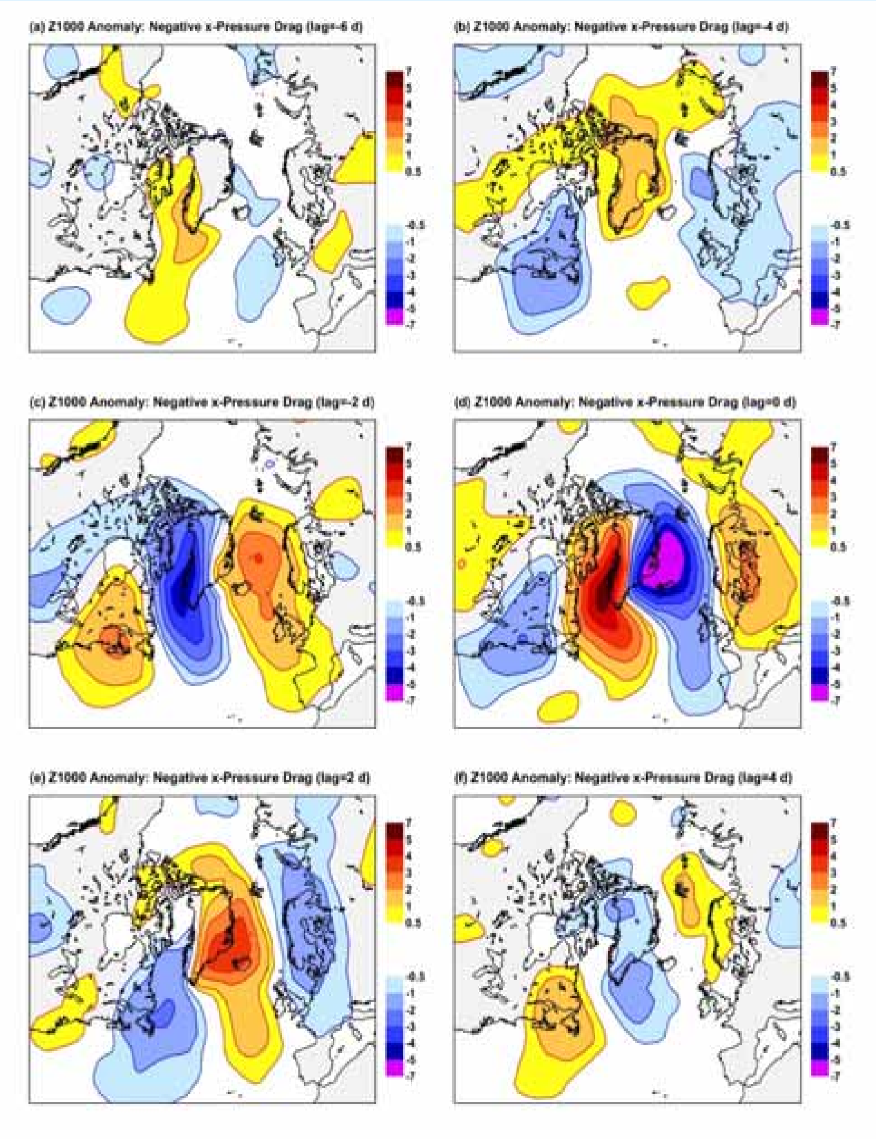

Z1000 associated with 'abnormal' pressure drag (high pressure on eastern slopes of Greenland)

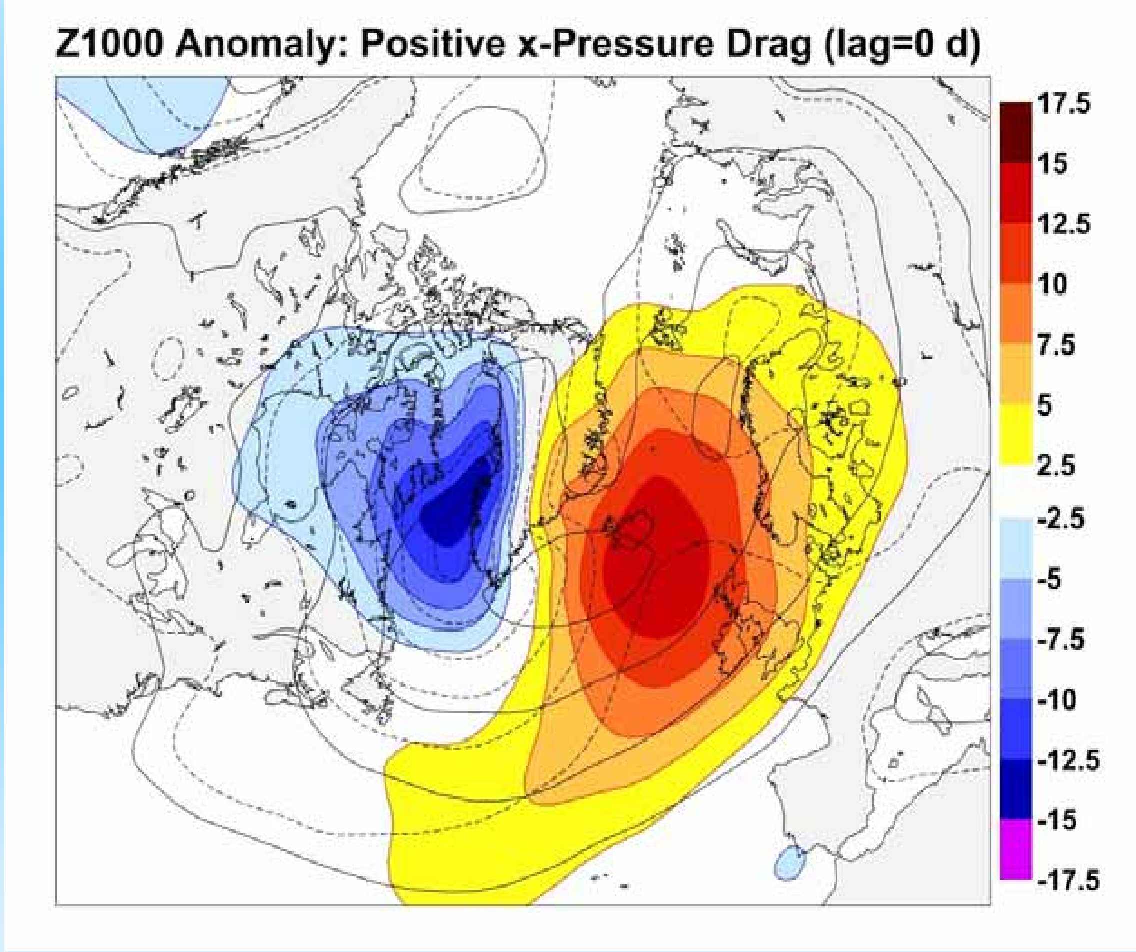

effect of model resolution on resolved pressure drag, surface friction and parameterized gravity wave stress

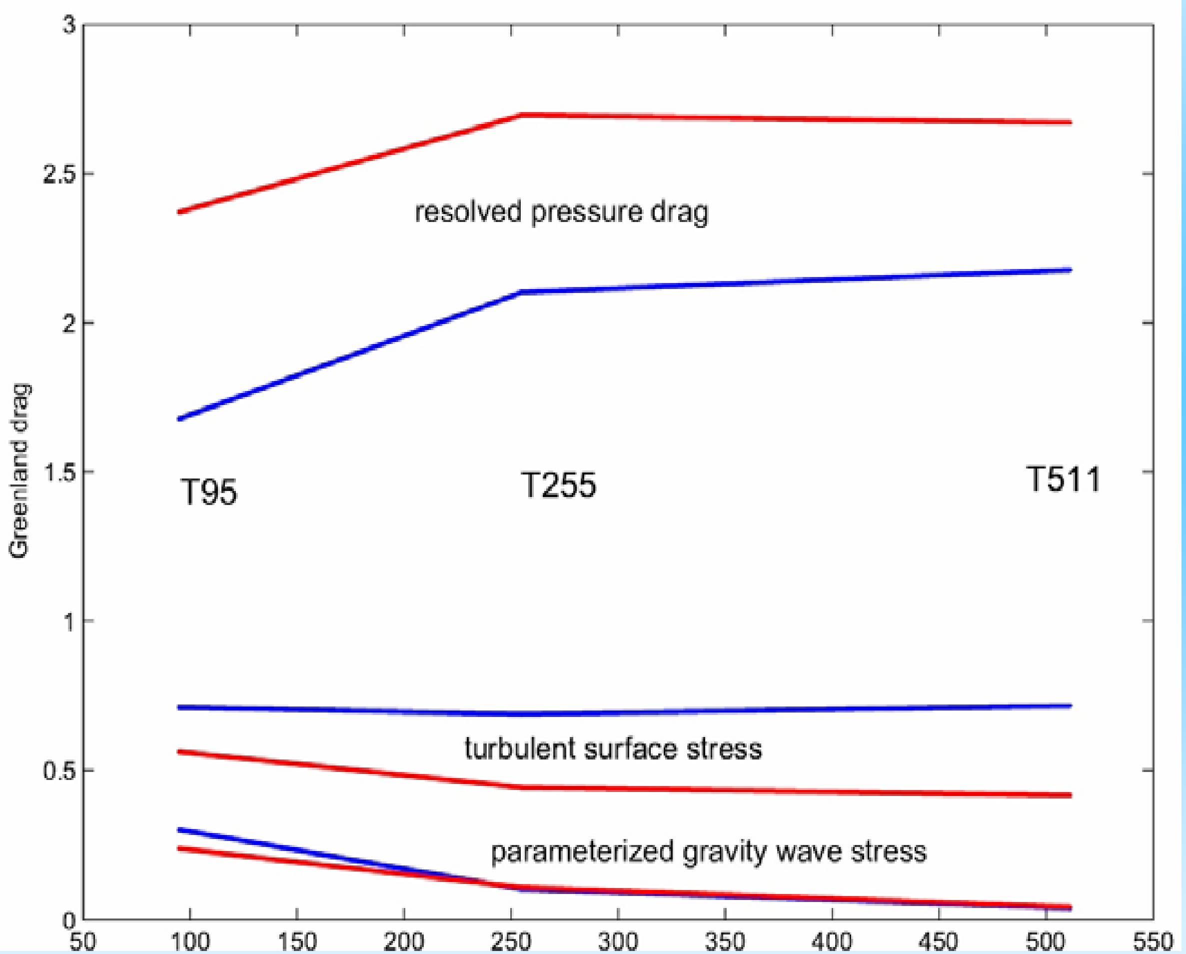

Storm tracks

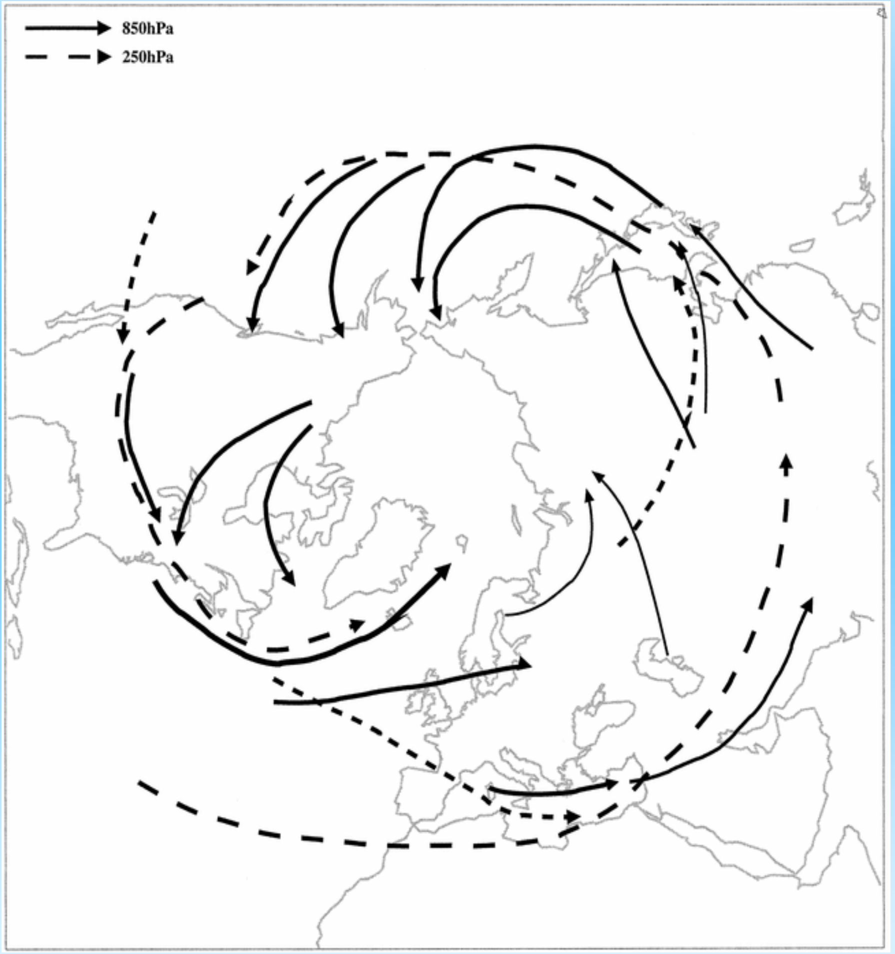

splitting of storm track, some lows moving northward on west side of Greenland (short lived), most moving north on eastern side. Cyclones are also split vertically by the 'knife-edge'

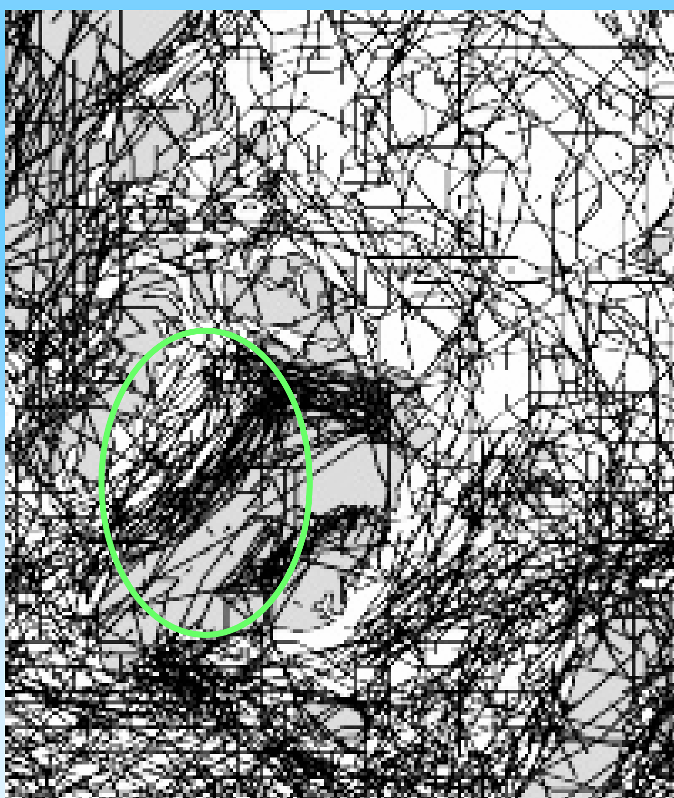

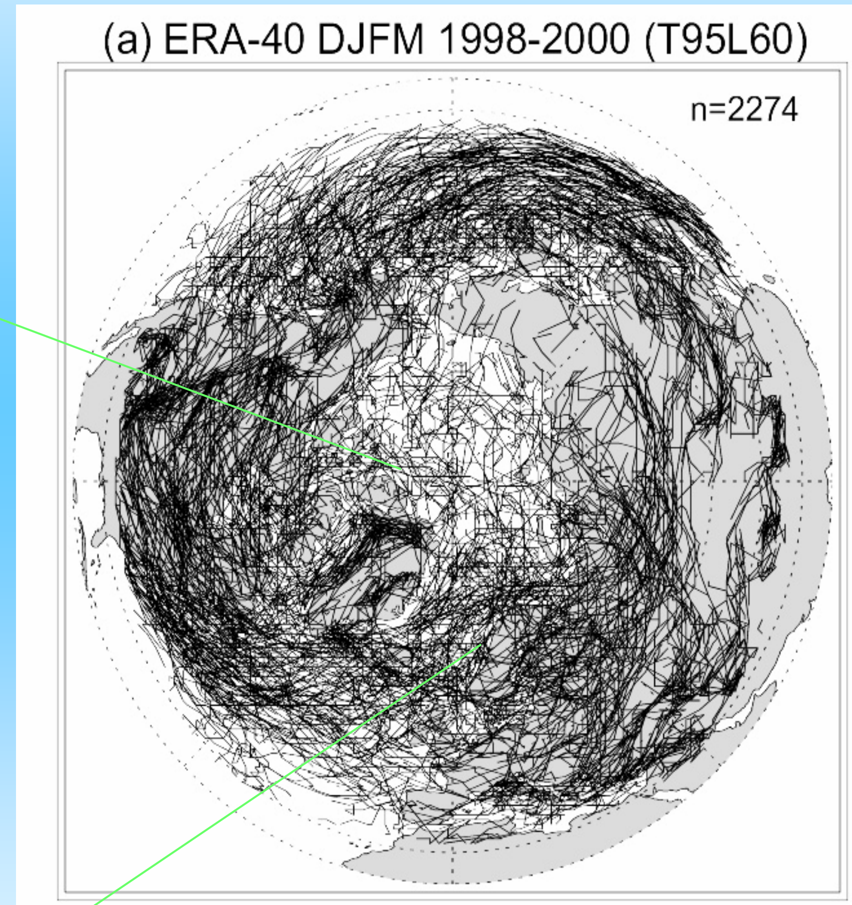

occurrence of cyclones in ERA-40 data, and at various model resolutions

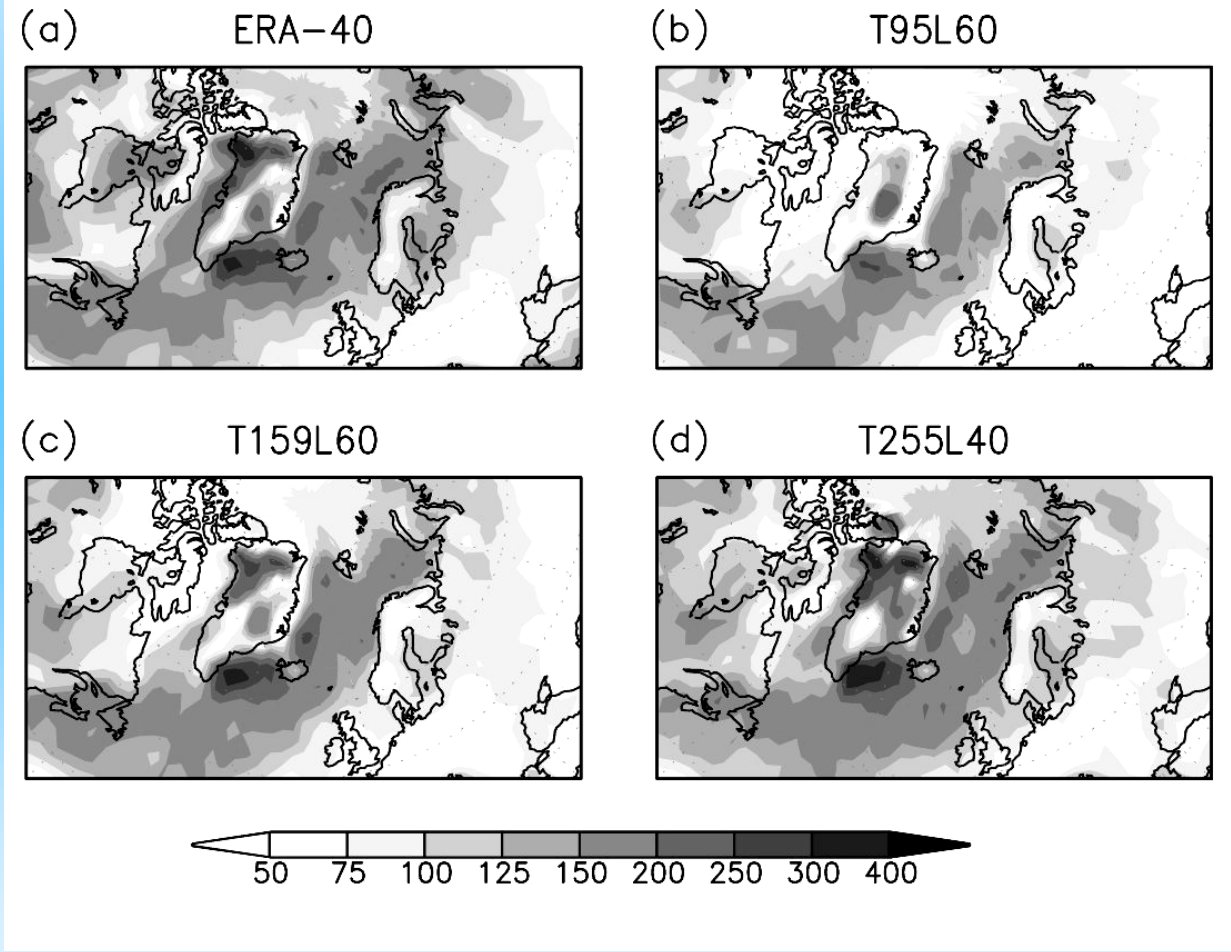

200 km

80 km

120 km grid

east-side storm tracks launched Irminger Sea (left) and Greenland Sea (right)

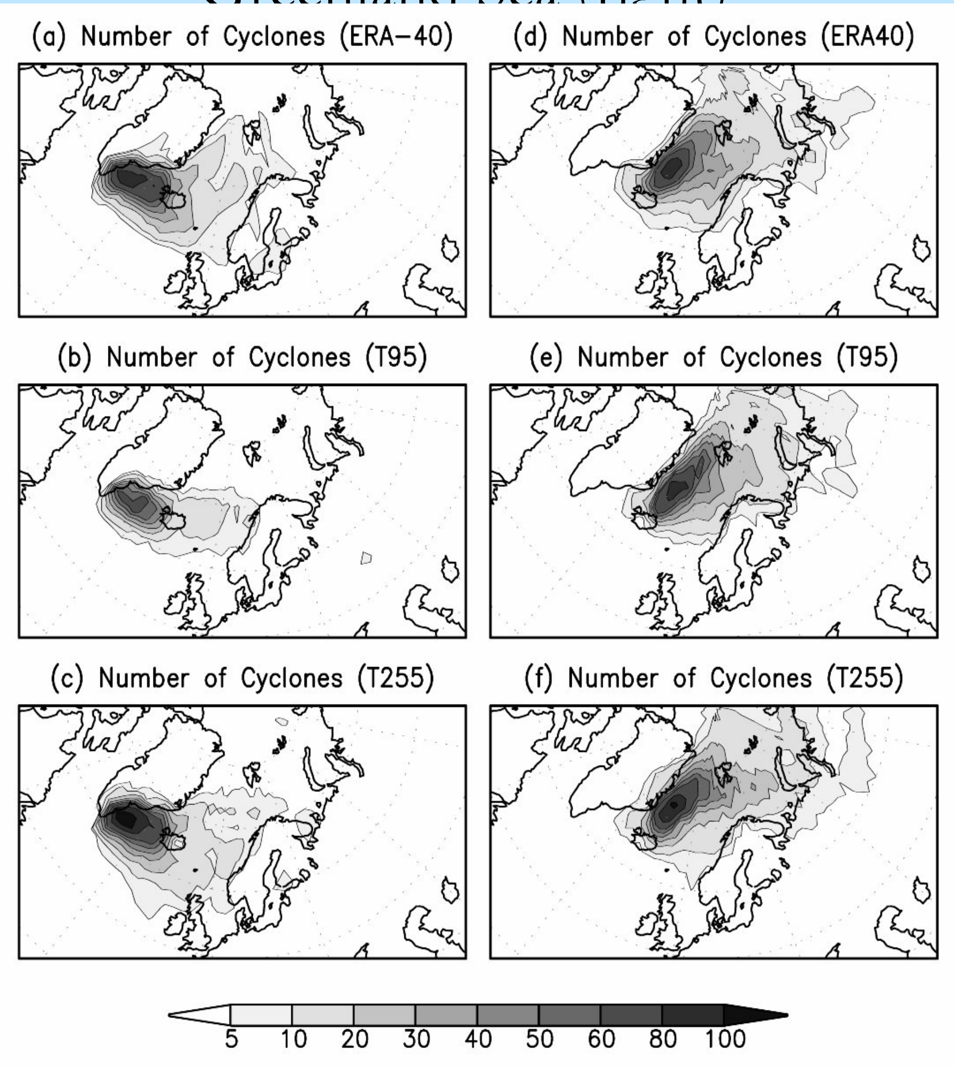

Two case studies, winter 2004/5 (strong, extraordinarily cold, elongated stratospheric polar vortex arrived early in the season)

Limpusaven et al JGR 2007 event

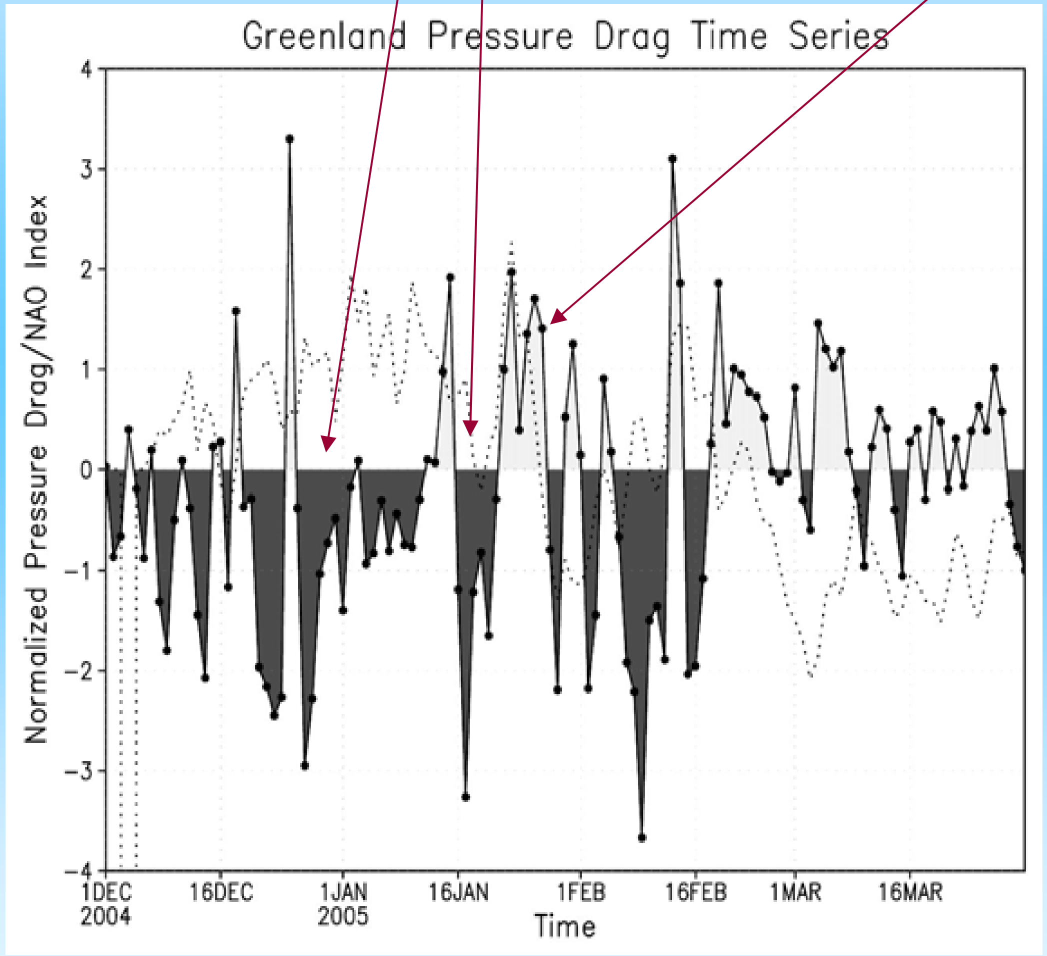

'normal' drag events (Greenland pushes atmosphere westward , low pressure to the east)

Θ on PV-2 surface (~tropopause) and SLP: Christmas 2004T511L60 ….3 storms in 10 days

Cold air sw … even at the tropopause lev

25 Dec 2004

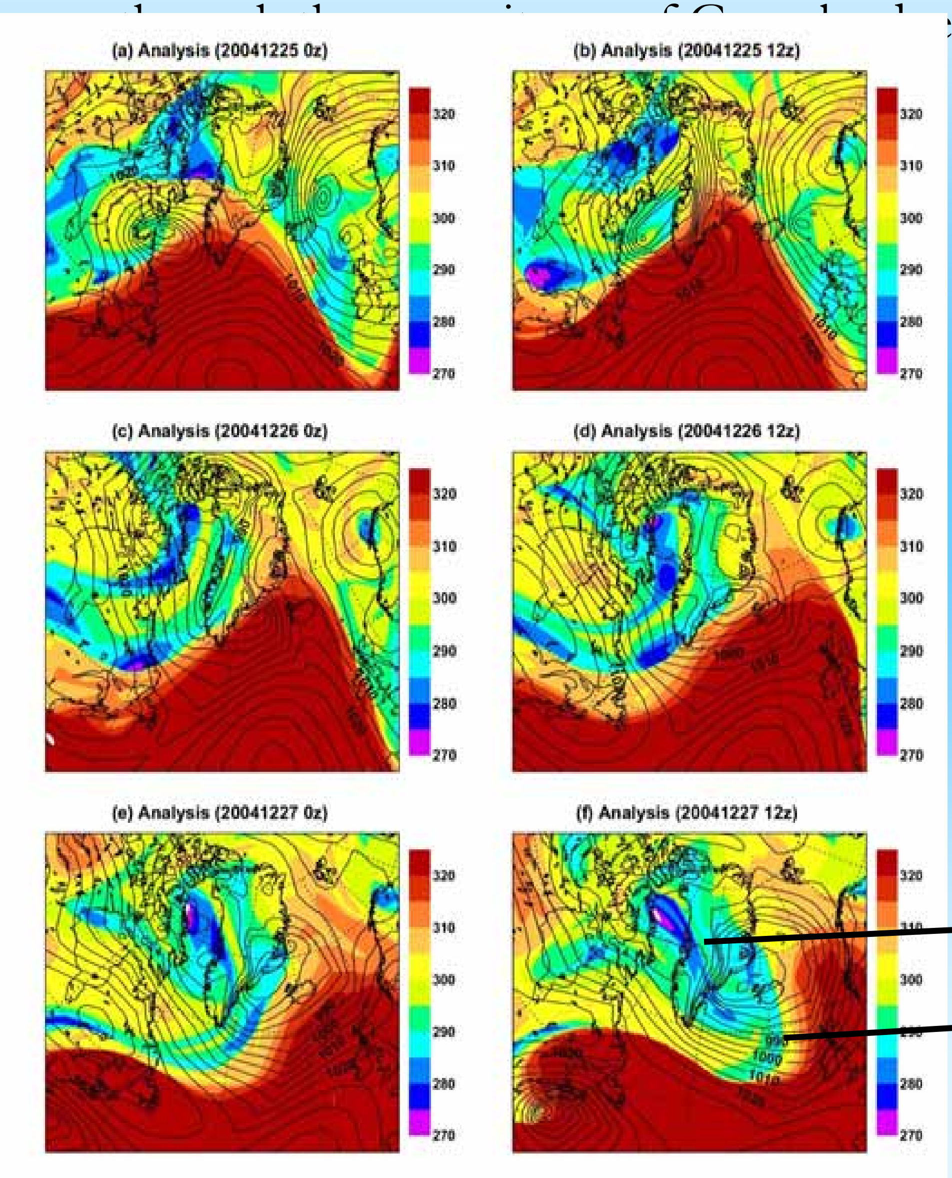

gap jet

tip jet

2 x $10^{-6} m^2 K s^{-1} kg^{-1}$

25-27 Dec 2004

surface winds

low-level vorticity

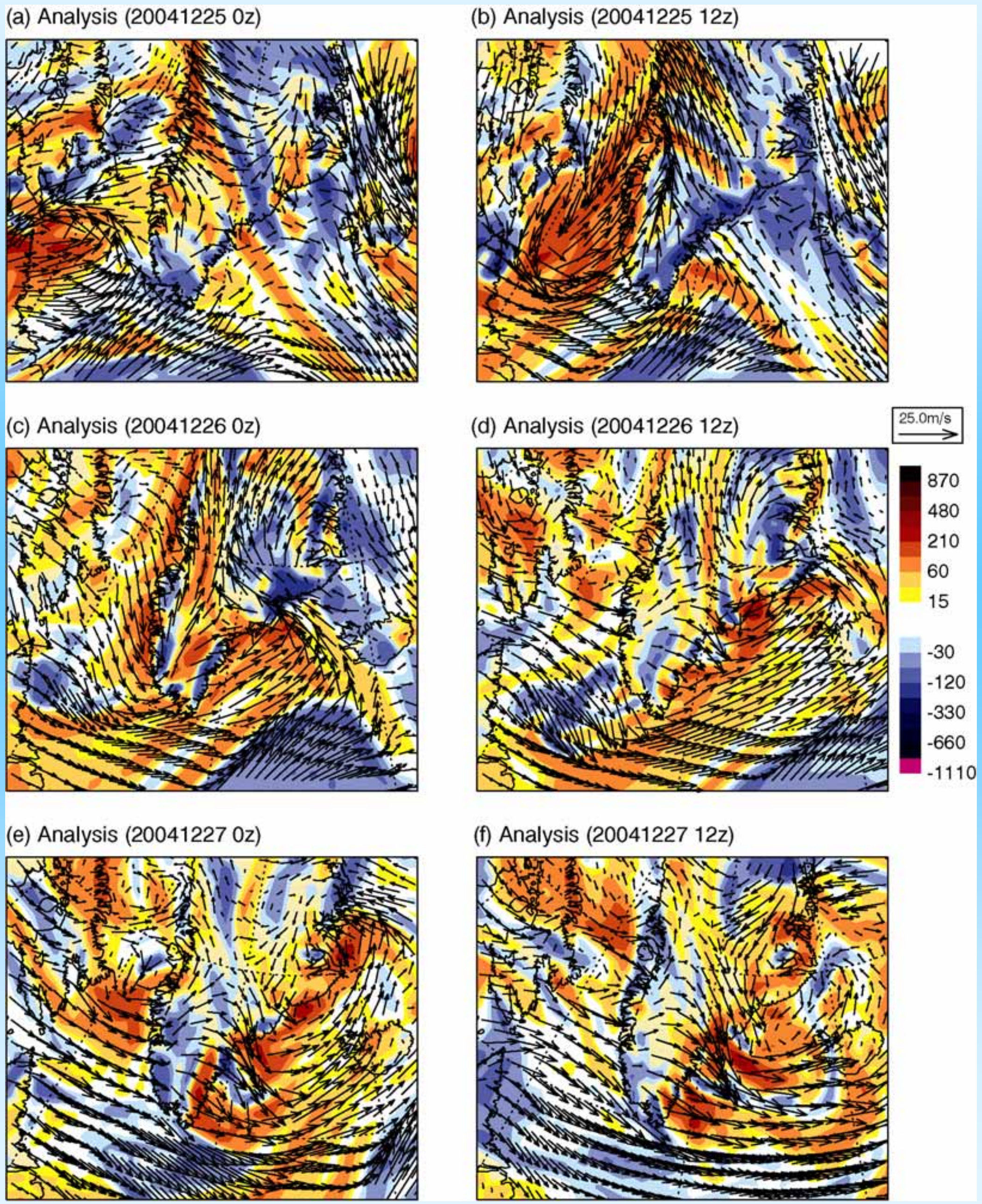

15-17 Jan 2005

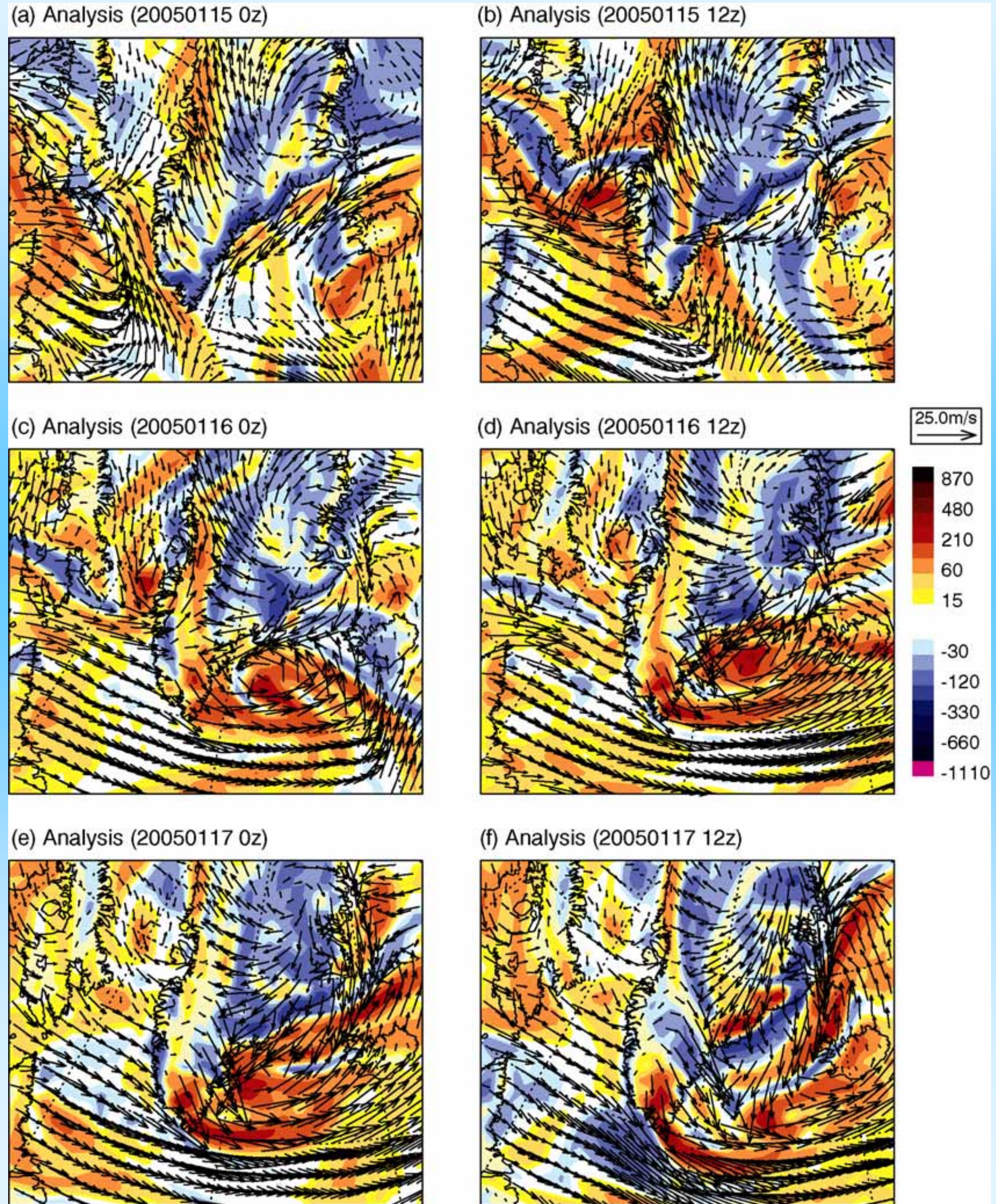

$0.31 \, f/N \, dU/dz$

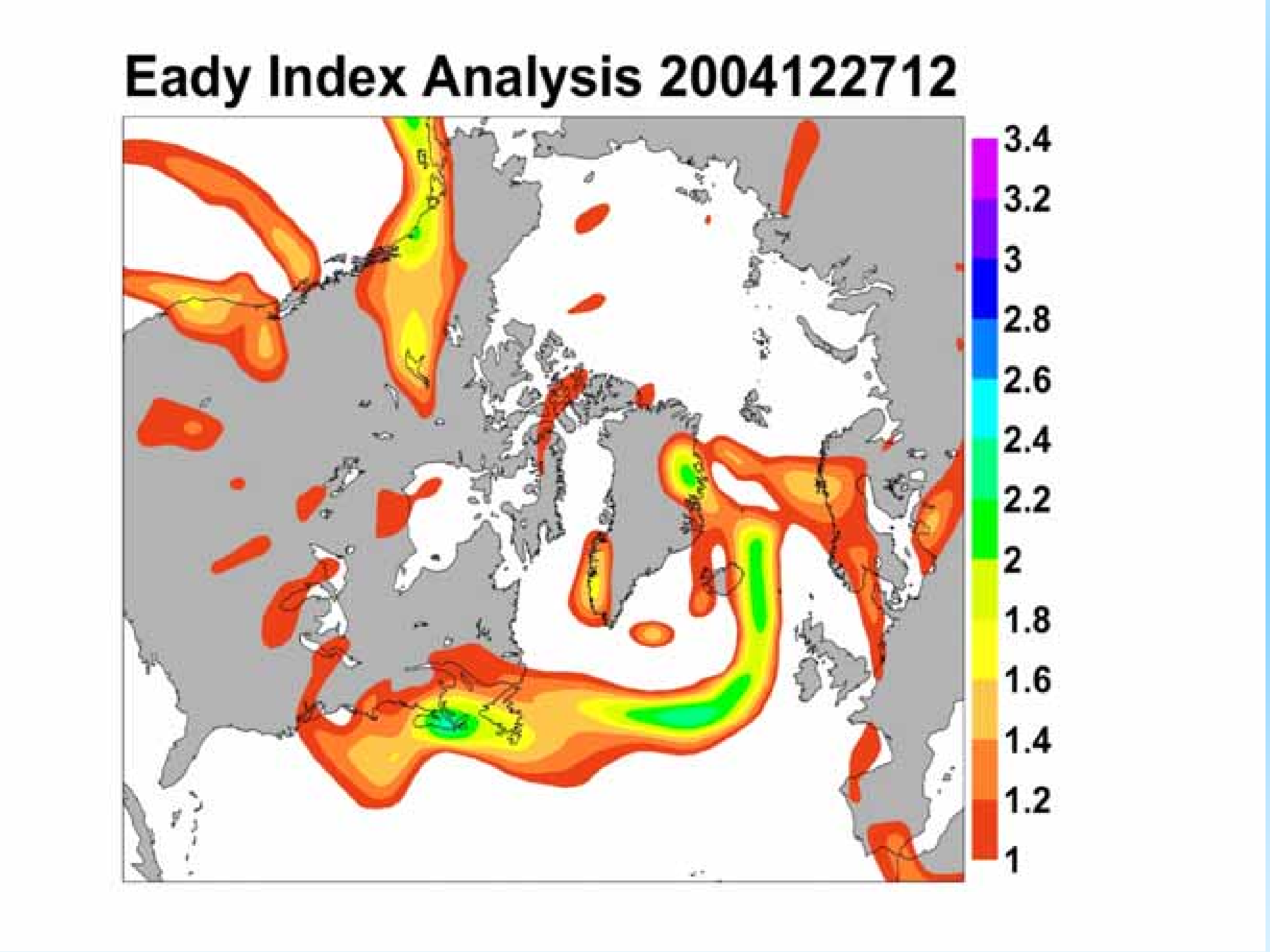

Eady Index Analysis 2004122712
3.4
3.2
3
2.8
2.6
2.4
2.2
2
1.8
1.6
1.4
1.2
1

Lagrangian back-trajectoies (using softward of H. Wernli)

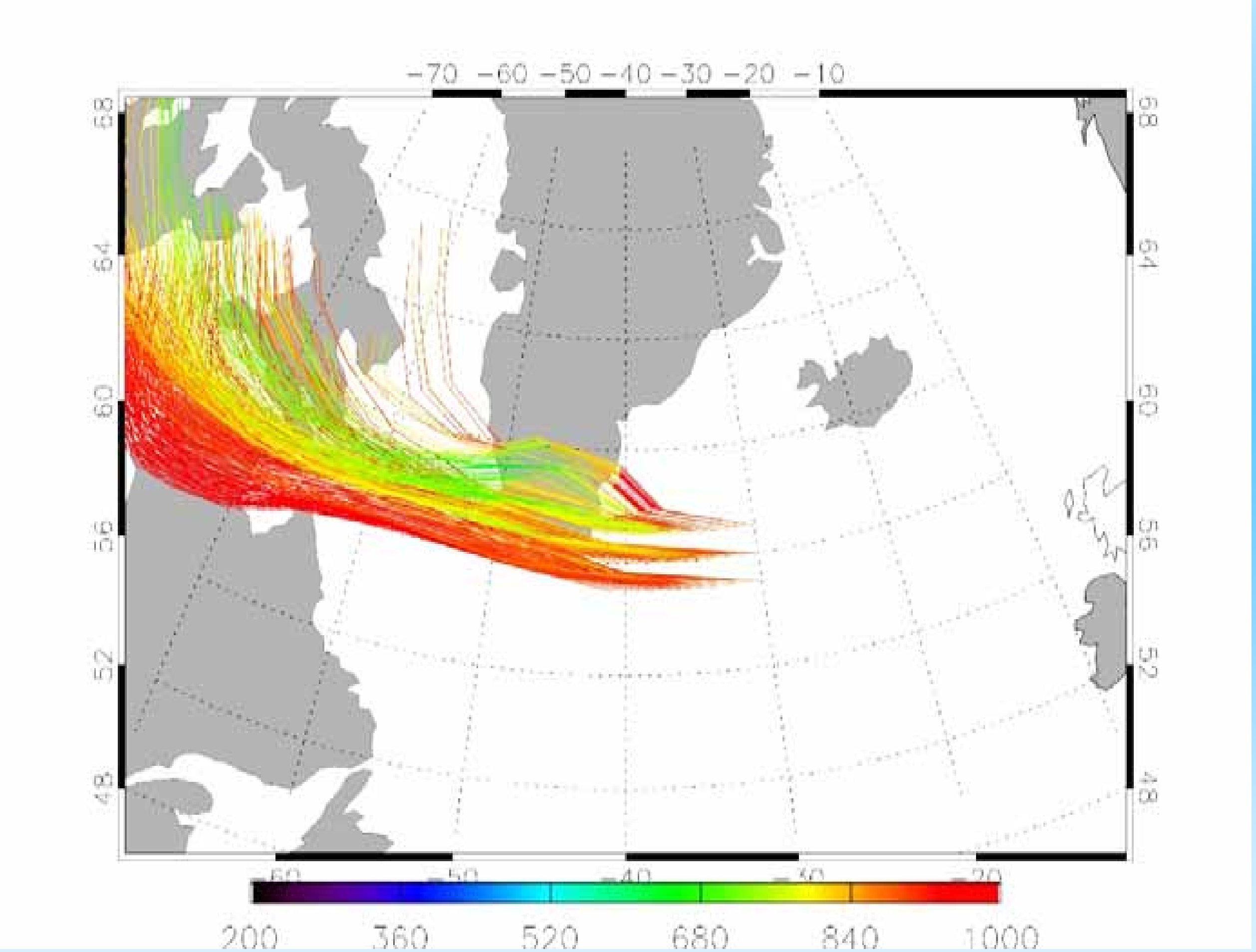

vorticity colors altitude colors

25-27 Dec 04

15-17 Jan 05

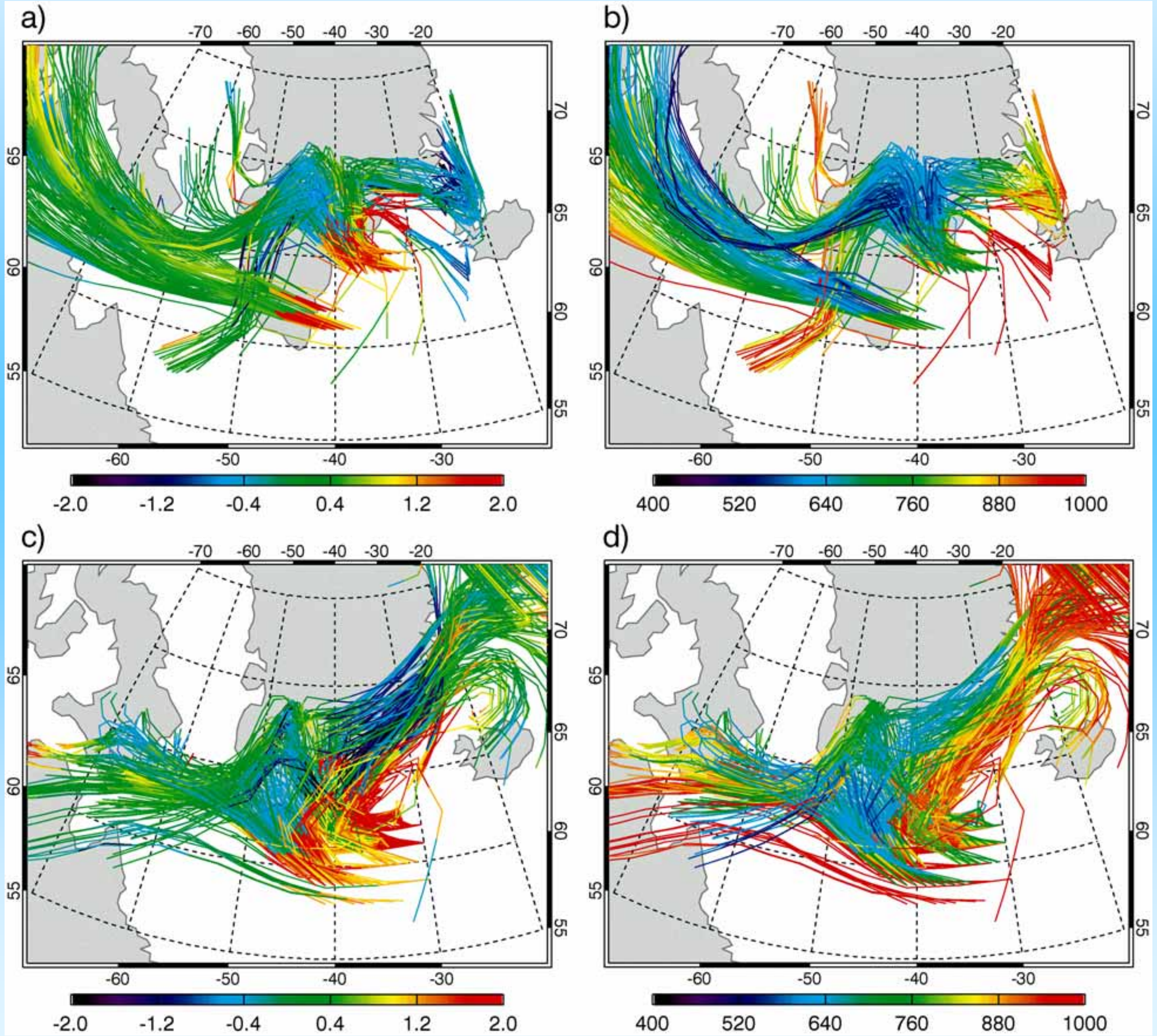

Effect on subpolar gyre of the Atlantic, and Greenland Sea: enhance air/sea heat flux: much intensified at higher model resolution

T95 T255 T799

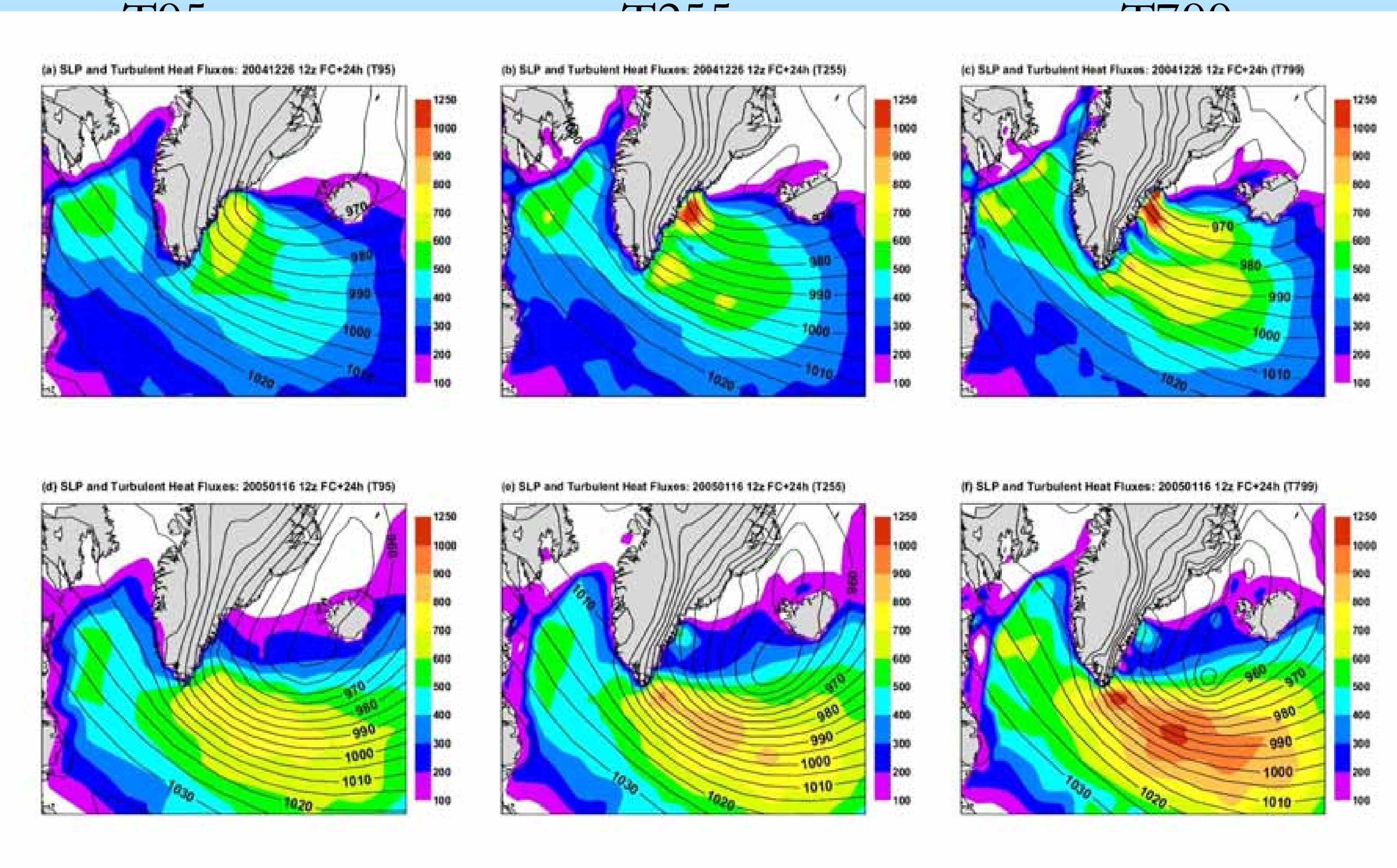

Principal eof of sea surface elevation, 1992-2006, which is mostly a simple trend, showing deceleration of the subpolar Atlantic gyre over 15 years

Häkkinen & Rhines 2004 Science

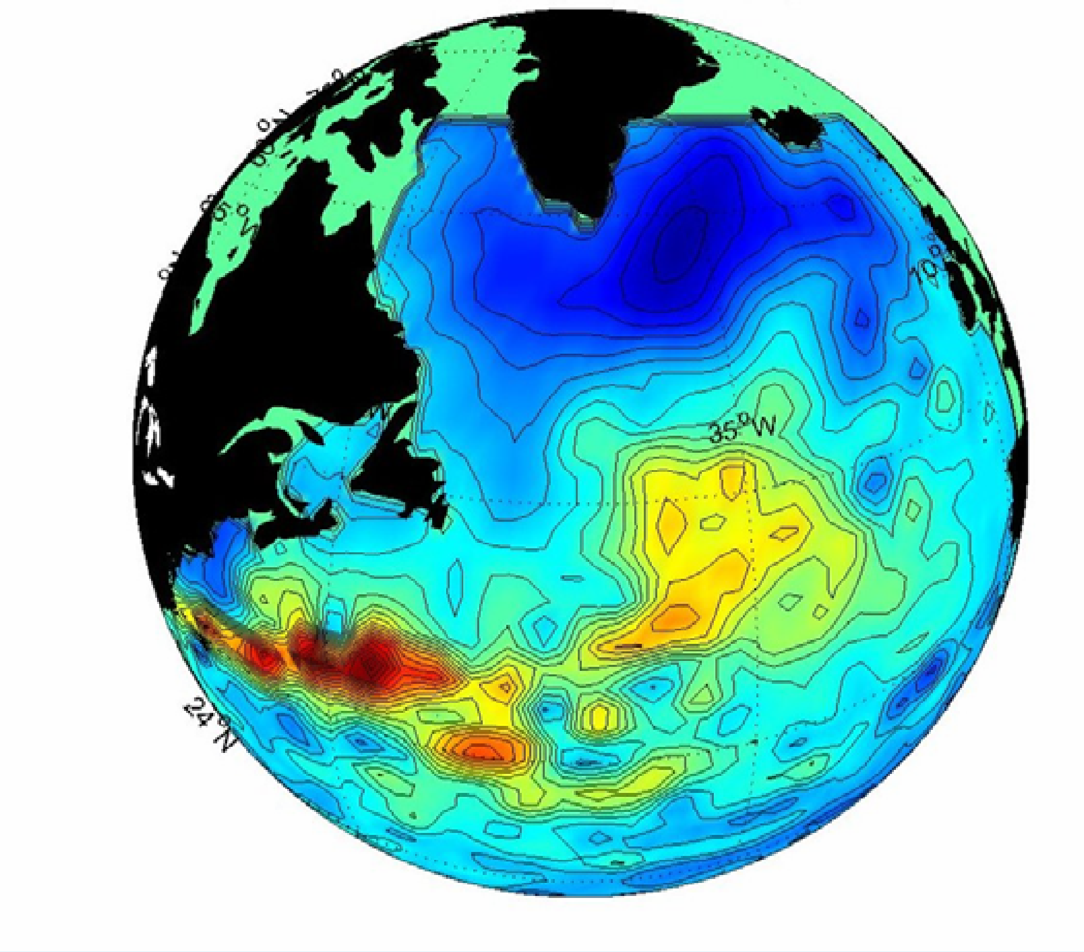

Tip jets and reverse tip jets:

Doyle & Shapiro Tellus 1999, Moore & Renfrew J Clim 2005, Pickart et al. Nature 2004

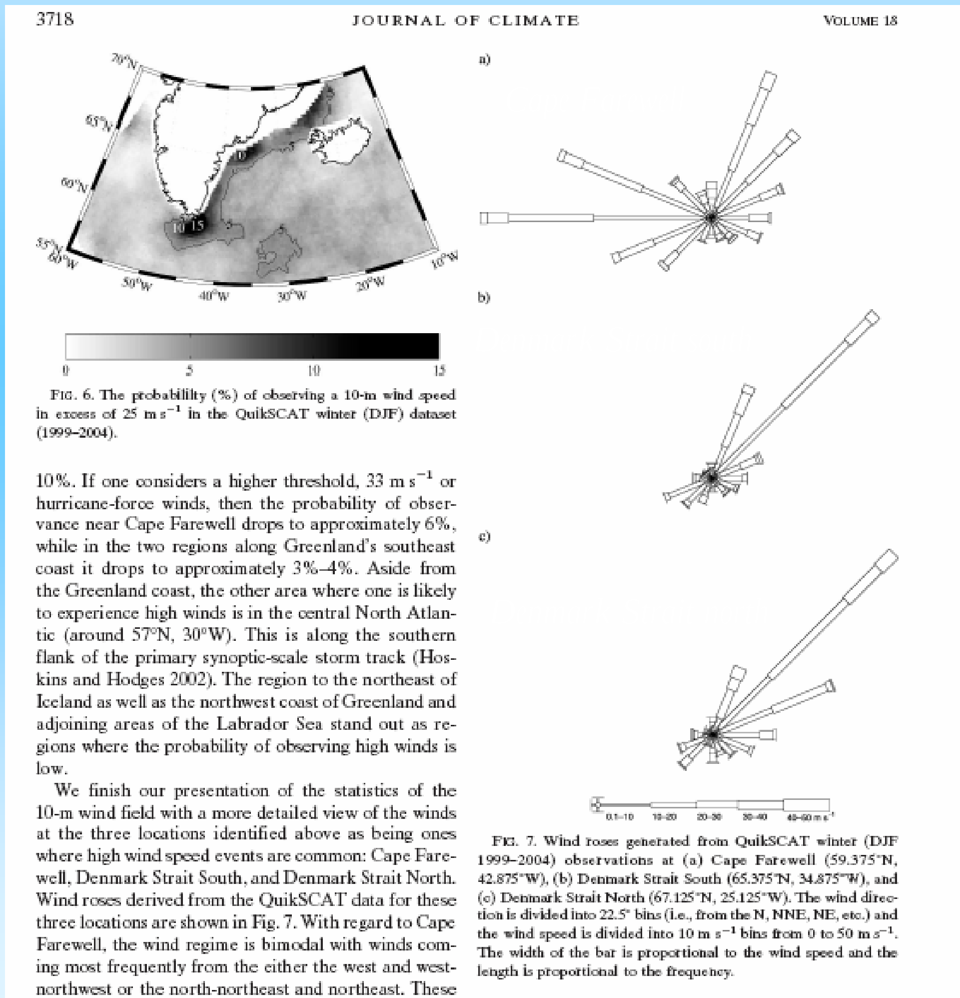

FIG. 6. The probability (%) of observing a 10-m wind speed in excess of 25 m s^{-1} in the QuikSCAT winter (DJF) dataset (1999–2004).

10%. If one considers a higher threshold, 33 m s^{-1} or hurricane-force winds, then the probability of observance near Cape Farewell drops to approximately 6%, while in the two regions along Greenland's southeast coast it drops to approximately 3%–4%. Aside from the Greenland coast, the other area where one is likely to experience high winds is in the central North Atlantic (around 57°N, 30°W). This is along the southern flank of the primary synoptic-scale storm track (Hoskins and Hodges 2002). The region to the northeast of Iceland as well as the northwest coast of Greenland and adjoining areas of the Labrador Sea stand out as regions where the probability of observing high winds is low.

We finish our presentation of the statistics of the 10-m wind field with a more detailed view of the winds at the three locations identified above as being ones where high wind speed events are common: Cape Farewell, Denmark Strait South, and Denmark Strait North. Wind roses derived from the QuikSCAT data for these three locations are shown in Fig. 7. With regard to Cape Farewell, the wind regime is bimodal with winds coming most frequently from the either the west and west-northwest or the north-northeast and northeast. These

FIG. 7. Wind roses generated from QuikSCAT winter (DJF 1999–2004) observations at (a) Cape Farewell (59.375°N, 42.875°W), (b) Denmark Strait South (65.375°N, 34.875°W), and (c) Denmark Strait North (67.125°N, 25.125°W). The wind direction is divided into 22.5° bins (i.e., from the N, NNE, NE, etc.) and the wind speed is divided into 10 m s^{-1} bins from 0 to 50 m s^{-1}. The width of the bar is proportional to the wind speed and the length is proportional to the frequency.

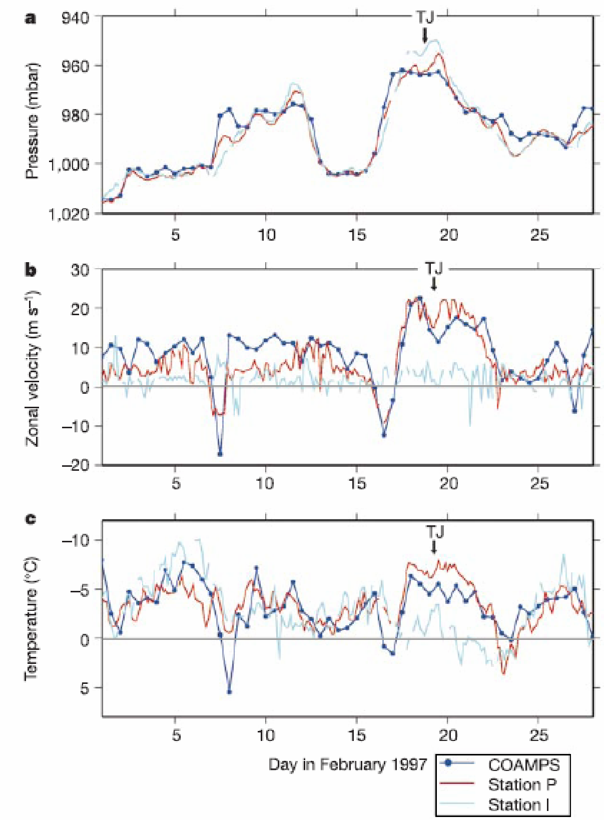

Figure 2 A tip-jet event recorded by Greenlandic meteorological land stations. The COAMPS model output (averaged over the region 59–60° N, 37–42° W) is compared with the observed meteorological time series (see key) for February 1997. The land station data are recorded every 3 hours (gaps indicate missing data); see Fig. 1 for the locations of the meteorological stations. The tip-jet event is denoted by TJ. **a**, Sea-level pressure. **b**, Zonal 10-m wind (positive is westerly). The COAMPS and station P winds are significantly correlated ($r = 0.72$); neither of them is correlated with the station I wind record. **c**, 2-m air temperature. The two meteorological station temperature records have been offset by 4° (warmer) for plotting purposes.

Forecast effect of high-pressure drag events is short-lived, particularly in Europe; skill of forecasting drag is high

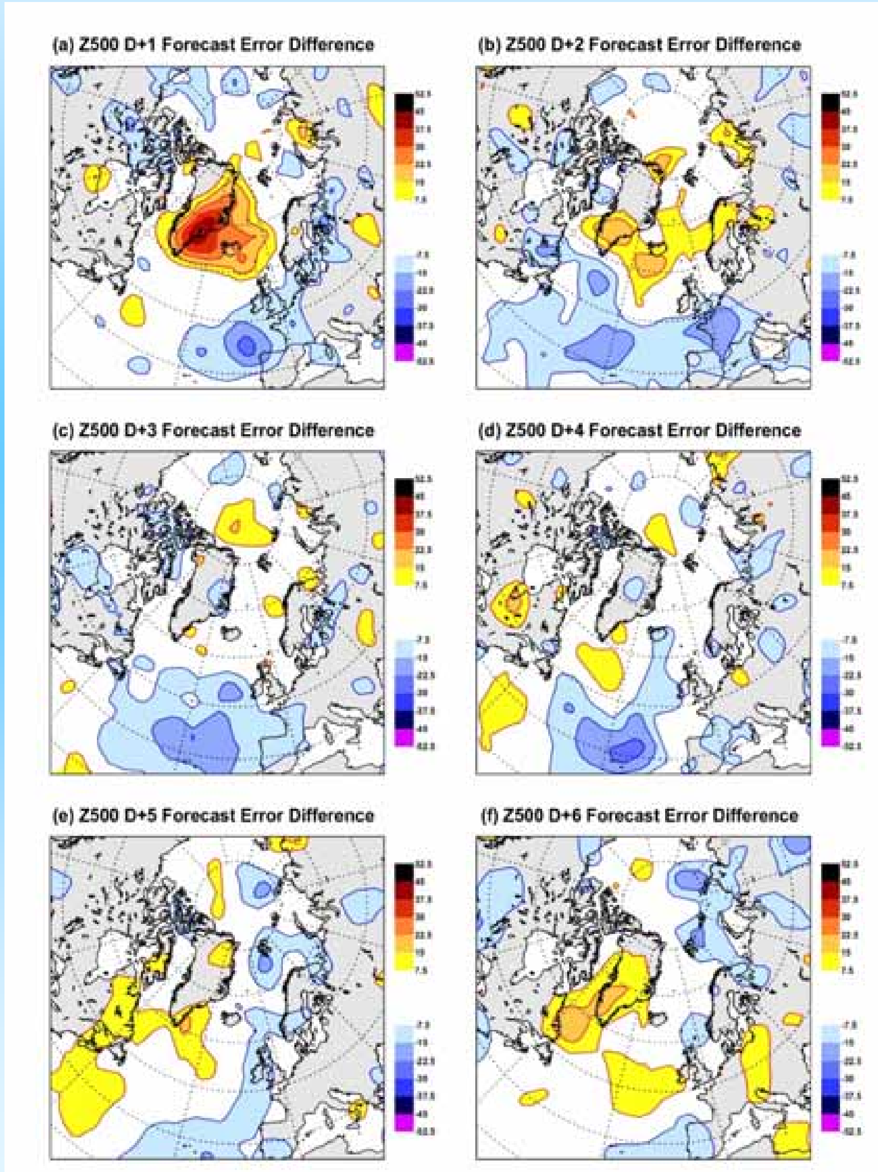

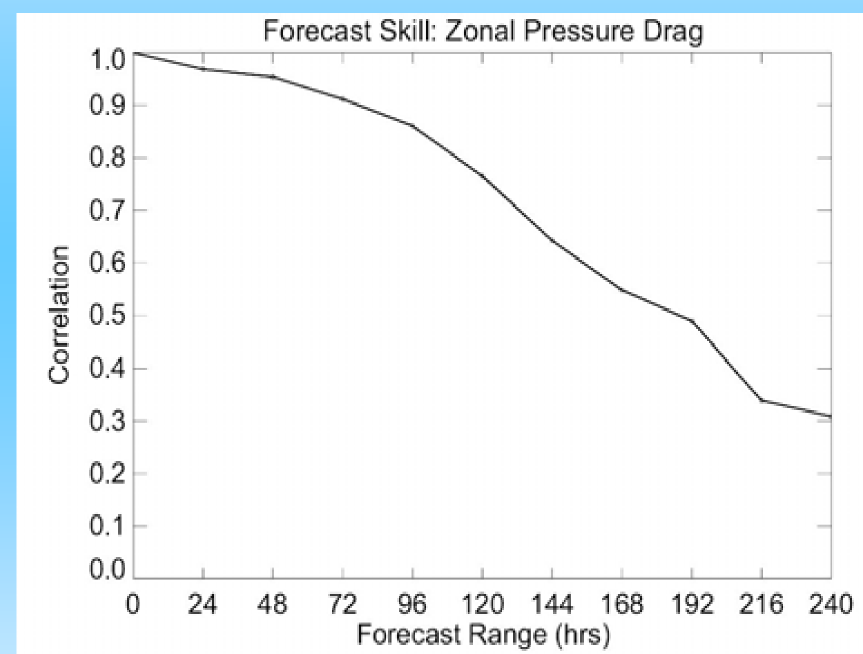

EP-flux: hemispheric impact; anomalous SPV acceleration (barotropization rather than simple mountain drag

note factor of 10 zoom for anomaly vectors

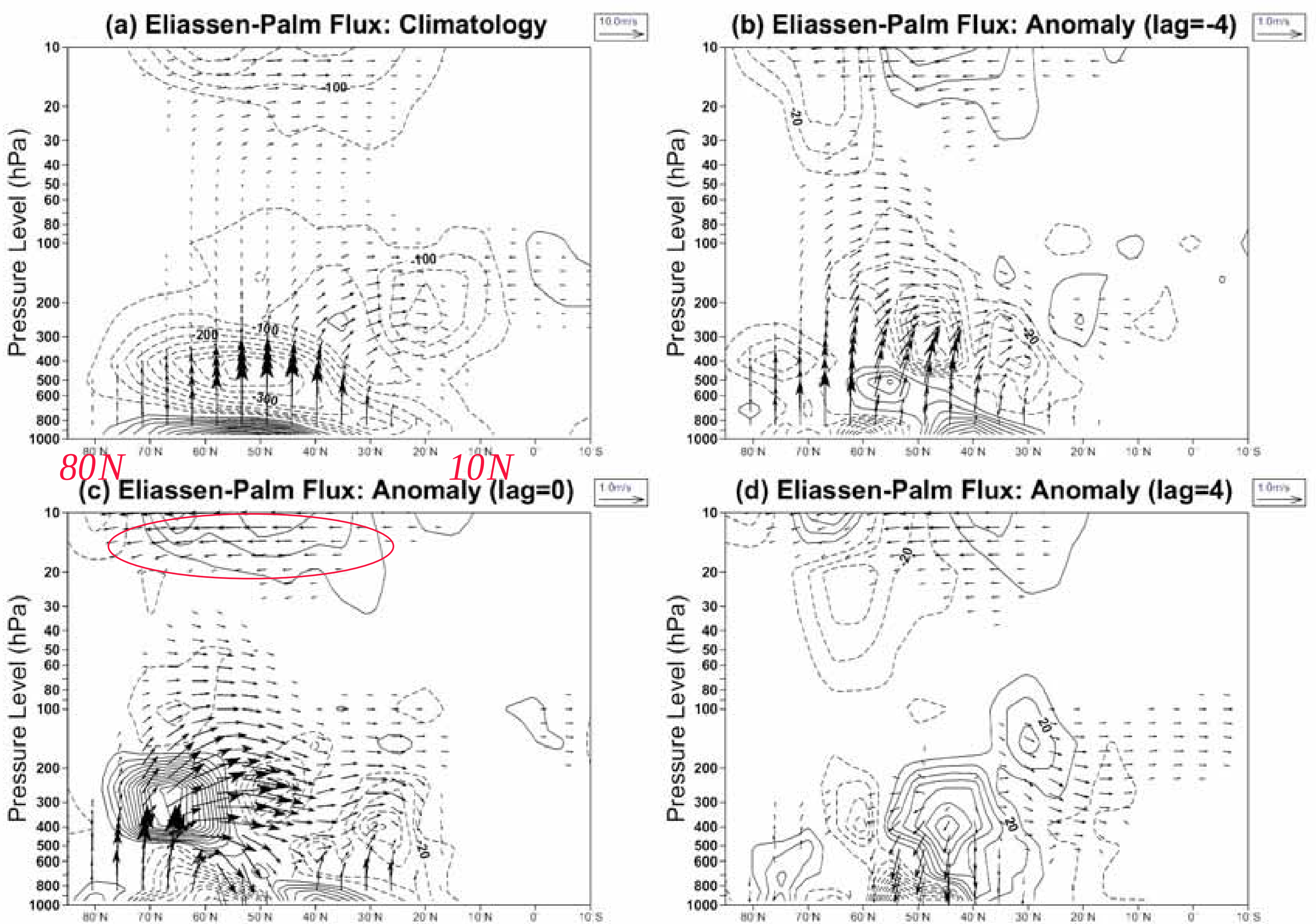

Egger *JAS 2006* finds that zonal momentum tendency can be opposite to expected push by pressure drag…due to imported meridional vorticity flux in transient eddies. Covariance fields wit[illegible]odel.

1474 JOURNAL OF THE ATMOSPHERIC SCIENCES VOL

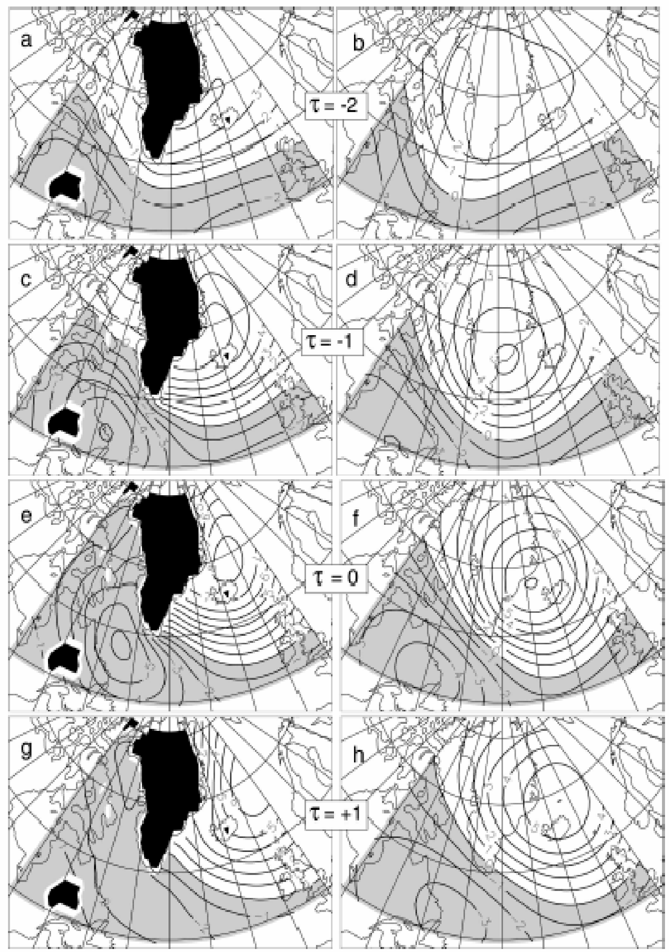

FIG. 6. Crosscovariance function $C(P, p|\tau)$ of the Greenland mountain torque at (left) $z = 500$ m and (right) $z = 5500$ m with the pressure field normalized by the standard deviation σ_P of P so that the resulting fields can be interpreted in hPa.

Gravity waves

Doyle & Shapiro Tellus 1999

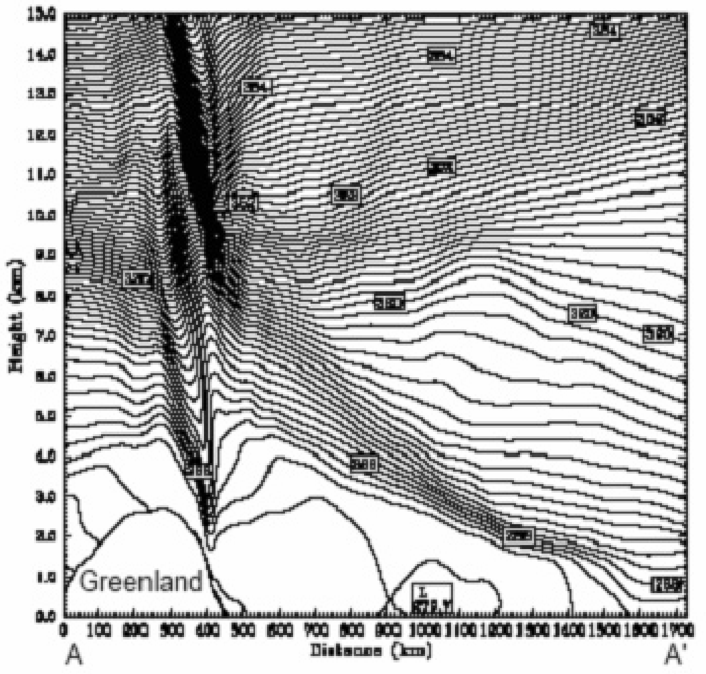

Fig. 6. Cross section of potential temperature (K) at 0000 UTC 10 November 2001, along the line AA' of Fig. 3.

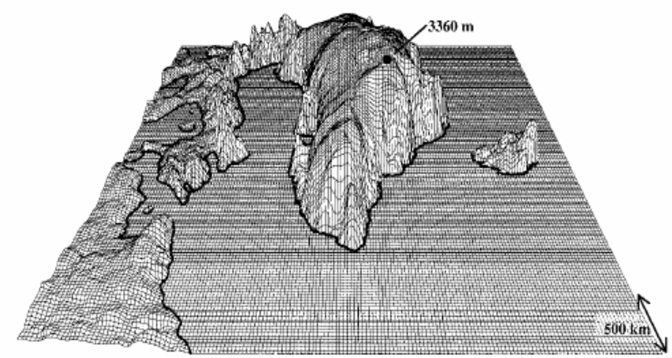

Three-dimensional depiction of the Greenland relief.

ECMWF model runs: high-pressure drag events develop downslope winds and upward propagating gravity waves reaching the stratosphere at T511, T799….resolutions higher than that used in ‘no-Greenland/Greenland’ model studies

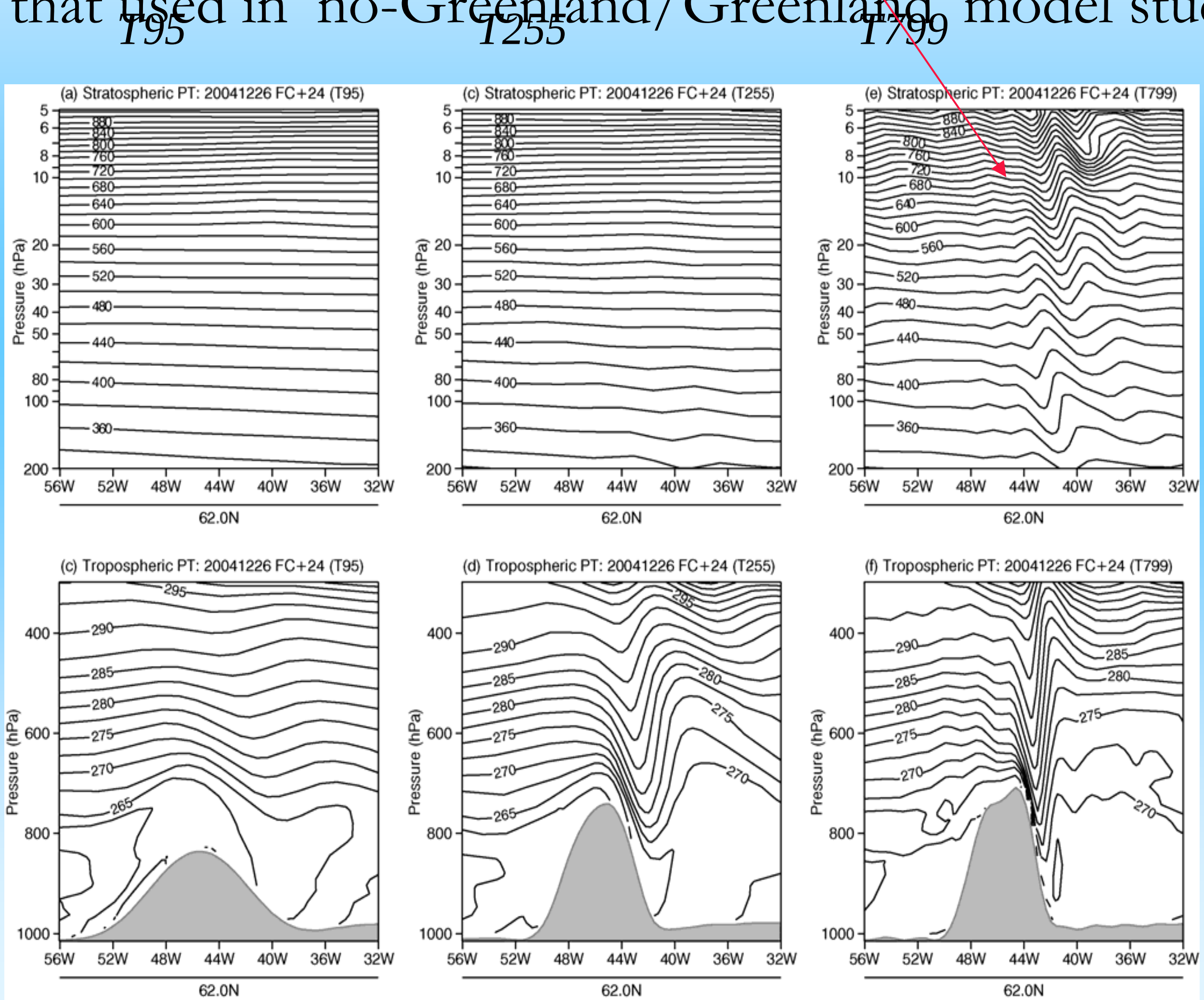

Downslope winds increase wavedrag (by Bernoulli) here in a layer of CO2

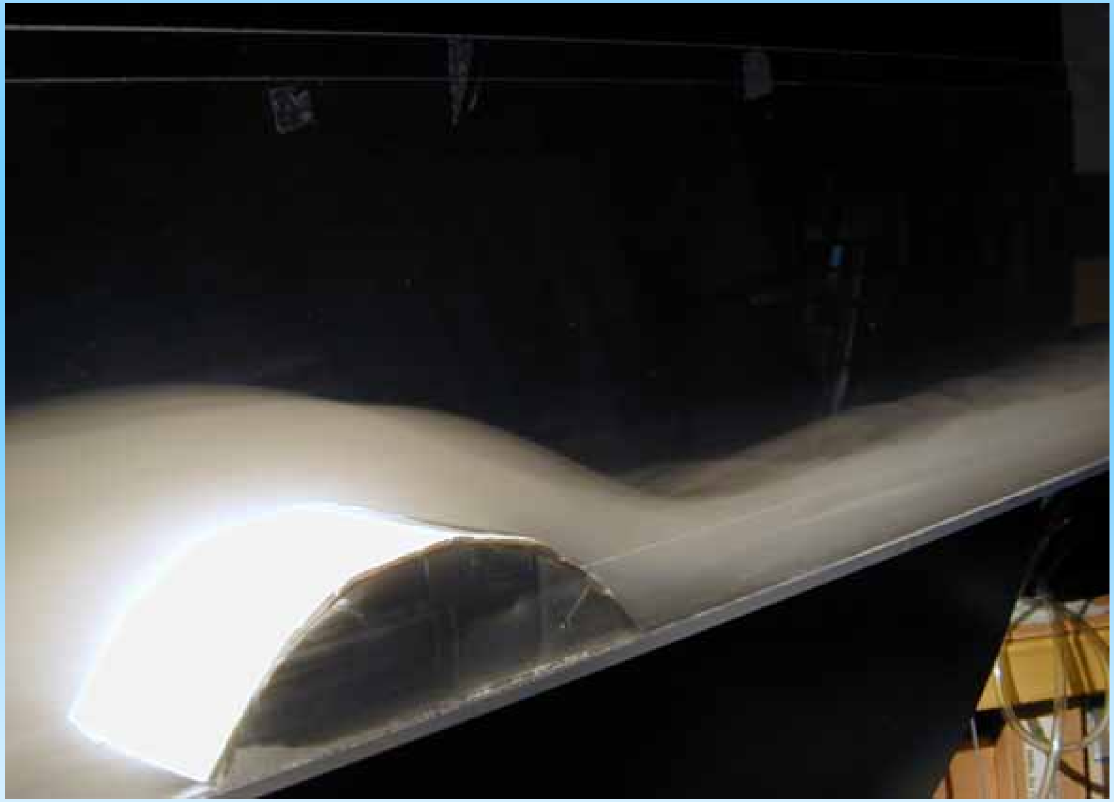

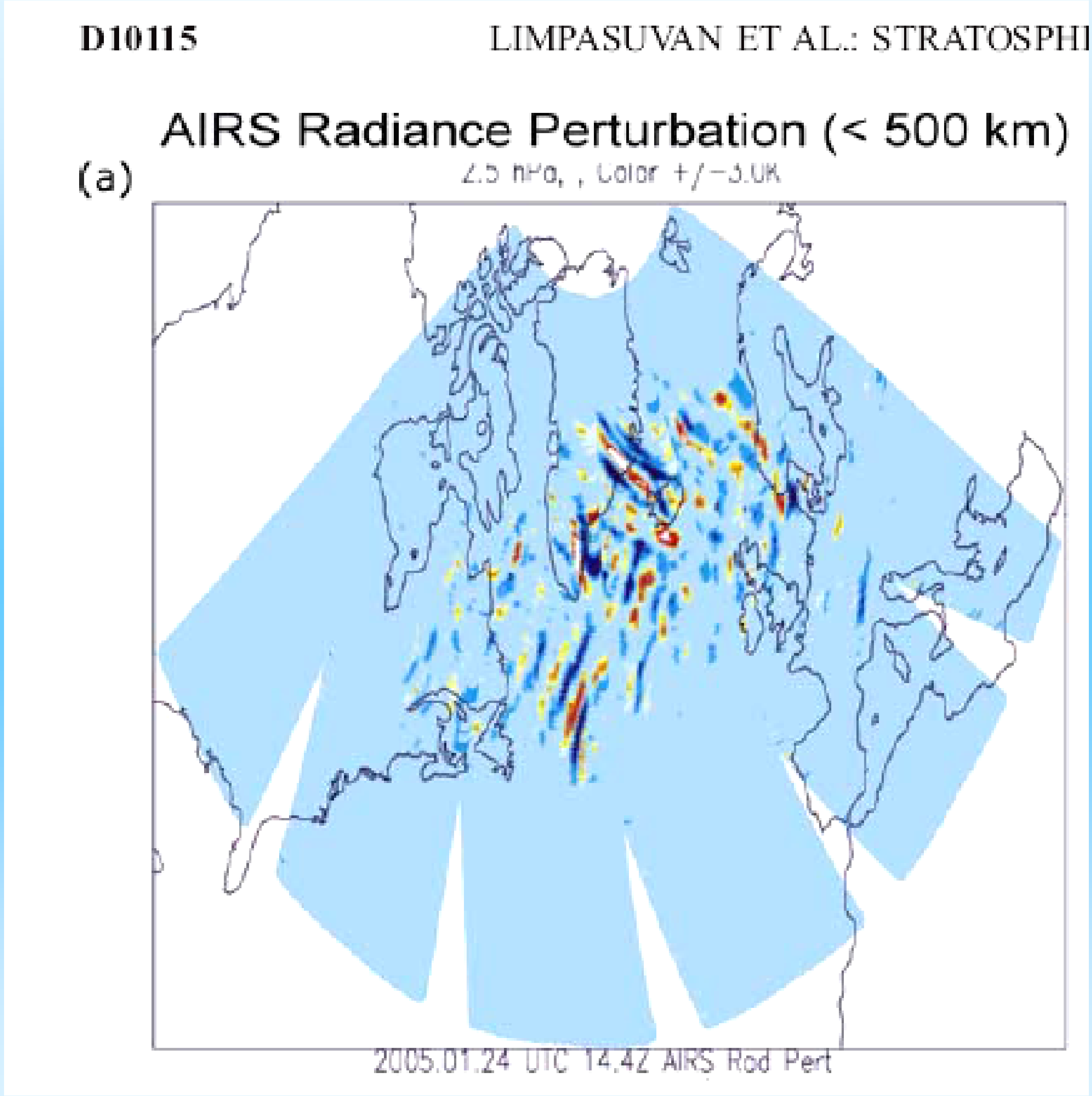

Limpusaven et al. JGR 2007

gravity waves decelerating SPV: at rates 10-120 m $sec^{-1} day^{-1}$

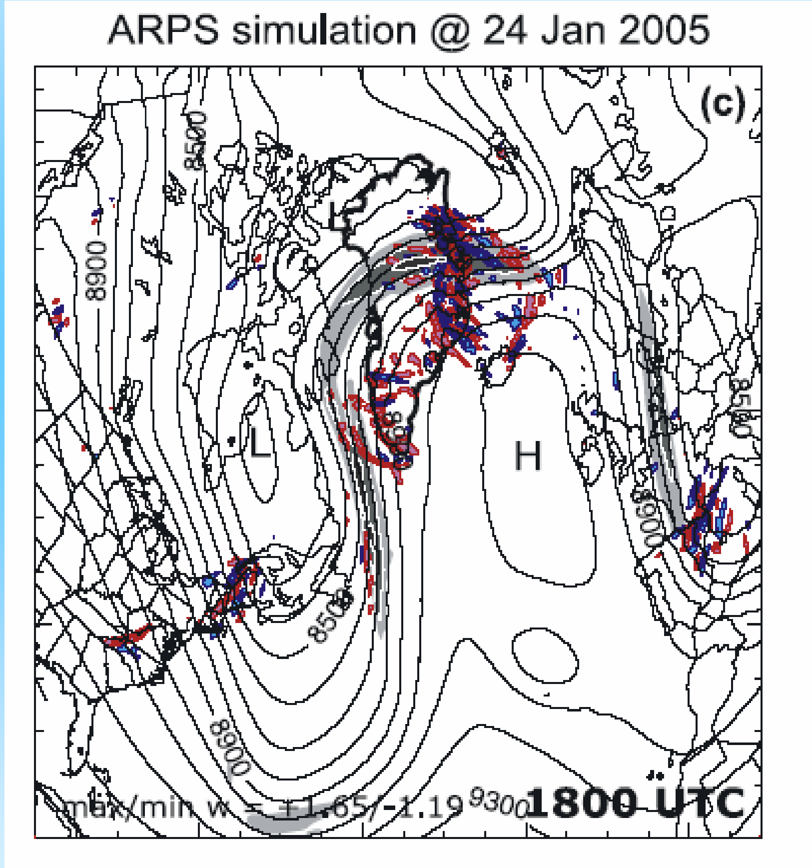

300 hPa dyn height *Limpusavan et al JGR 2007*

24 Jan 2005..an 'abnormal' pressure drag event (would lead to westerly accel of atmos)

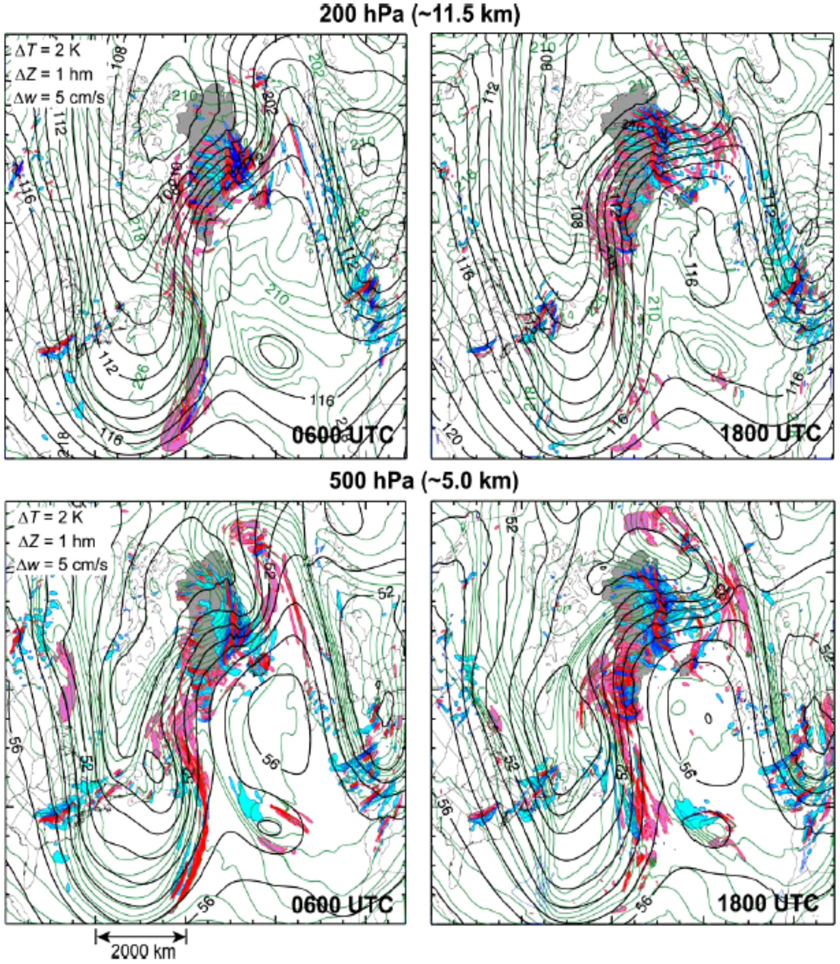

Figure 4. (Top row) ARPS simulations at 0600 UTC and 1800 UTC of 24 January 2005 and at 200 hPa. The height field (Z, in hectometer) and temperature field (T, in Kelvin) are given as black and green contours, respectively. The vertical wind (w) is given as filled color contours; upward (downward) motion is shown in red (blue). Contour intervals are indicated. (Bottom row) As above except at 500 hPa. Greenland and Iceland are shaded in gray.

Limpusavan et al. JGR 2007

Mel Shapiro's Greenland flights

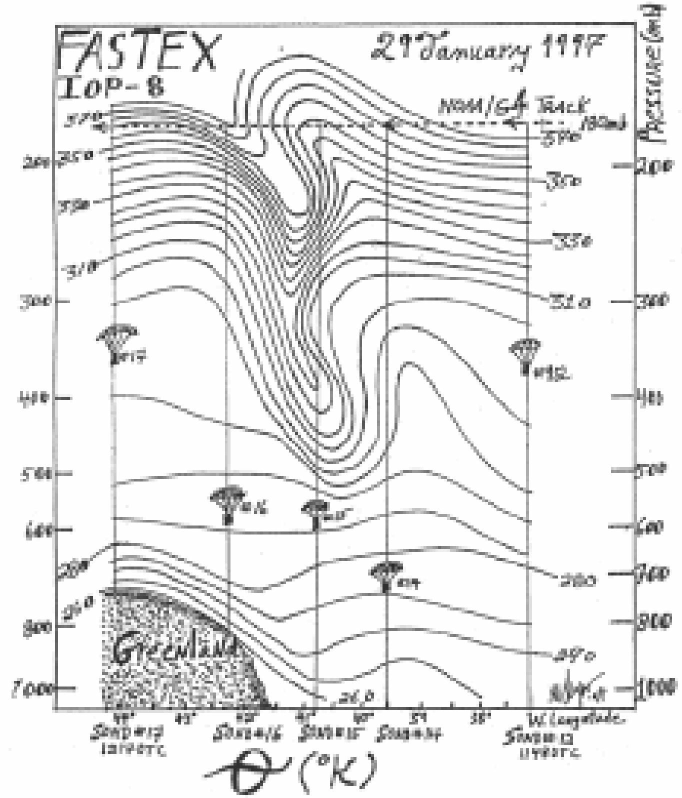

Fig. 5. Cross section of potential temperature (K) at ~1200 UTC 29 January 1997 derived from dropsondes (numbered 12-17) from the NOAA/G-4 aircraft.

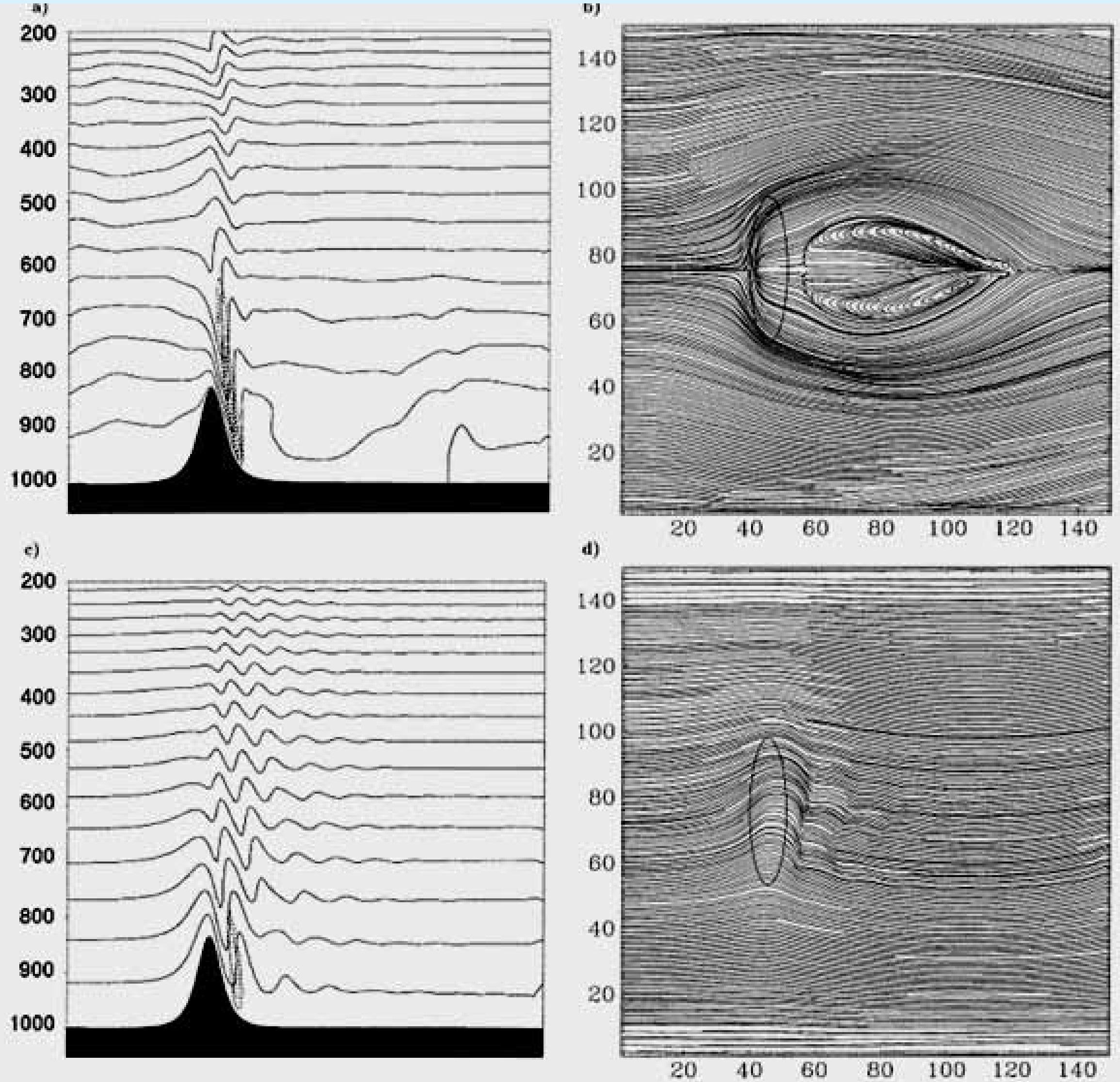

FIG. 1. Comparison of simulations excluding and including the Coriolis force. (a) A cross section of a flow with $\hat{h} = 1.5$ and Ro = ∞, taken at the axis of symmetry at $t^* = 34.56$ showing potential temperature (K, solid) and turbulent kinetic energy (J kg^{-1}, dashed). The isentrope contour interval is 2 K and the TKE contour interval 1 J kg^{-1}. (b) Streamlines at the surface at the same time. The topography is shown at 0.35h. (c), (d) As in (a), (b) but with Ro = 0.42.

Ro = ∞
Nh/U = 1.5

Ro = 0.42
Nh/U = 1.5

Petersen, Olaffson, Kristjannson JAS2003

Schär (*JAS 93)*: PV is transported along the intersections of the Bernoulli-function and isentropic surfaces in a statistically steady flow….

$$PV\ flux: \vec{J} = \nabla\theta \times \nabla B$$

$$B = enthalpy + \tfrac{1}{2}|\vec{u}|^2 + \Phi$$

$$\approx c_p T + \tfrac{1}{2}|\vec{u}|^2 + gz$$

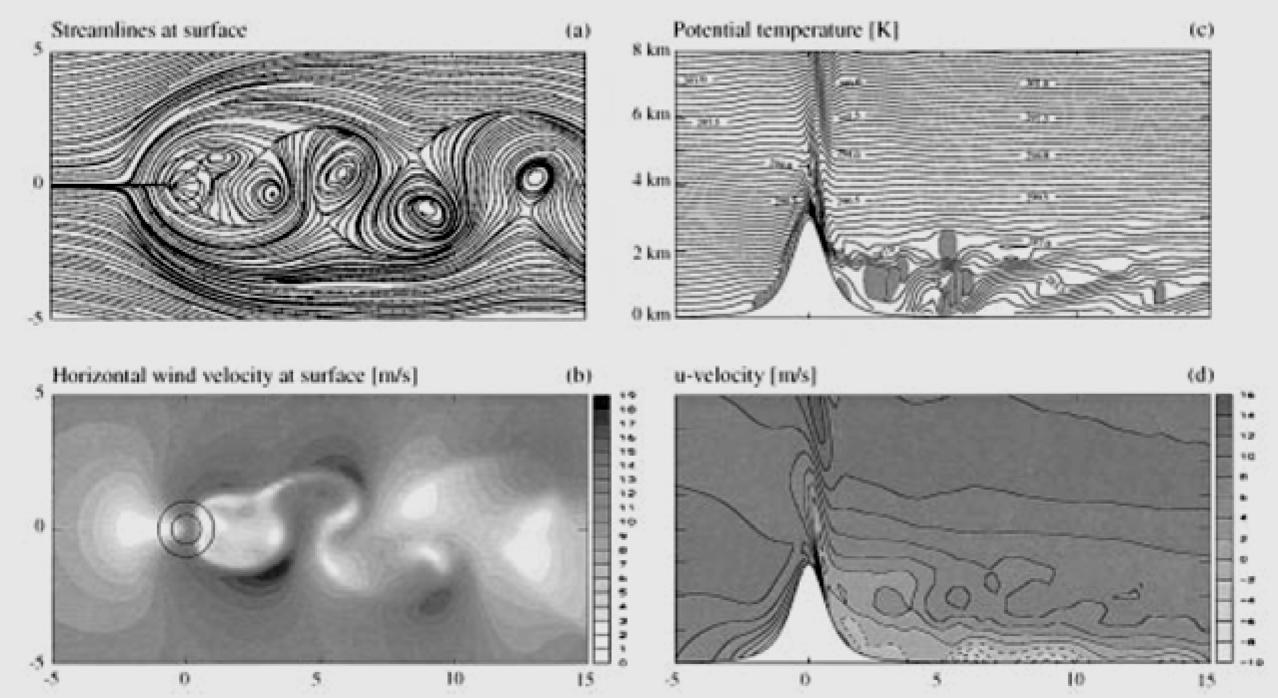

Schär & Durran JAS 97

also: tip horiz vorticity to make vertical vorticity *Rottuno et al. JAS 99*

Ertel potential voticity generation by breaking lee gravity wavesL the PV generation as well as the gravity-wave momentum flux alter the geostrophic circulation

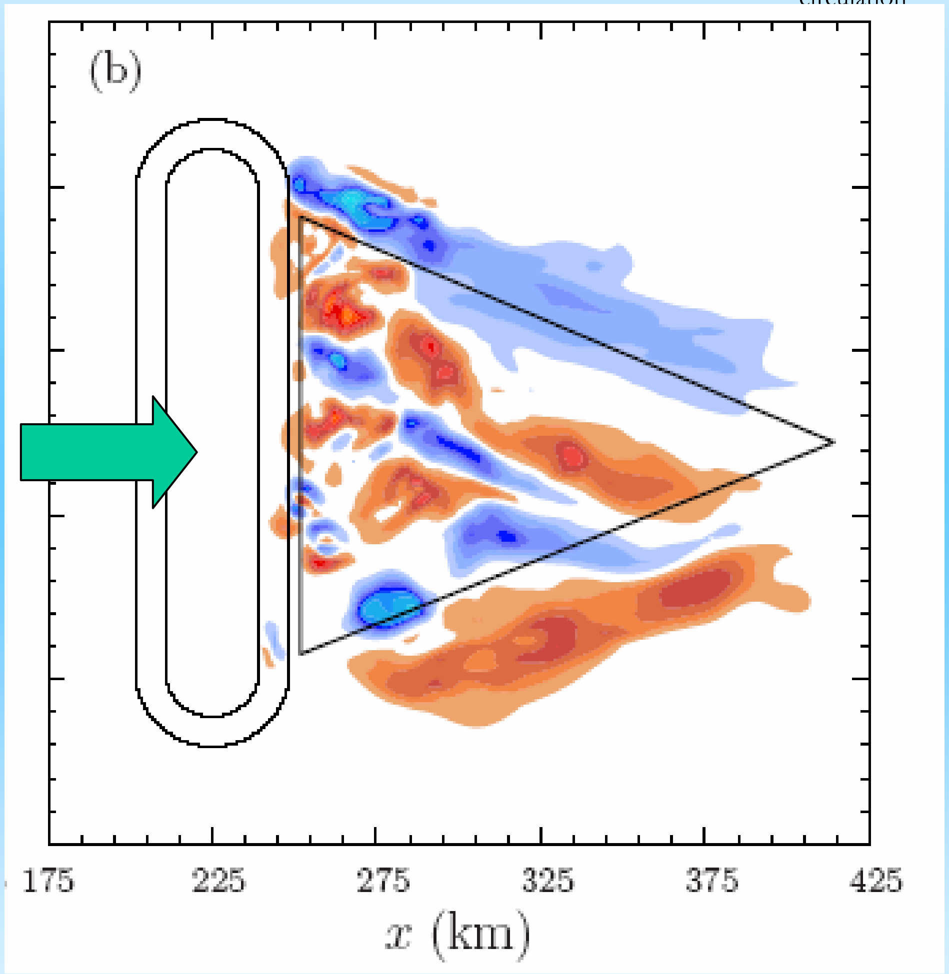

$$\frac{\partial q}{\partial t} + \nabla \cdot \mathbf{J} = 0,$$

$$\mathbf{J} = \nabla\theta \times \nabla B,$$

Chen, Hakim & Durran, JAS 2007 subm

PV and zonal flow generation in flow over a 1.5 km high mountain

(dipole of PV, decelerated wake)

Chen, Hakim & Durran, JAS 2007 in press

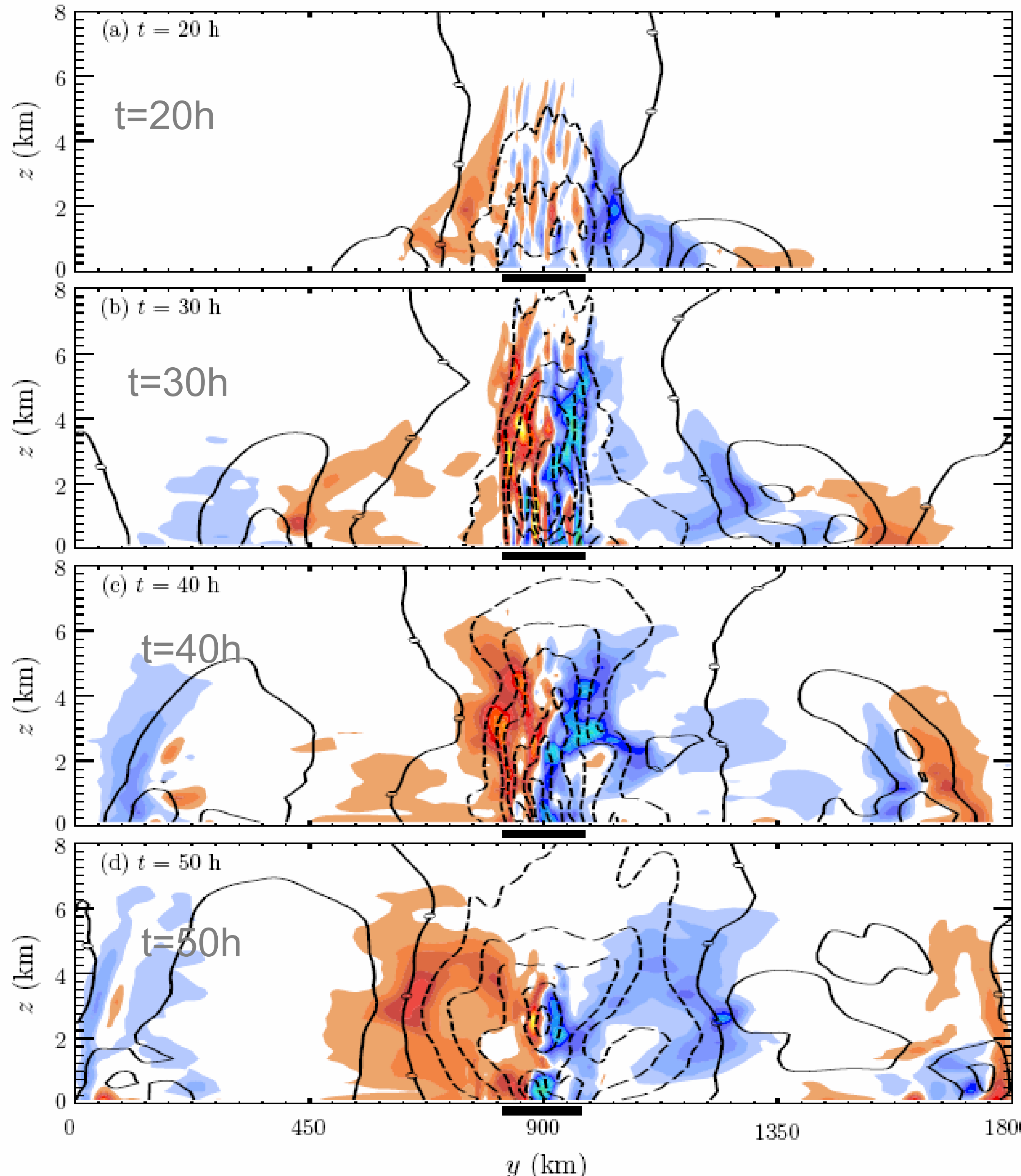

Overturning circulations

-

Some 'burning' questions for which we thought we knew the answers:

(i) What drives the global meridional overturning circulation (MOC) of the oceans --- buoyancy or mechanical mixing induced by winds and tides?

(ii) Is high-latitude sinking and the deep, cold branch of the MOC a dominant member of the meridional heat and fresh-water transport?

(iii) Does the ocean circulation substantially warm western Europe?

More generally, does heat transport by oceanic general circulation affect atmospheric climate?

(iv) What are the paths of upwelling of deep waters in the global oceanic MOC?

(v) Where are the crucial sites for convection and water-mass transformation ?

(vi) What is the quantitative rate of water-mass production for the several components of the North Atlantic DeepWater (for example, Labrador Sea Water), and how are they altered before being 'delivered' to the global MOC?

(vii) How do convection and mixing drive diffusive overturning at many scales, reaching to the distant circulation.

Oceanic overturning circulations: coexisting with ‘horizontal gyres of wind-forced circulation

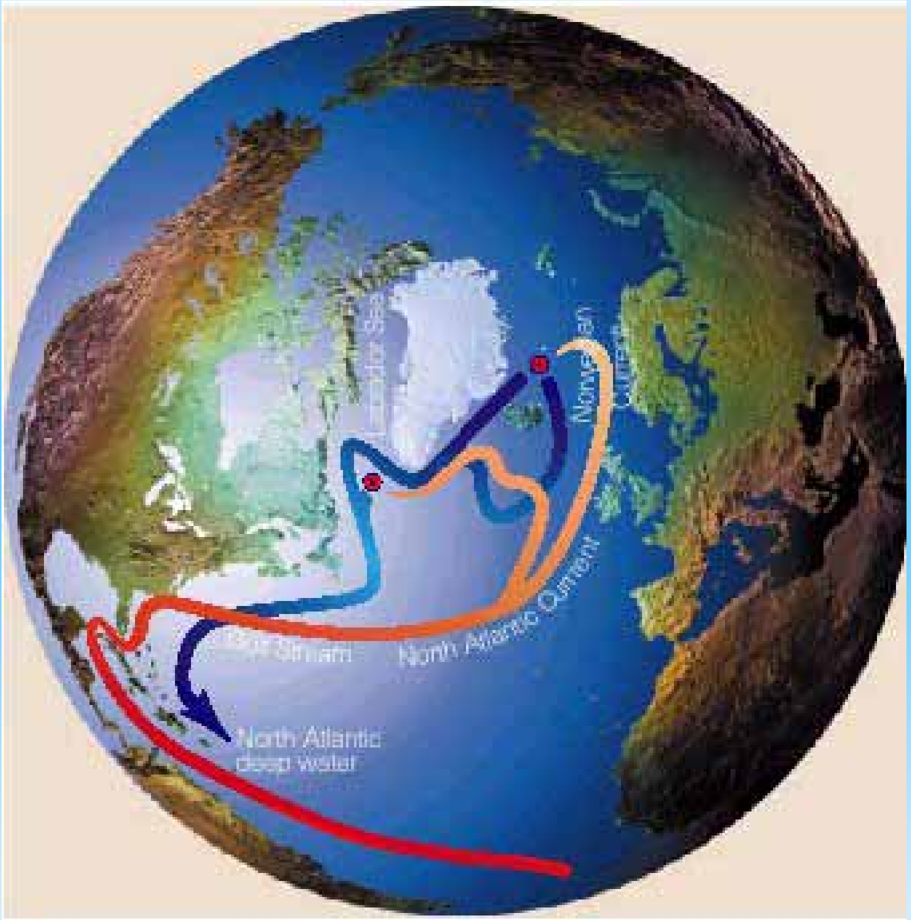

- MOCs have an easier time in the oceans than in the atmosphere:

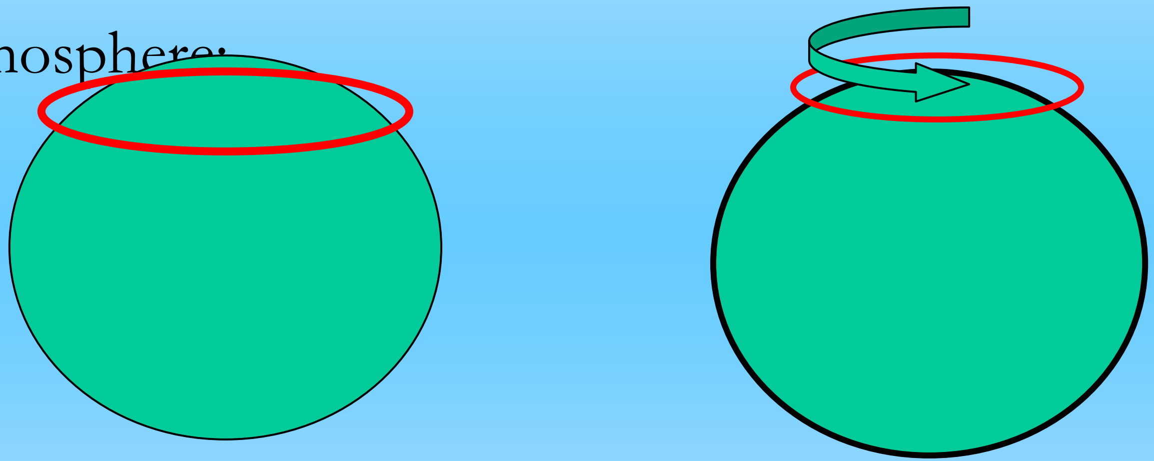

a ring of air moved 1000 km north gains westerly velocity of 100 m sec^{-1} There is not enough energy available to utilize this mode: the Hadley cell is limited in north-south extent. Forces (eddy momentum flux from PV stirring) and non-symmetric circulation are required to support extensive meridional excursion.

channels and conduits for heat- and fresh-water transport

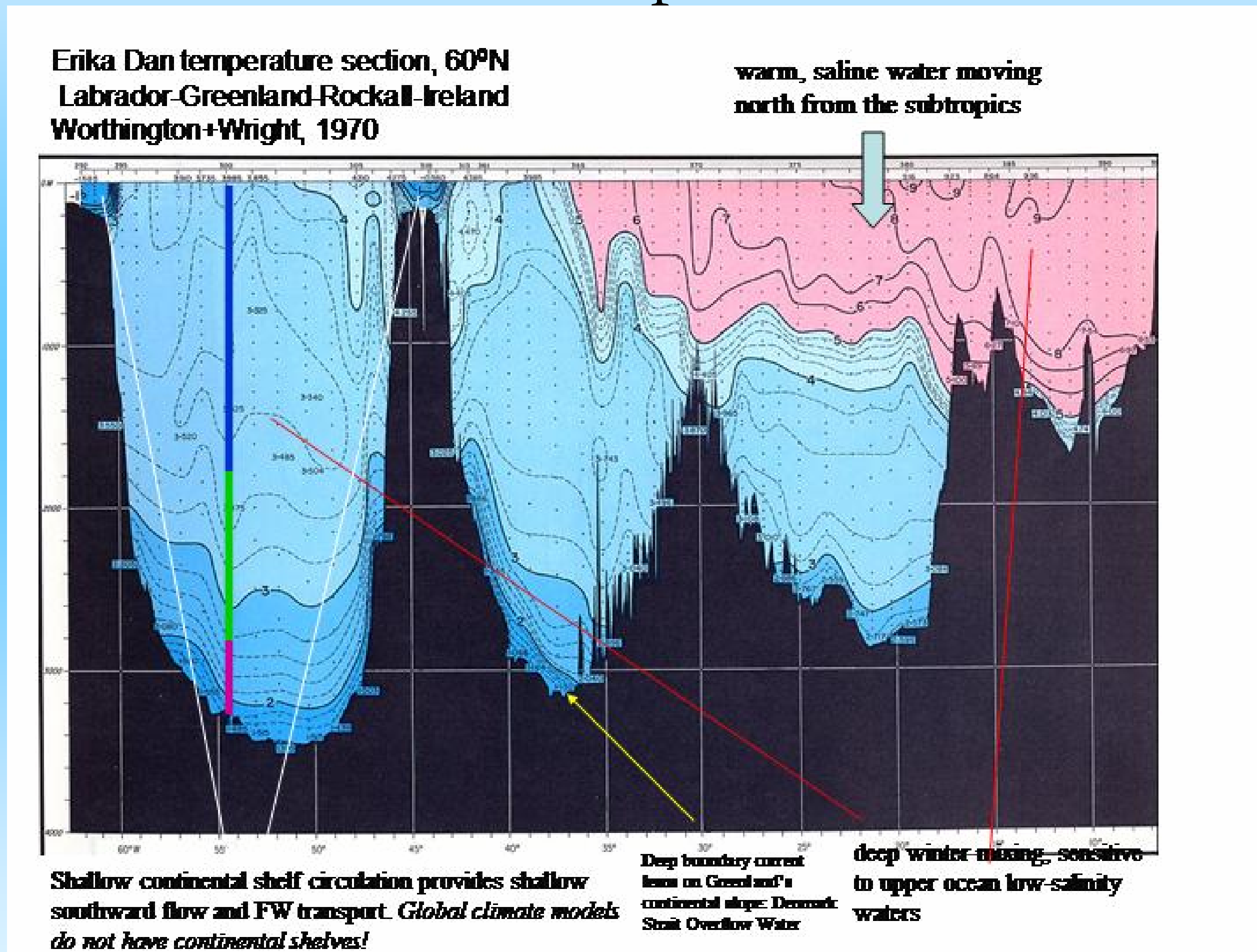

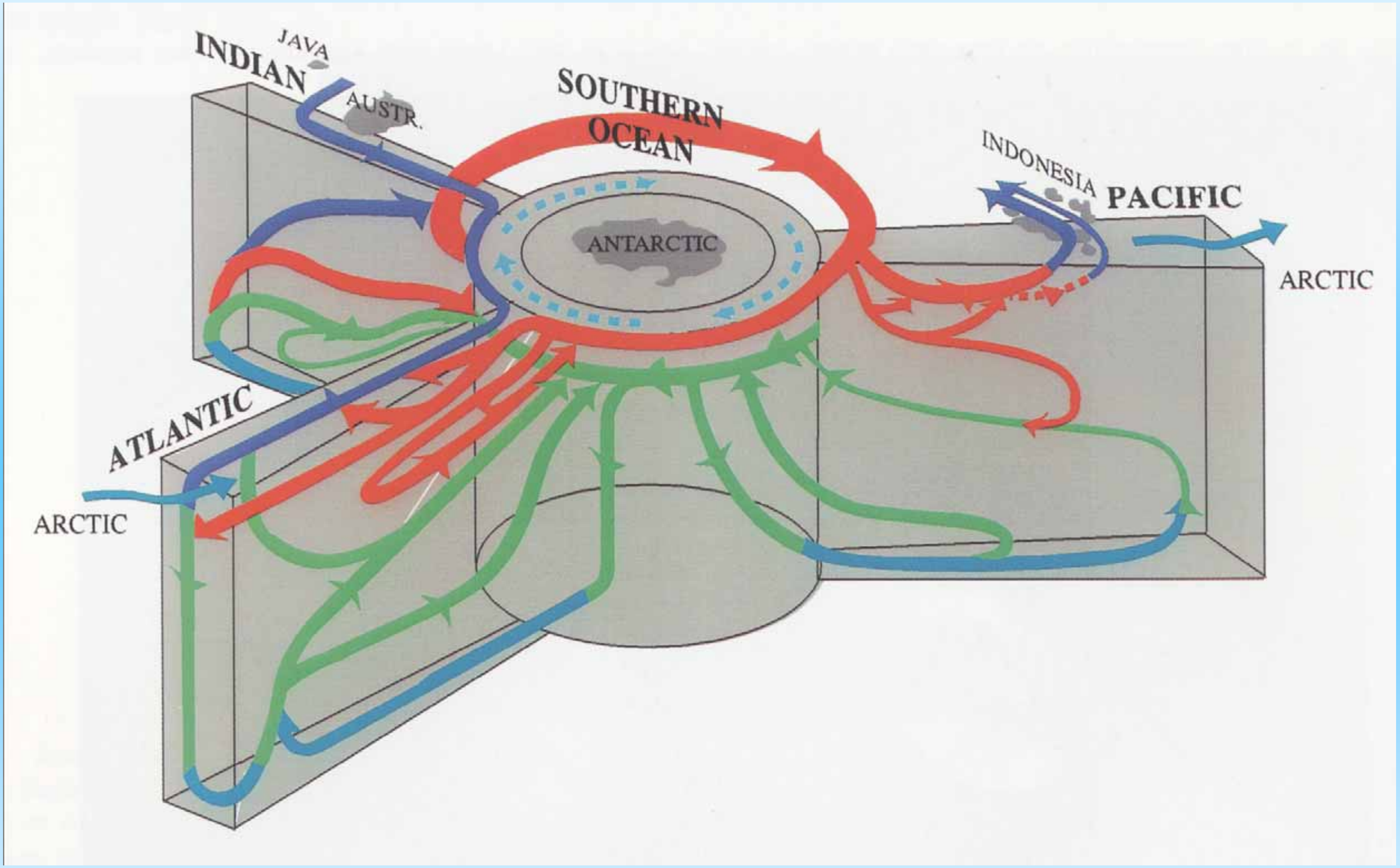
INDIAN
JAVA
AUSTR.
SOUTHERN OCEAN
INDONESIA
PACIFIC
ARCTIC
ANTARCTIC
ATLANTIC
ARCTIC

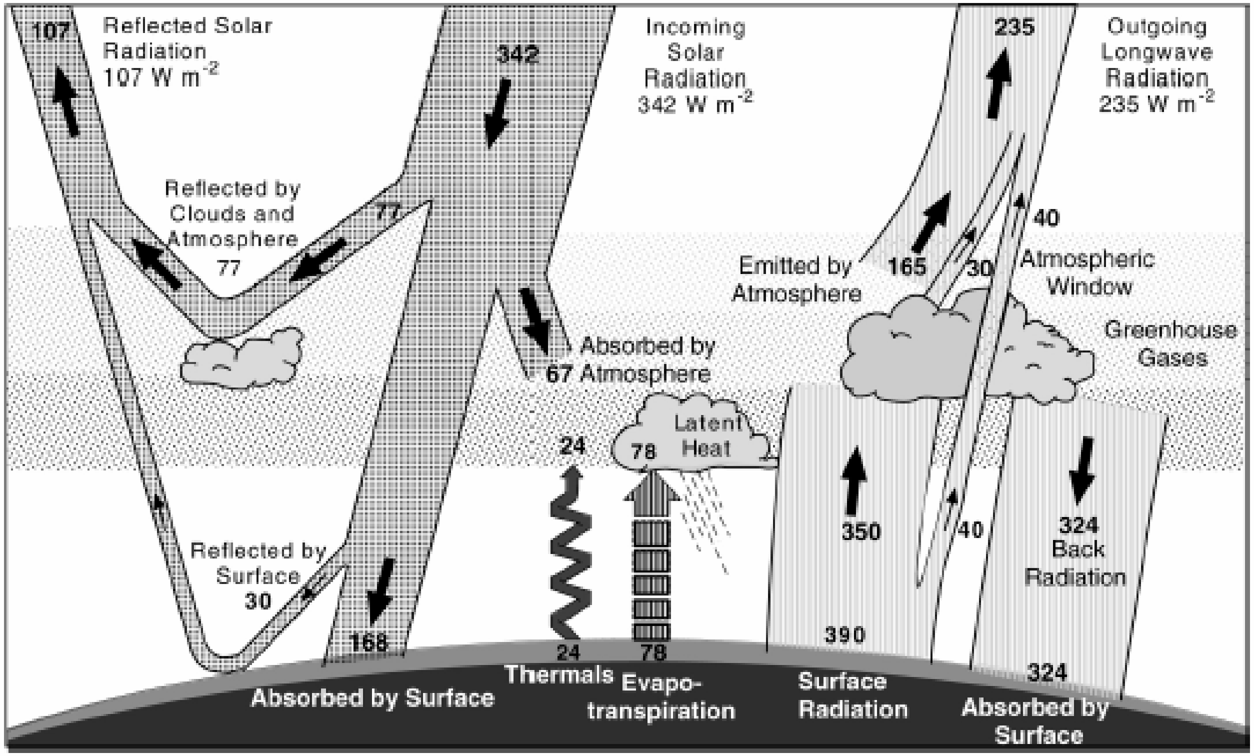

(31%)

Figure 1. The earth's radiation balance. The net incoming solar radiation of 342 W m^{-2} is partially reflected by clouds and the atmosphere or at the surface, but 49% is absorbed by the surface. Some of that heat is returned to the atmosphere as sensible heating and most as evapotranspiration that is realized as latent heat in precipitation. The rest is radiated as thermal infrared radiation and most of that is absorbed by the atmosphere and re-emitted both upwards and downwards, producing a greenhouse effect, as the radiation lost to space comes from cloud tops and parts of the atmosphere much colder than the surface. From Kiehl and Trenberth (1997).

consider the differences between tropics and Arctic…(a)at 60N latitude the sunshine incident per unit area is 50% of the full intensity with the sun overhead; (b) the albedo (whiteness) is greater

source: IPCC-01 / TRENBERTH

solar radiation (kilowatt-hours per square meter, per day)
varies with latitude and season (here neglecting the great effect of cloudiness)

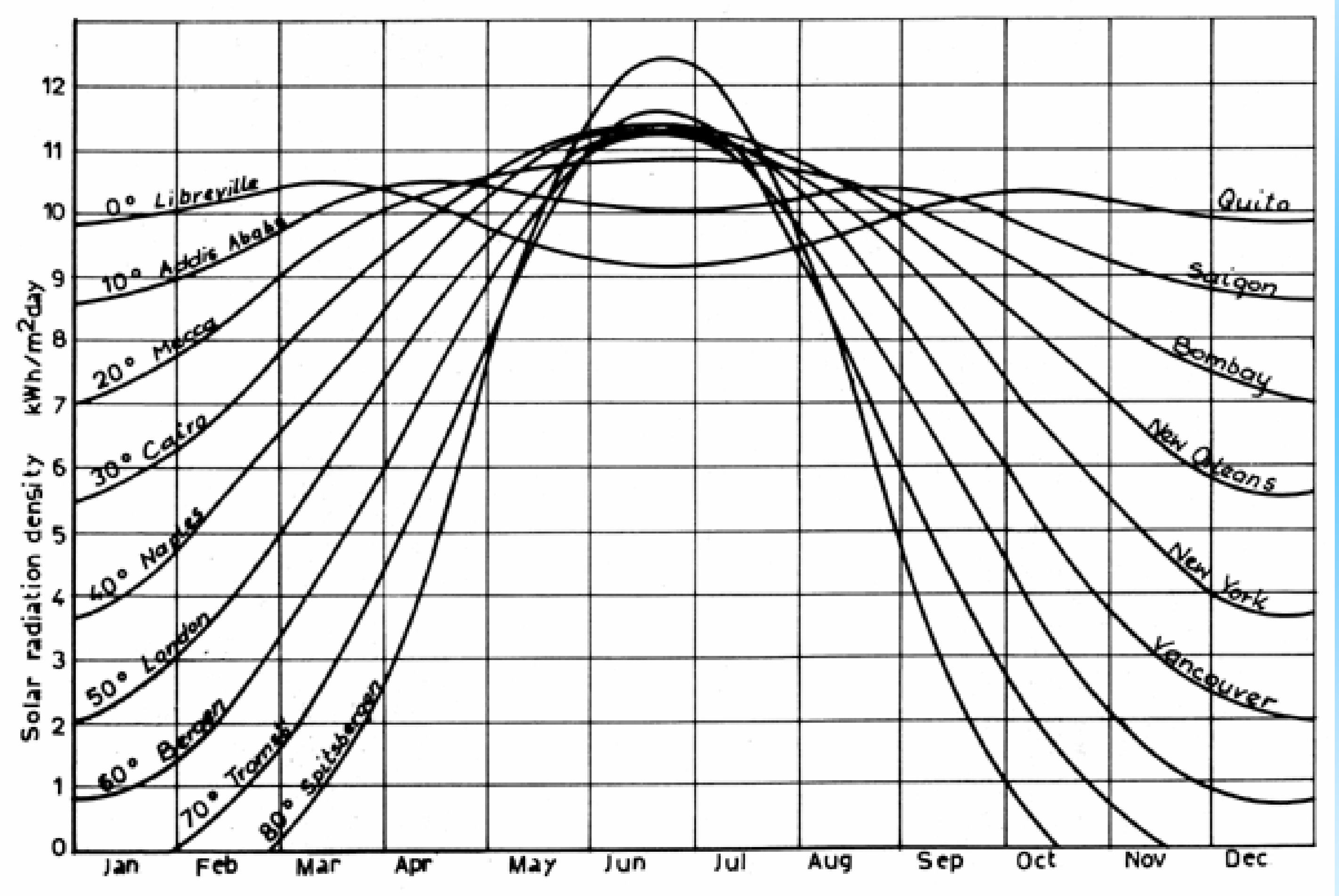

www.fao.org/DOCREP/003/X6541E/X6541E03.htm

Variation of Temperature With Latitude

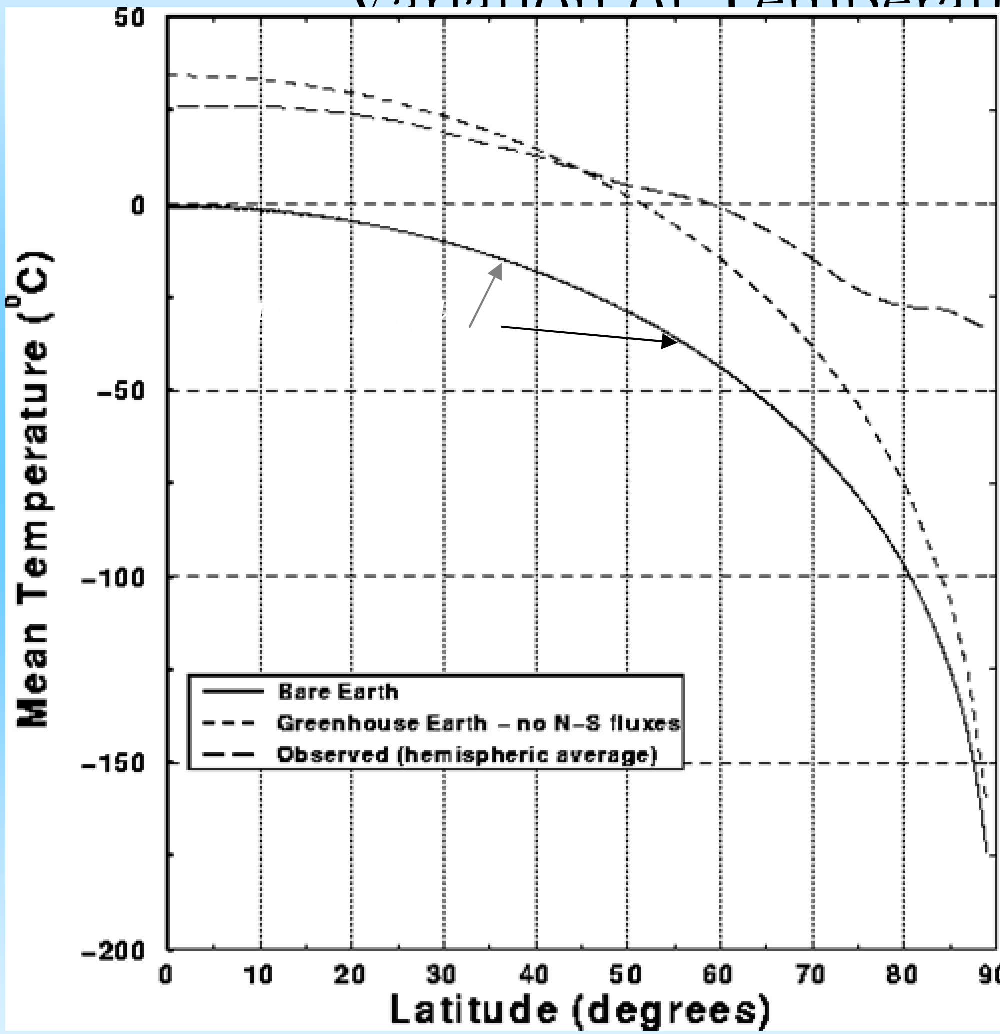

- A simple radiative calculation gives an Earth with the correct average T, but wrongly distributed meridionally (north-south)

slide from K.Carslaw, Univ. of Leeds

Figure 1.5. *Vertical profile of the temperature between the surface and 100 km altitude as as defined in the U.S. Standard Atmosphere (1976) and related atmosphere layers. Note that the tropopause level is represented for midlatitude conditions. Cumulonimbus clouds in the tropics extend to the tropical tropopause located near 18 km altitude.*

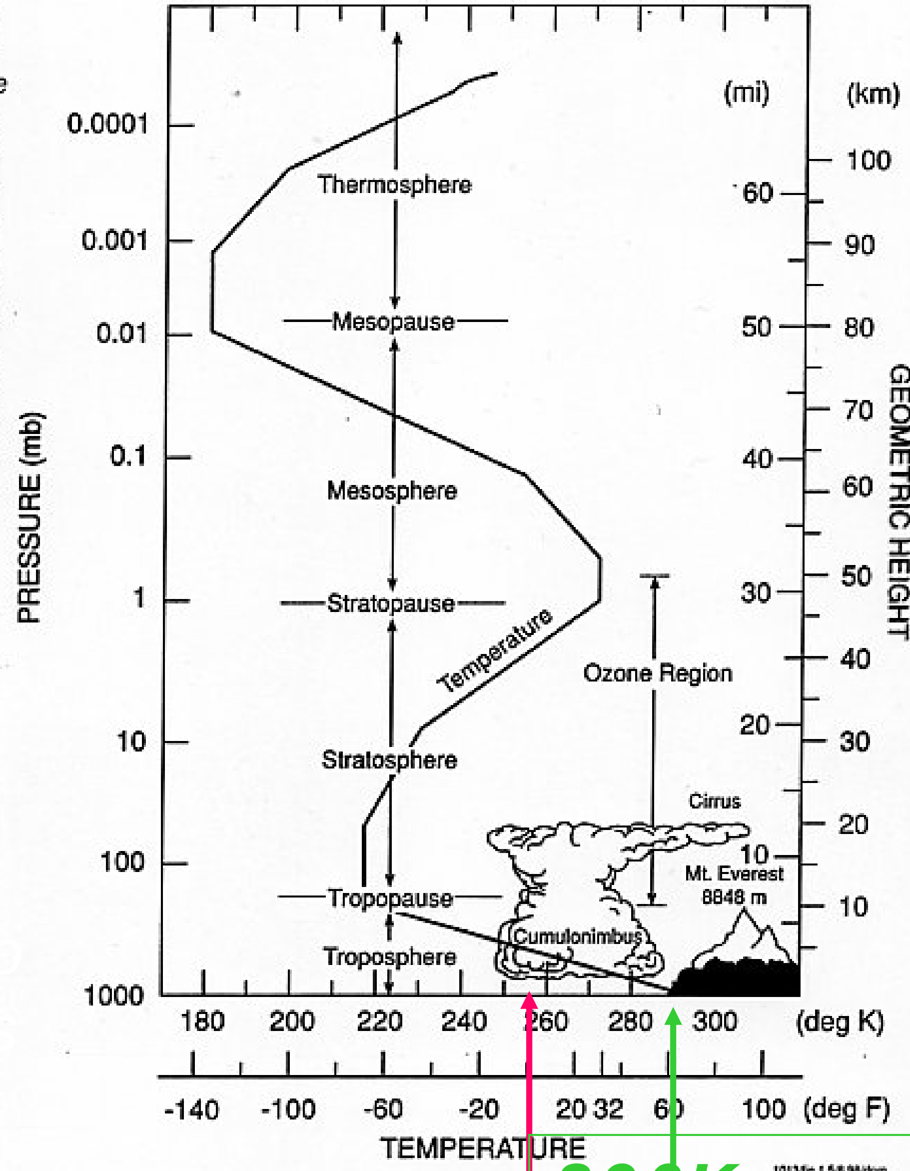

290K = average surfac

about 250K,

255K (-18^{0}C)..the simple radiation

Global meridional heat transport divides roughly equally into 3 modes:

1. atmosphere (dry static energy) $c_p T + \Phi$ (Bryden & Imawaki 2002) gz
2. ocean (sensible heat) $c_p \theta$
3. joint atmosphere/ocean mode: water vapor/latent heat transport Lq

The three modes of poleward transport are comparable in amplitude, and distinct in character (sensible heat flux divergence focused in tropics, latent heat flux divergence focus in the subtropics) (based on Keith (Tellus 1995) climatology, similar to more modern: Trenberth *et al.* J.Clim 2003)

HEAT- AND MOISTURE FLUX STRONGLY COUPLED

(residual method, TOA radiation 1985-89 and ECMWF/NMC atmos obs: redundant obs (air-sea flux)

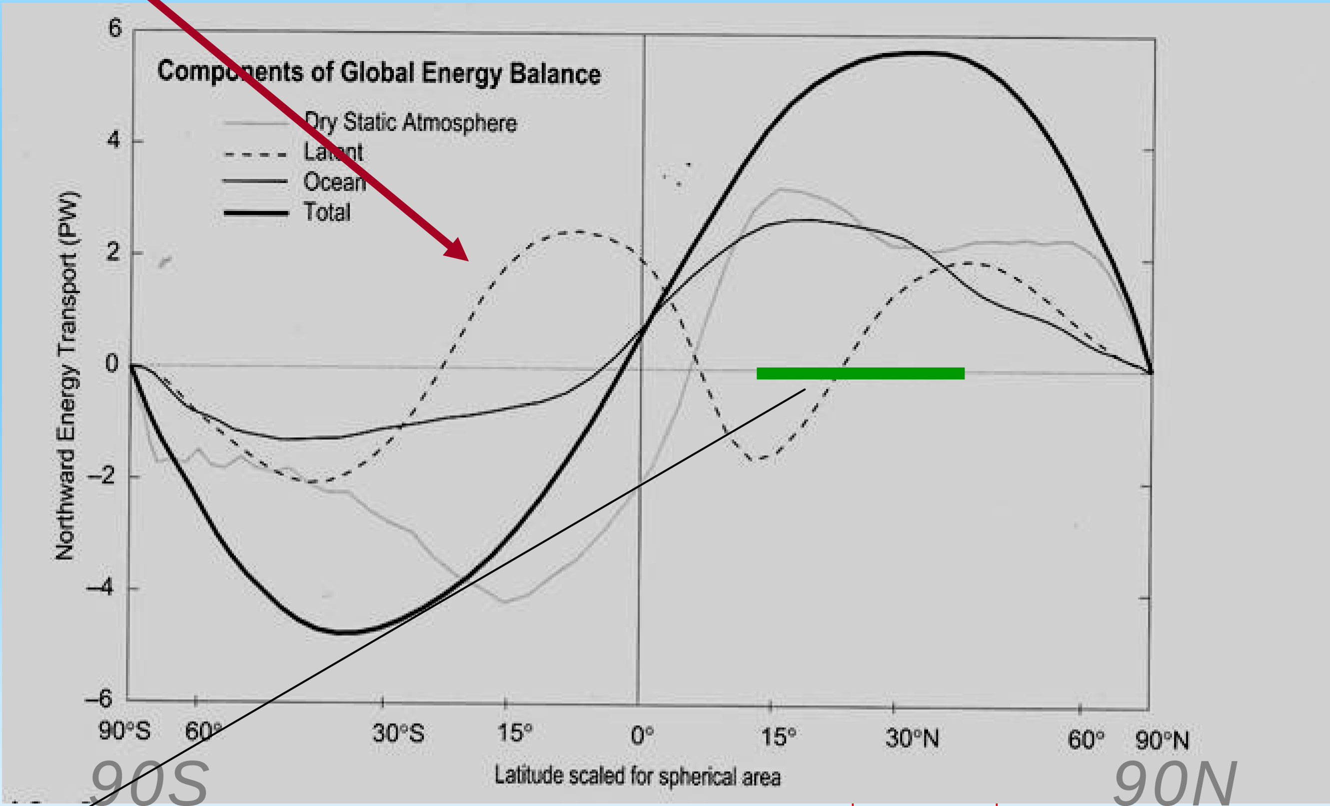

the northern subtropics show extremely active upward air/

Error est.: ± 9% at mid-latitude; Bryden est 2.0 ±0.42 pW at 24N very similar numbers from Trenberth & Stepaniak,QJRMS 04

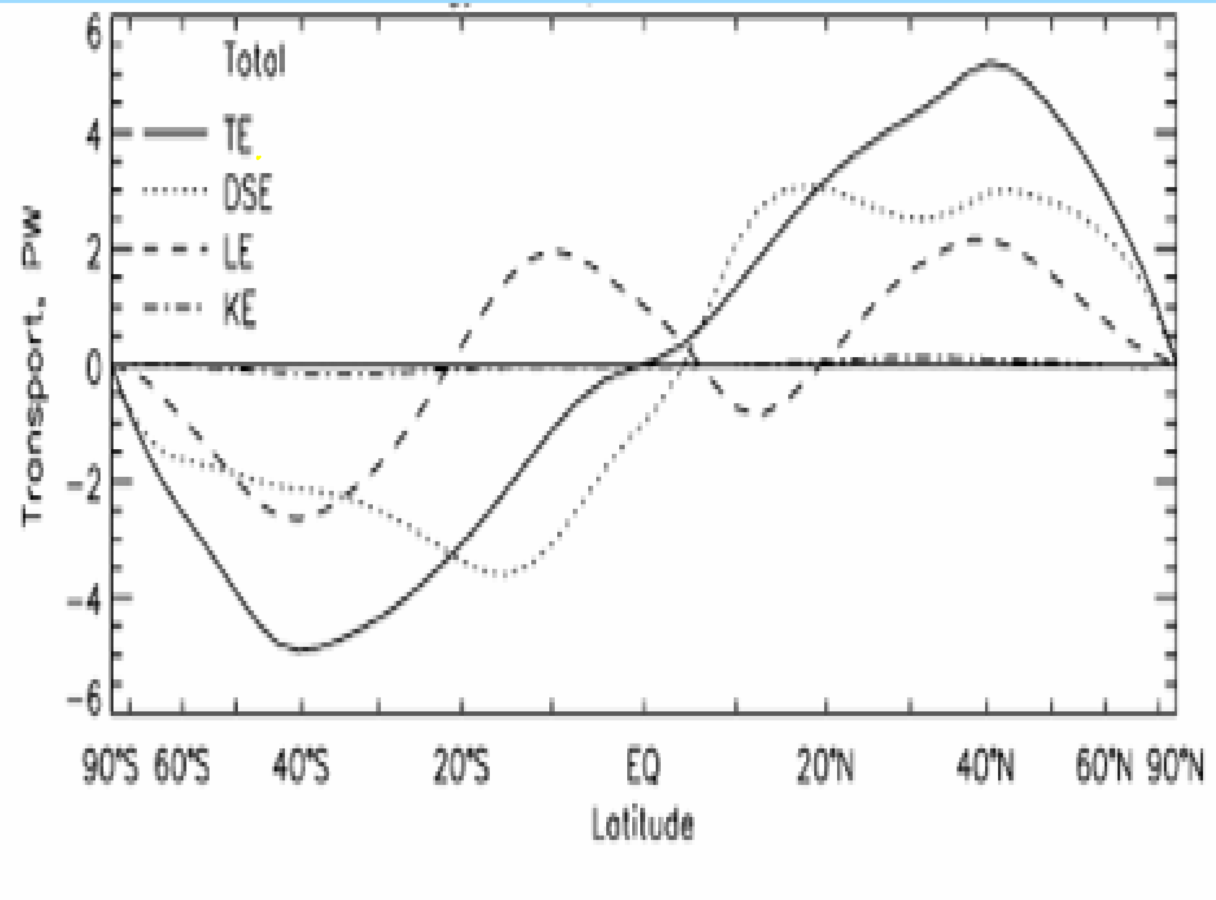

Flux of fresh water by the atmosphere is concentrated in the Pacific and Atlantic storm tracks

globally it carries ~ 2 petawatts of latent heat flux … which is ~0.7 Sverdrup (0.7 megatonnes/sec) of freshwater flux

1993 JFM

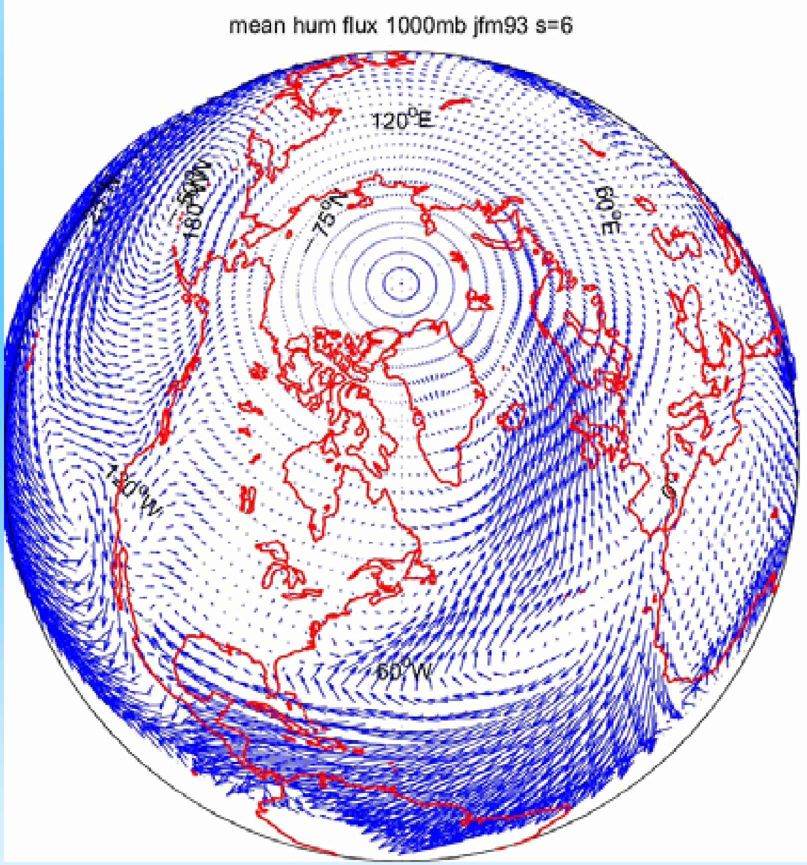

1996 JFM

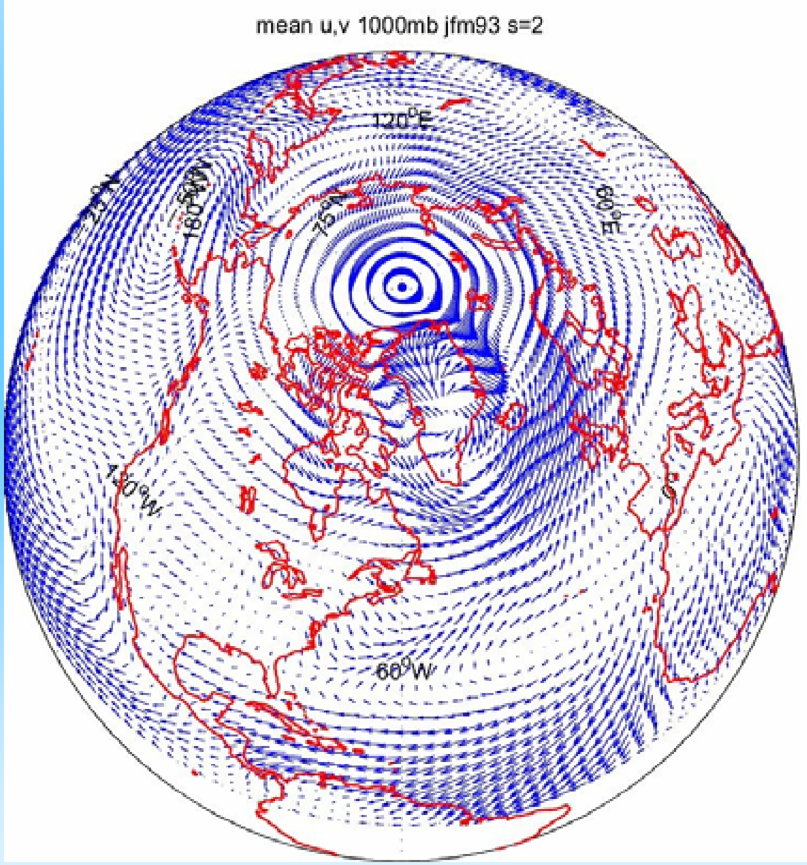

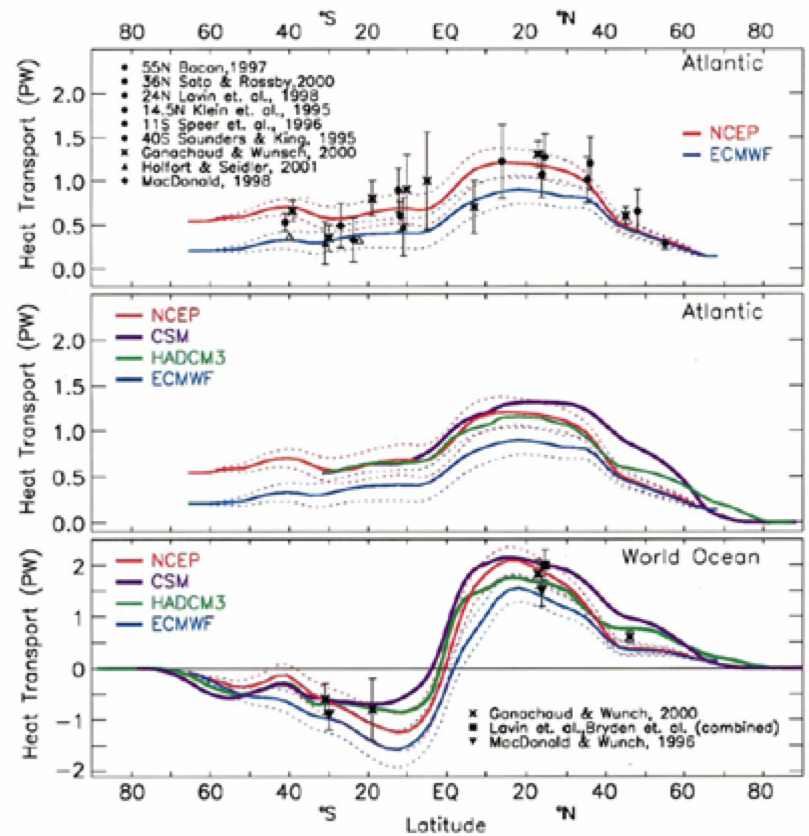

Fig. 6. The northward ocean heat transports from the NCEP-derived and ECMWF-derived products are compared (top) for the Atlantic Ocean with direct ocean estimates from sections, as identified in the key. The dashed curves show the ±1 std err for the derived transports. Where given in the original source, error bars are also plotted and the symbol is solid. Slight offsets in latitude are introduced where overlap would otherwise occur. Several sections are not exactly along a latitude circle, notably those for Bacon (1997) at ~55°N and the Saunders and King (1995) section along 45°S (South America to 10°E) to 35°S (Africa), plotted at 40°S. (middle) Comparison of the derived results with transports from the HADCM3 (years 81–120) and CSM (years 250–299) coupled models for the Atlantic. (bottom) Results for the global ocean along with those from Macdonald and Wunsch (1996) at 24°N and 30°S, and at 24°N the combined Lavin et al. (1998) and Bryden et al. (1991) and for Ganachaud and Wunsch (2000).

merid. heat transport at 35N: 78% A, 22% O;   18N: 50% A, 50% O

- So, ventilation of the tropics by atmosphere + ocean MOC's provides ~ 5 pW (5 x 10^{15} W); distributed over the area of the Earth between 0N and 30N, averages 5 x 10^{15} W/πR^2 = 39 W m^{-2}, delivering the same amount per m^2 to the Earth north of 30N.

  Fully as much heat is carried in the atmosphere by 0.8 Sverdrups (megatonnes s^{-1}) moisture flux ~ 2 pW as by dry static energy flux. (using the heat of vaporization, 2.25 MJ/kg)

  (It is useful to talk about both oceanic and atmospheric mass (water or air) transports in Sverdrups (Sv):

  Gulf Stream 30-120 Sv

  Antarctic Circumpolar Current~ 180 Sv

  Atlantic MOC ~ 16-20 Sv

  westerly winds/jet stream ~ 500 Sv

  atmospheric MOC ~ 50 -100 Sv

Qnet, net atmosphere-ocean heat flux, watts/m^2 (Keith Tellus 95)
(annual average)

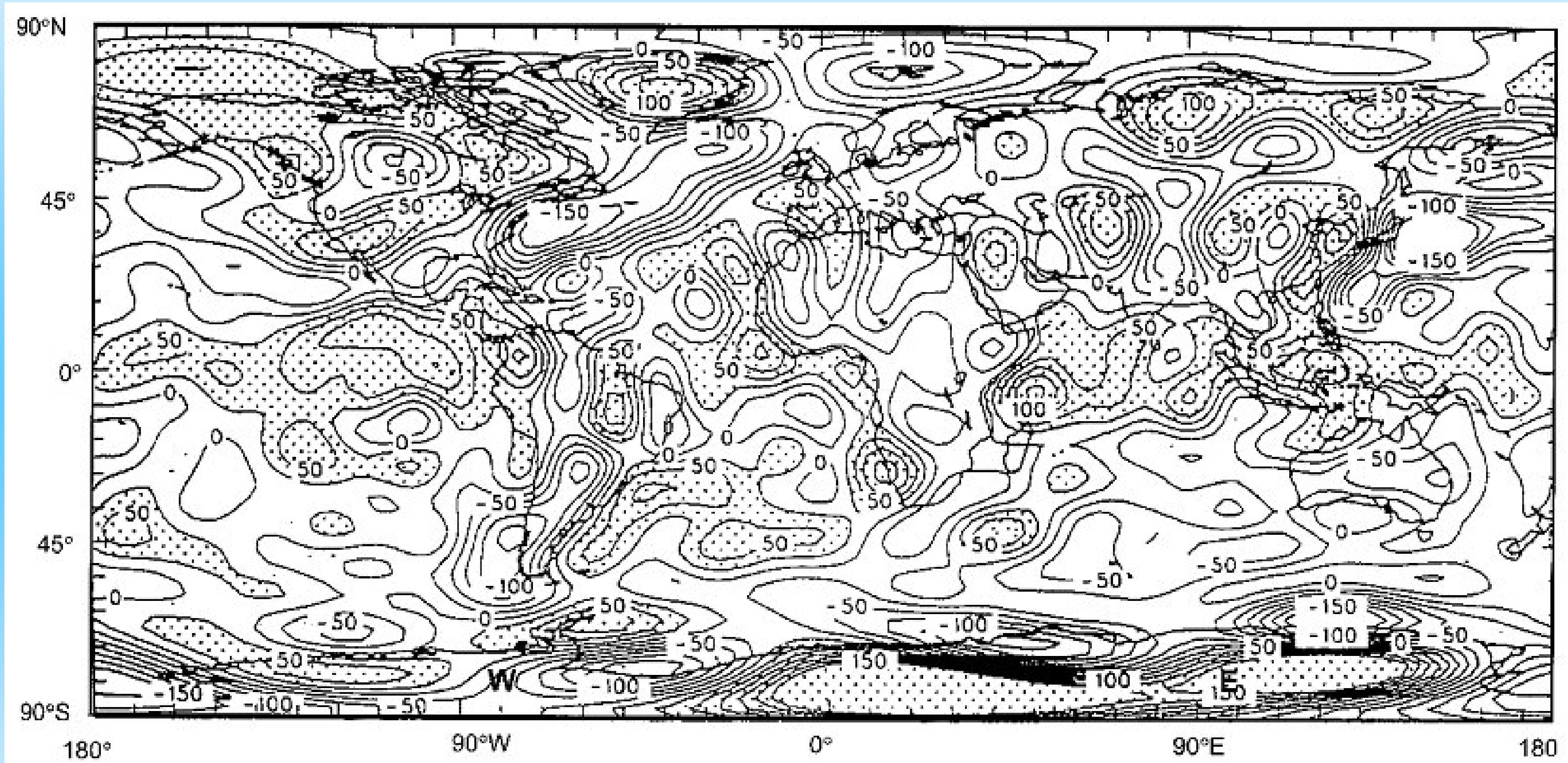

It should be noted that because the sun heats the ocean, O,
but does not cool the atmosphere, A, the most useful maps
of Qnet for A will differ those for O by the short-wave insolation.

Where is air-sea heat flux most intense? January (W m-2) (SOC/NOC1.1a climatology based on COADS)

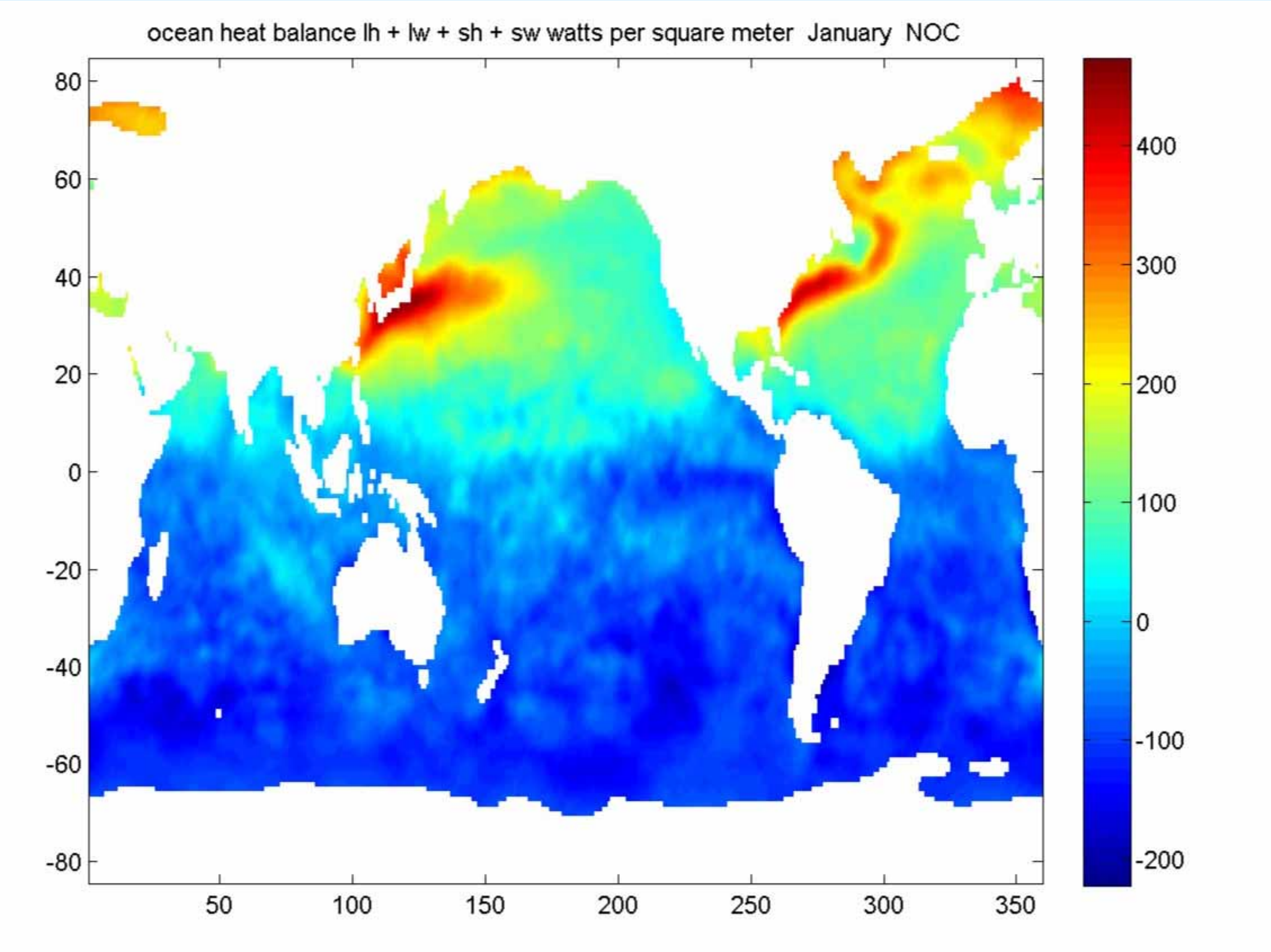

The air/sea heat flux seen by the atmosphere (latent+sensible+long-wave rad)
and by the ocean (latent+sensible+long-wave + short wave solar rad)

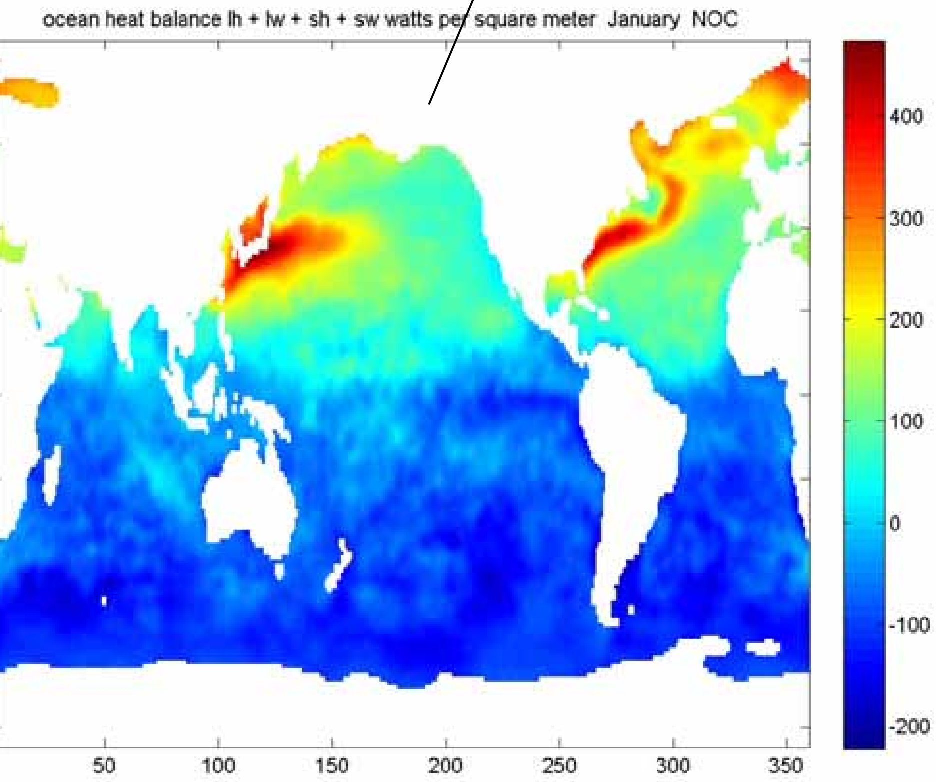

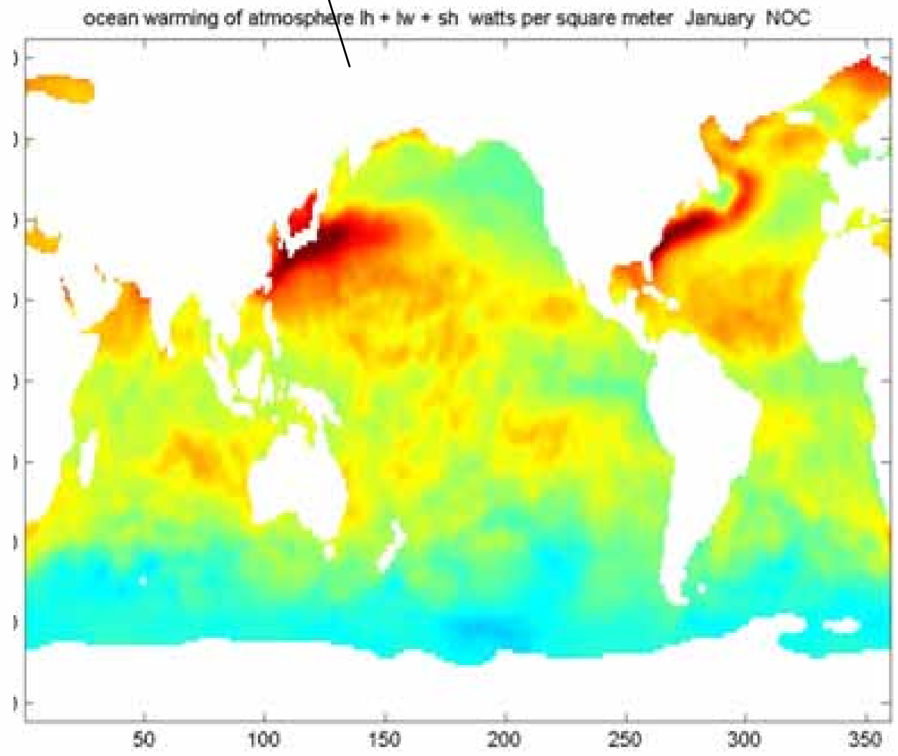

Annual average ratio of convergence of heat flux by ocean circulation divided by annual average heating of the atmosphere by ocean: (LH+SH+LW+SW)/(LH+SH+LW)

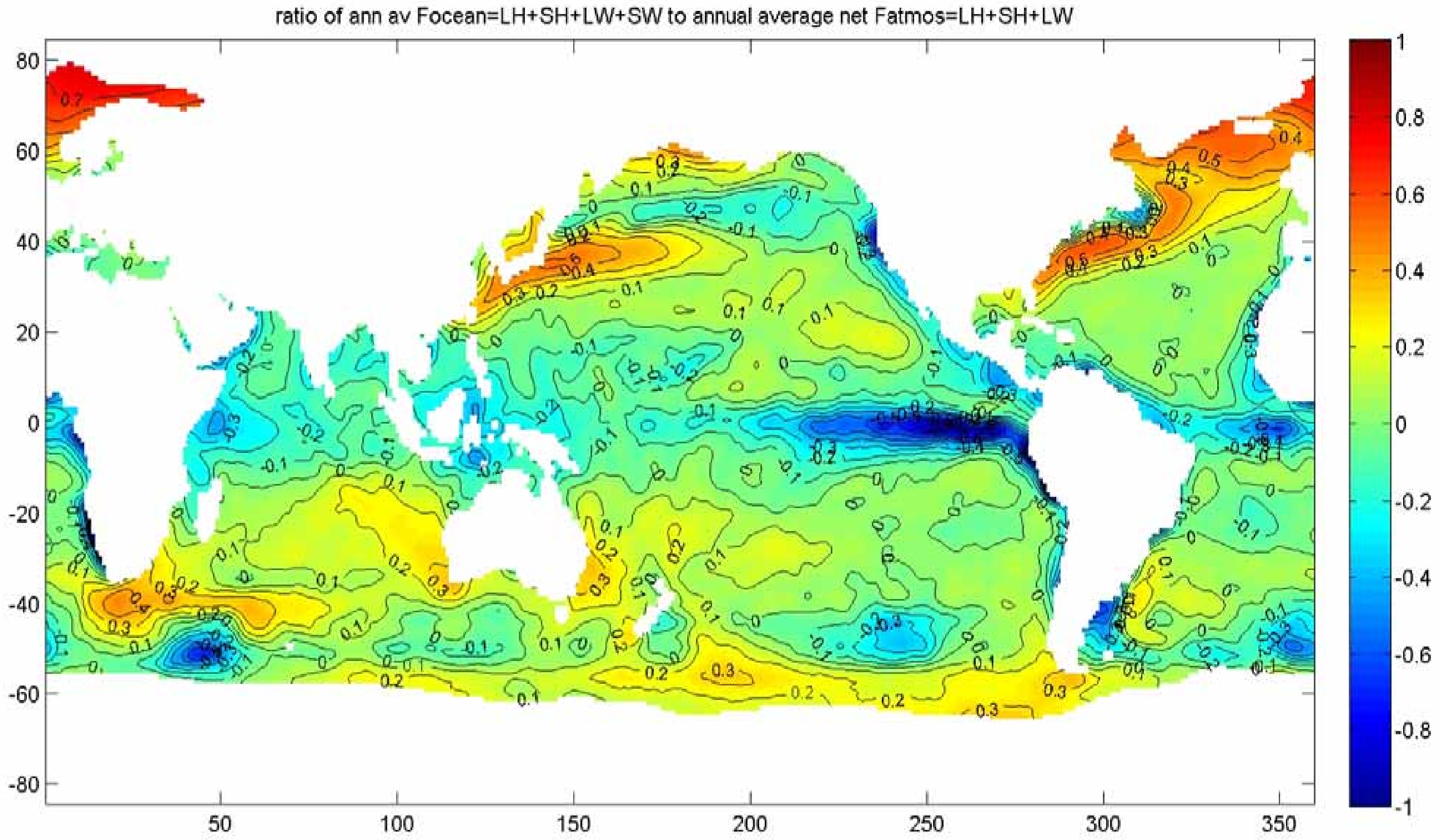

cold-air outbreaks: a source of deep convection (surface air temperature, 2 Jan 1993)

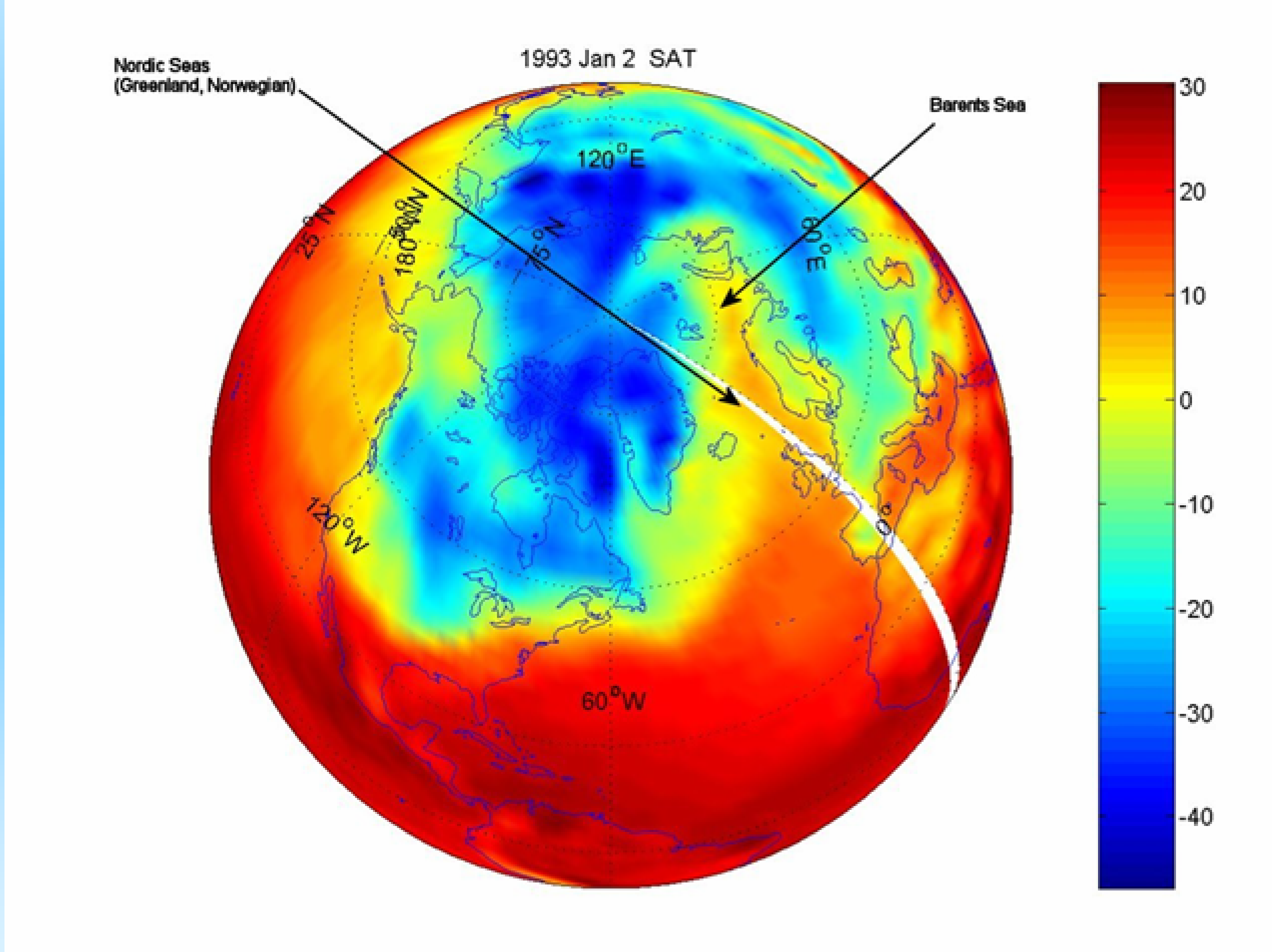

Held et al. (J.Clim.02) 100mb-1000mb diabatic heating for January

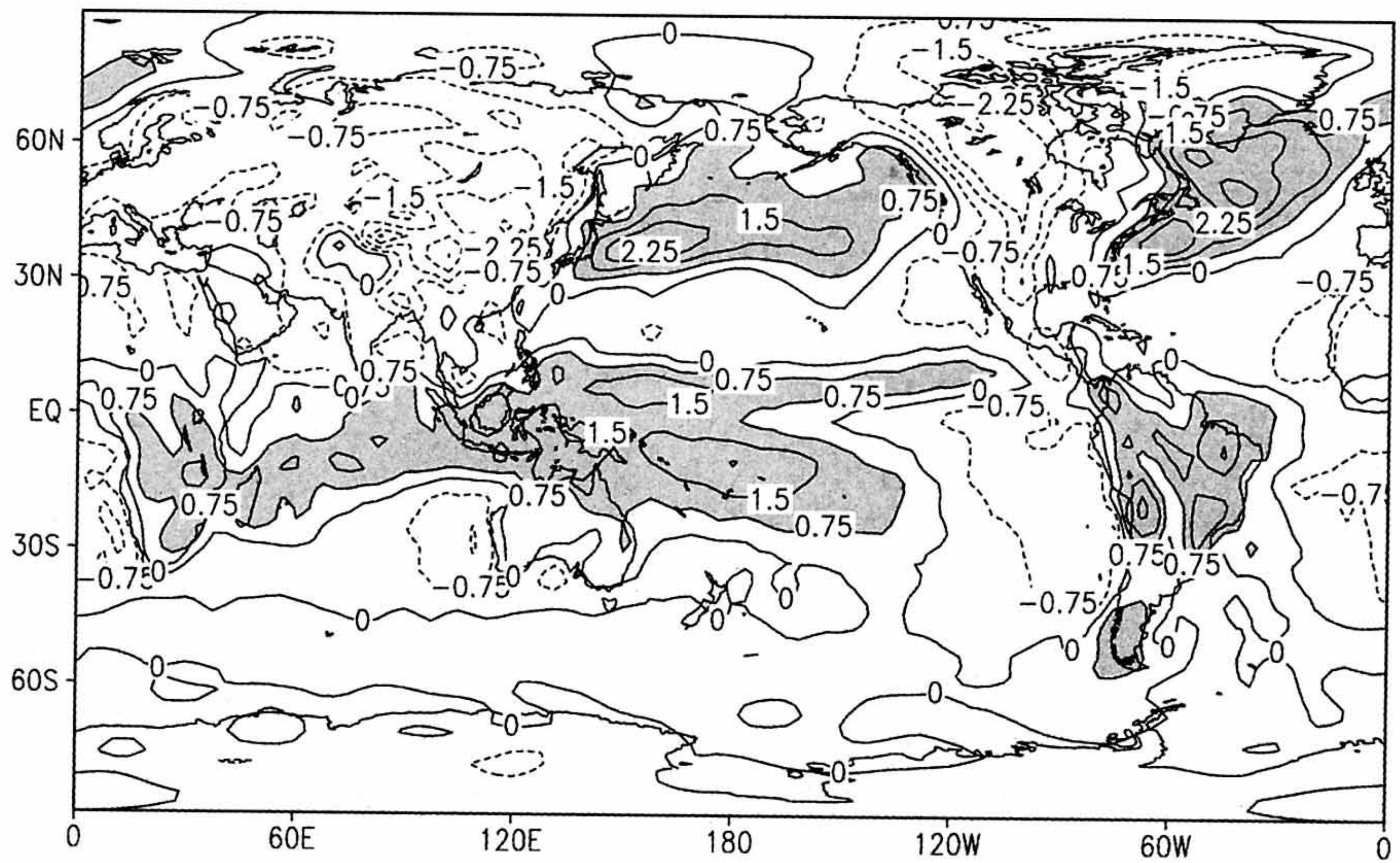

FIG. 8. The column-averaged diabatic heating field in Jan obtained from the NCEP–NCAR reanalysis as described in the appendix. The contour interval is 0.5 K day^{-1}.

A baroclinic vortex created by injecting water at mid-depth into a stratification

Note purple dye shows azimuthal velocity exists above and below the water mass:

The MOC (meridional circ) driving 3 vortices

cyclone

anticyclone

cyclone

PV inversion: using a model of convective destruction of PV. The modelled or diagnosed PV field is associated with a field of azimuthal circulation, displaced mass, and interacts with the meridional overturning circulation

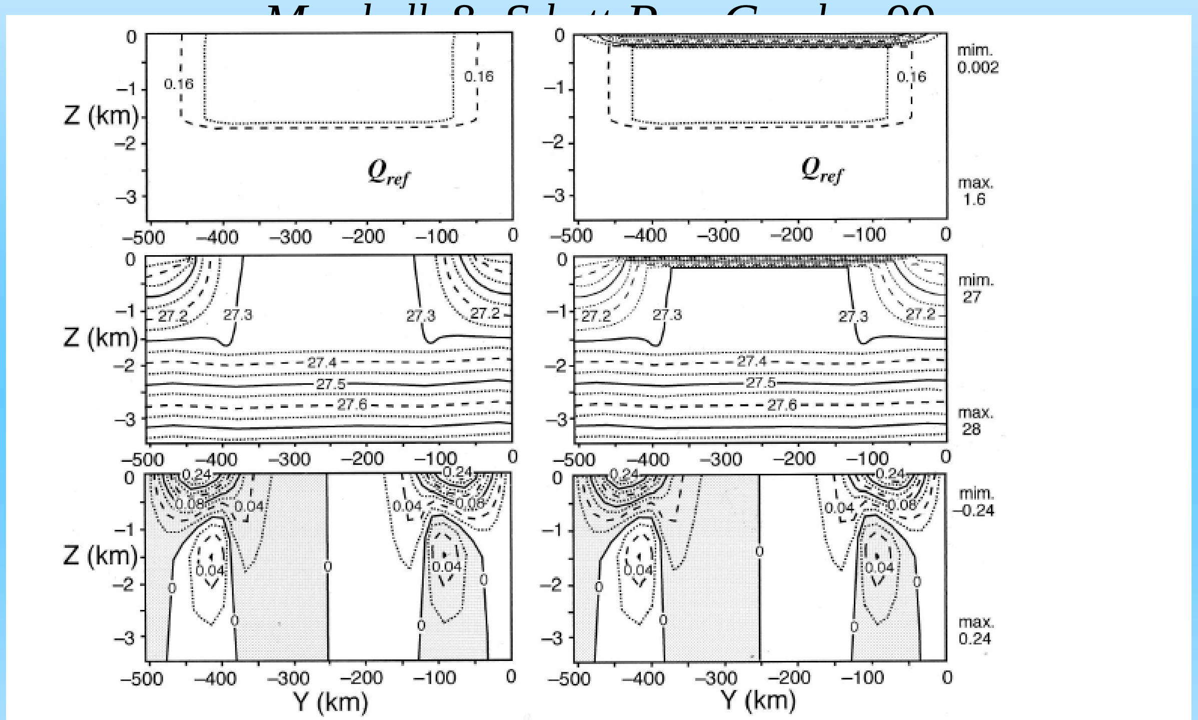

Figure 37. PV inversion for a mixed patch with (a) inhomogeneous and (b) homogenous boundary conditions at the surface. PV distribution, isopycnals, and currents are plotted. In Figure 37a the potential density at the sea surface is specified and an idealized interior PV anomaly inverted to give the hydrography and azimuthal velocity of a baroclinic vortex. In Figure 37b an interior PV field identical to that of Figure 37a is used, but now the cold surface is represented by a sheet of high PV just beneath the upper boundary, which is prescribed to be an isopycnal surface. Note that in Figure 37b, unlike Figure 37a, the isopycnals cannot cut the upper surface, which itself is an isopycnal.

viscous overturning in a rotating cylider:
the radial/vertical plane transmits stress from the top plate (which is at rest in the laboratory frame) and the bottom of the cylinder (which is rotating)

The Ekman layers are very thick!

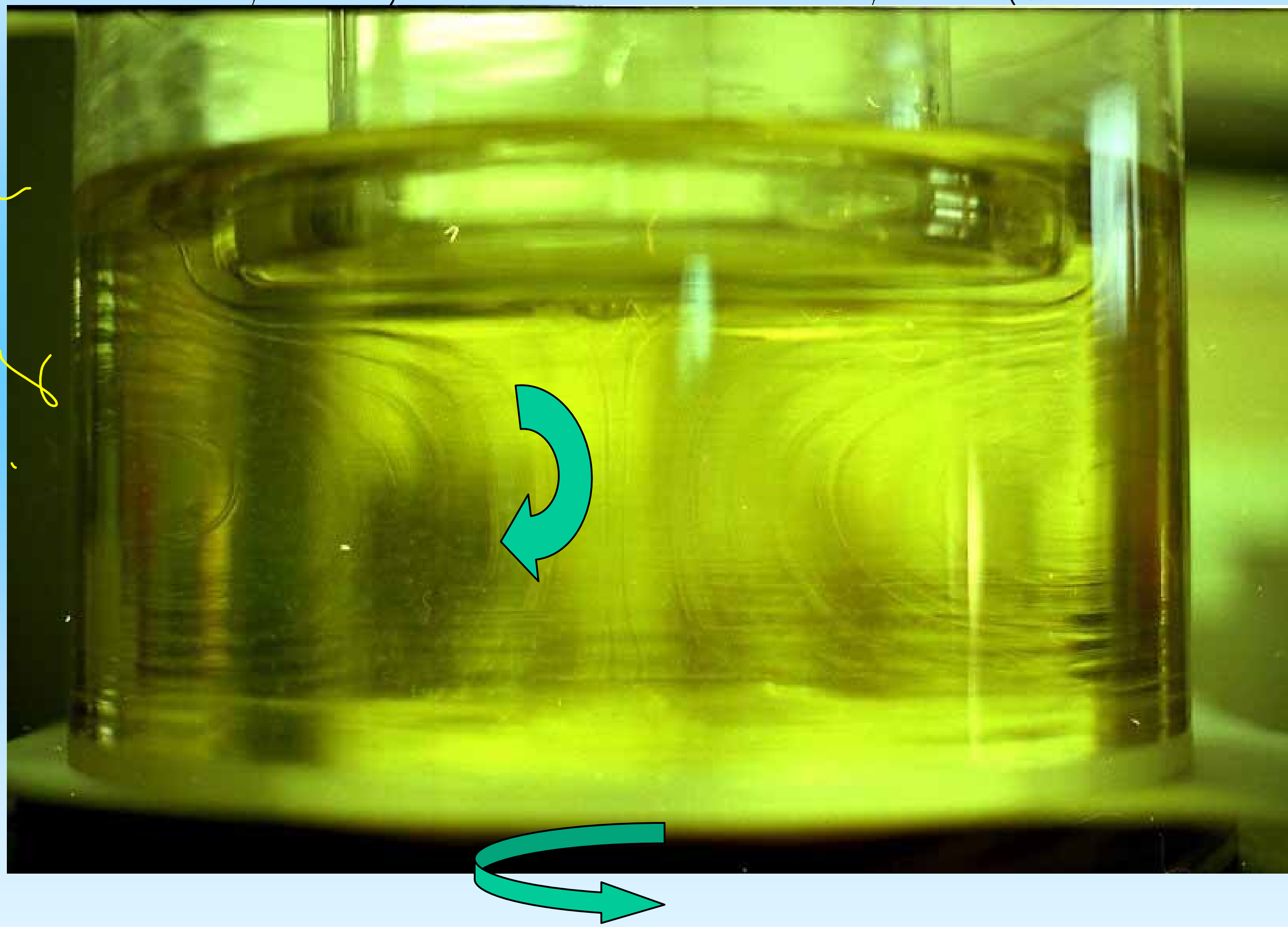

sugar syrup

Overturning cells in an annulus of fluid between concentric cylinders (the inner cyclinder is rotating, the outer cylinder is stationary (Taylor-Couette flow).

The cells transmit torque between the solid cylinders more strongly than would pure viscous diffusion.

(The same 2D equations govern thermal convection, and the Nusselt number expresses the analogous increase in heat flux above the diffusive rate).

MOCs organized by double diffusion

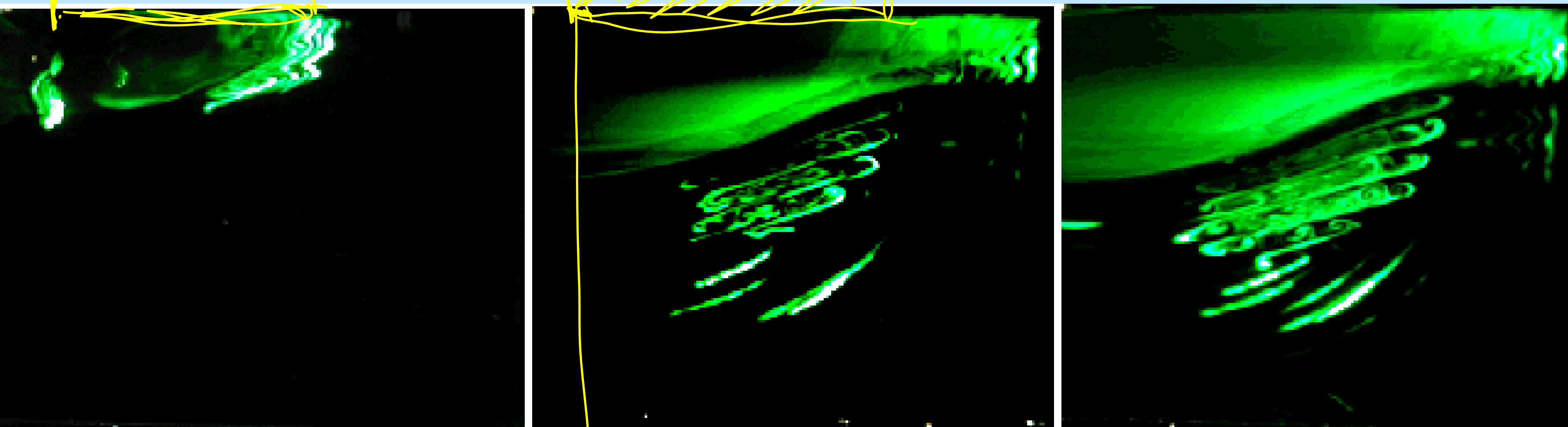

disk drives an anticyclone (warm eddy) in uniformly stratified fluid

Sink-driven flow in a rotating, stratified fluid: the cyclonic spin of the fluid would be resisted by bottom Ekman friction (and all radial inflow concentrated there in this tornado vortex); However, stable stratification resists and forces continuing MOC within the fluid. The azimuthal velocity

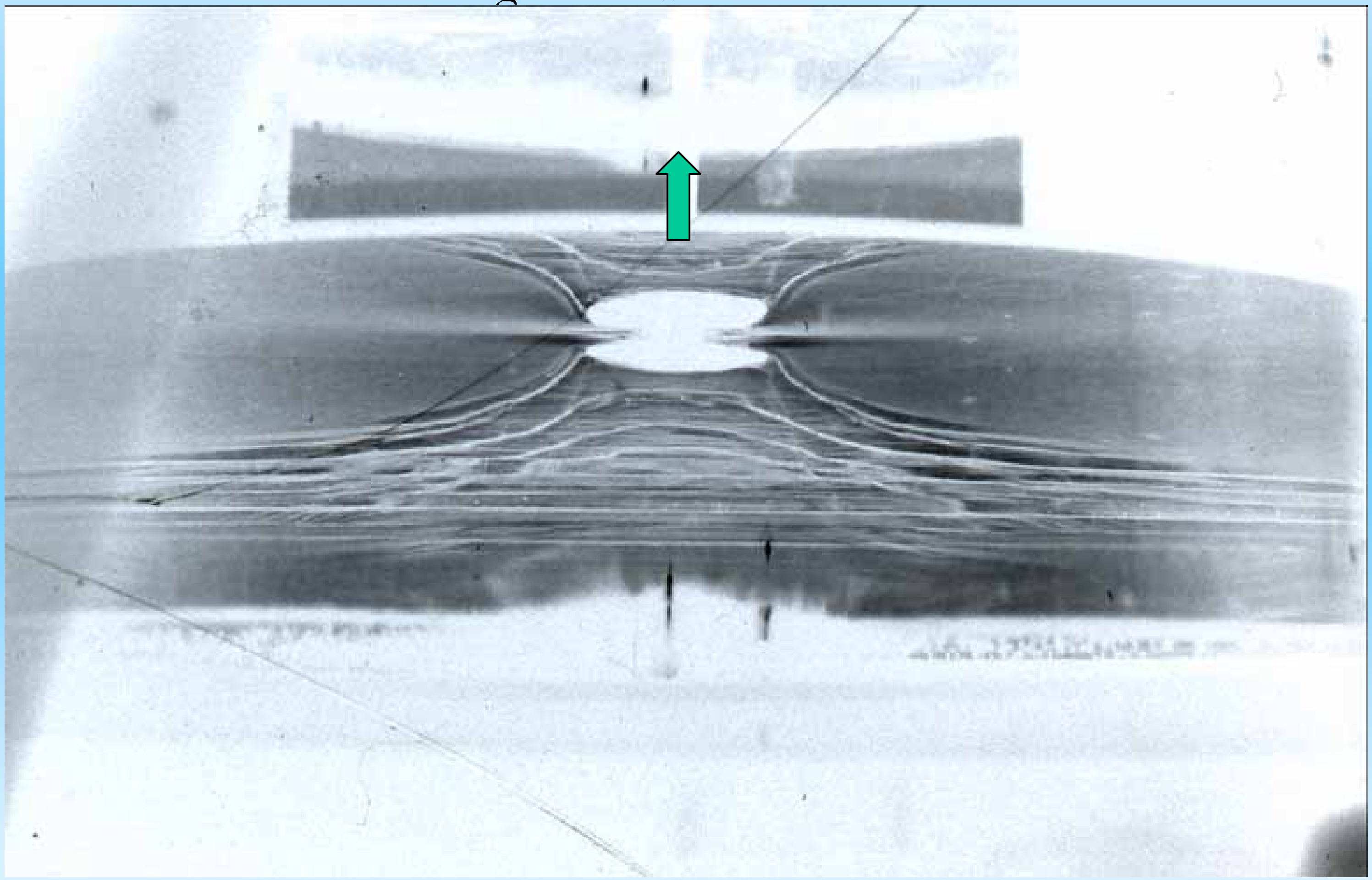

GFD lab, Univ of Washington

Dense plume flowing down a sloping valley in a rotating fluid (model of dense downslope flows in the Weddell Sea)

Elin Darelius, Univ of Washington GFD lab

particle paths are helical, with Ekman driven meridional overturning transmitting the boundary stress into the fluid. (Looking up the sloping valley)

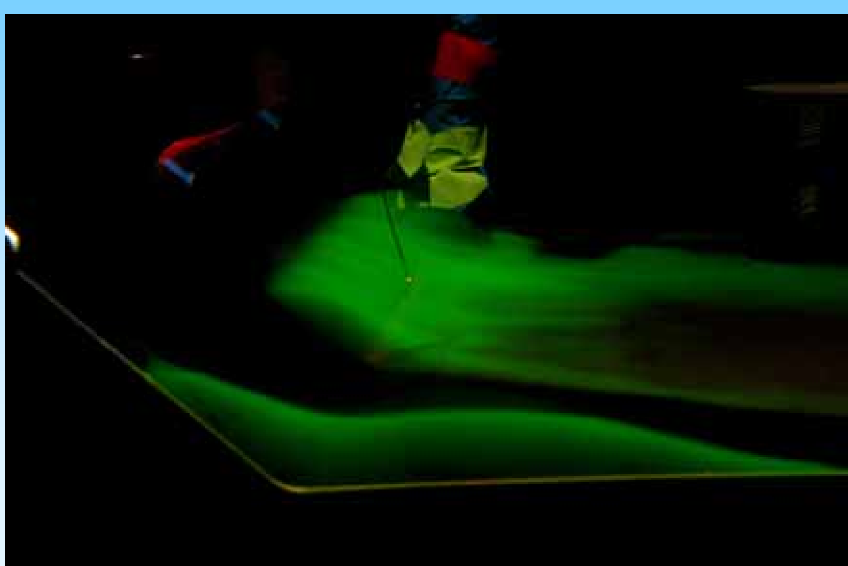

Figure 17: *The "Ekman Helix" traced out by dye injected in the bottom boundary layer seen a) up the canyon and b) from above. The secondary circulation causes a particle to follow a helix like path down the canyon.*

The zonally averaged overturning streamfunction, North Atlantic/Arctic model of Häkkinen driven by NCEP winds and temperatures

This image of the ocean circulation is the usual output of climate models; many essential processes are made invisible…the east-west detail of the previous slides. These 'details' are likely to be essential to understanding the global ocean transports.

The tendency for dominant sinking south of Greenland in low-resolution climate models is widespread: here in density- latitude space the streamfunction reveals higher latitude sinking and dense overflows.

The difference is expected from the east-west tilt of potential density surfaces, so that equal and opposite meridional velocities at the same depth z may have very different densities.

y-z space

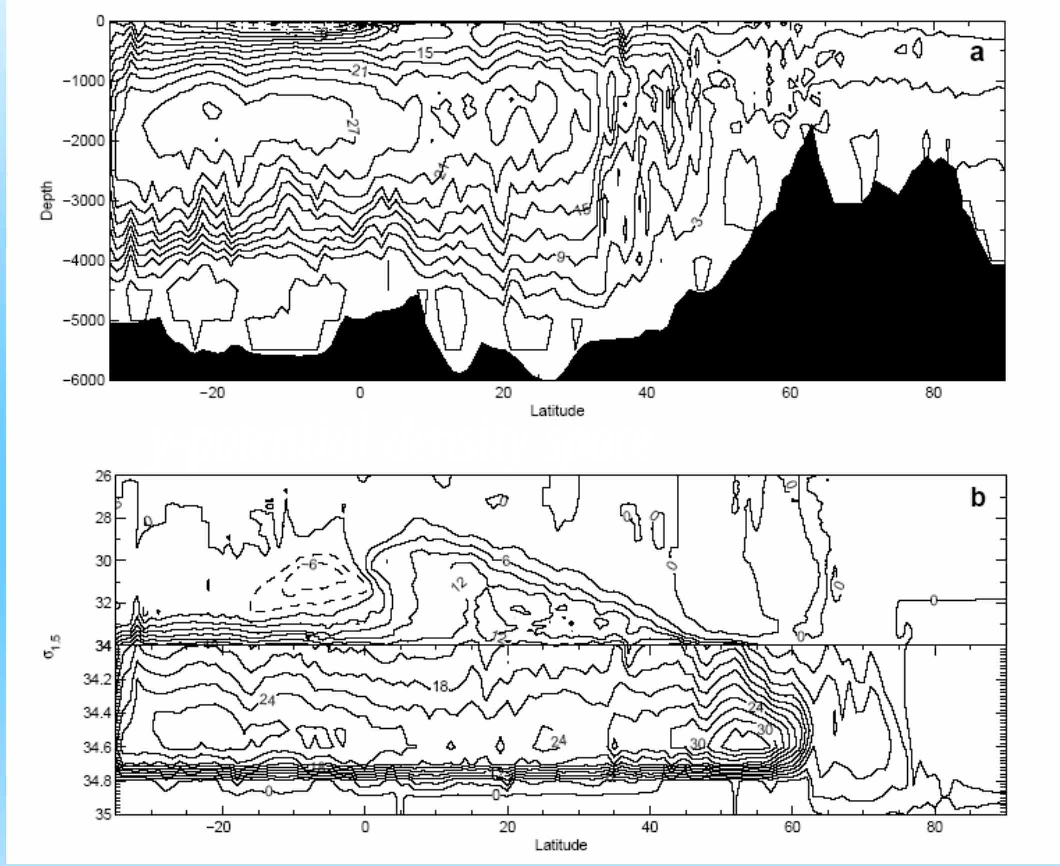

35S *90N*

Bailey, Hakkinen, Rhines 2003

Lumpkin & Speer's JPO 03 discussion of the Atlantic MOC, here plotted against potential density and latitude. Even though we know there is much east-west structure (boundary currents, horizontal gyres as in Reid's maps) the zonally averaged MOC 'looks like' the simple 2-dimensional box models

S

O_2

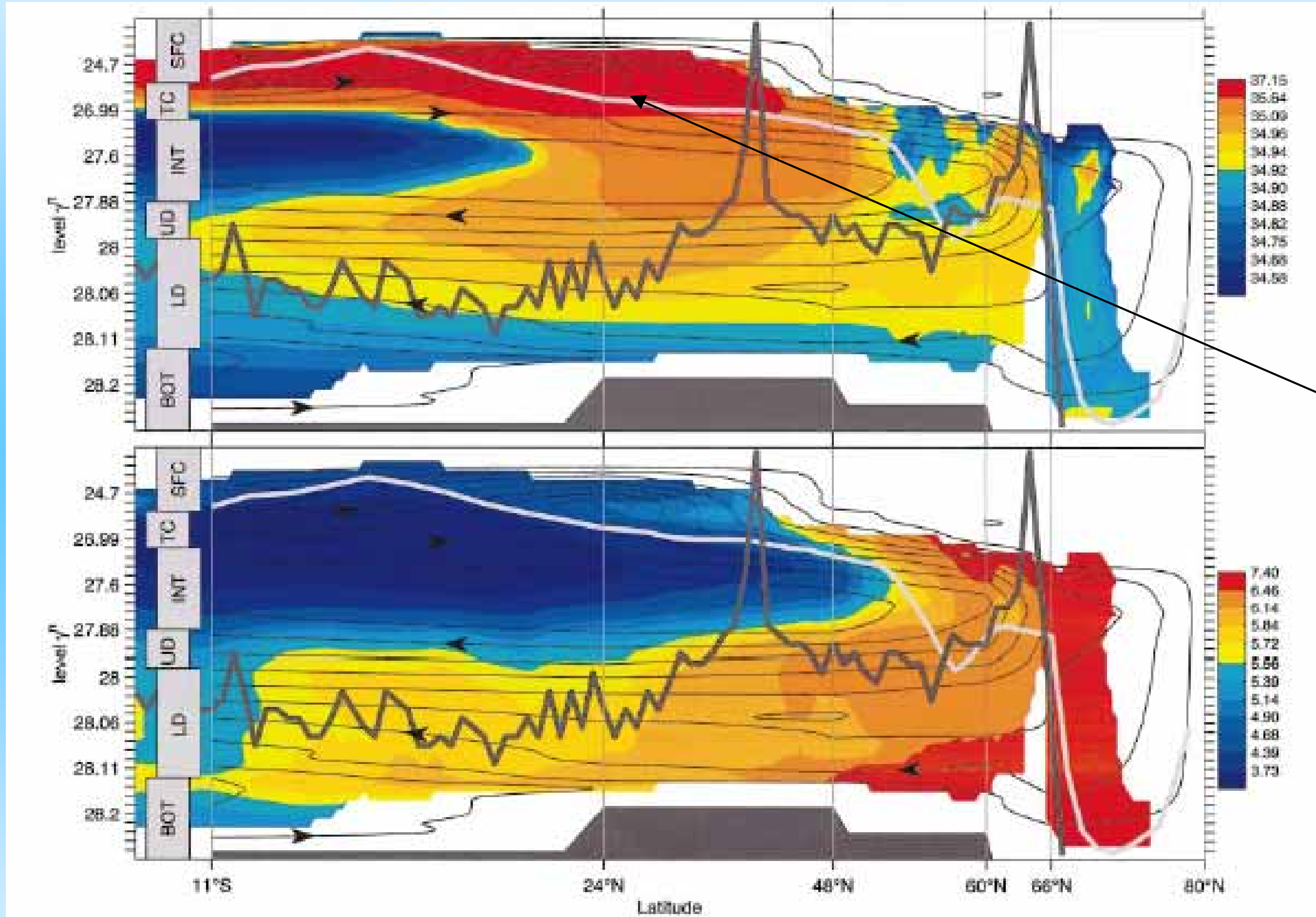

sea surface

FIG. 9. Side view of the North Atlantic meridional overturning, contoured in 2-Sv intervals, superimposed on zonally averaged (top) salinity and (bottom) oxygen (mL L^{-1}) calculated from climatology (Gouretski and Jancke 1998). Light gray curve: densest outcropping layer, estimated from COADS climatology. Dark gray curve: crest of the Mid-Atlantic Ridge, including the Azores Plateau and Iceland.

Lumpkin & Speer JPO 2003

Figure 4. Vertical-meridional section of salinity at 24°W in the South Atlantic. Data sources are as in Fig. 2, and the heavy dashed lines are the potential density surfaces highlighted in that figure. The salinity minimum diving down at 52°S and heading north is AAIW. The salinity maximum below that, starting from the South Atlantic and rising and growing weaker into the Weddell Sea is NADW. The highlighted density surfaces were chosen to include this salinity maximum.

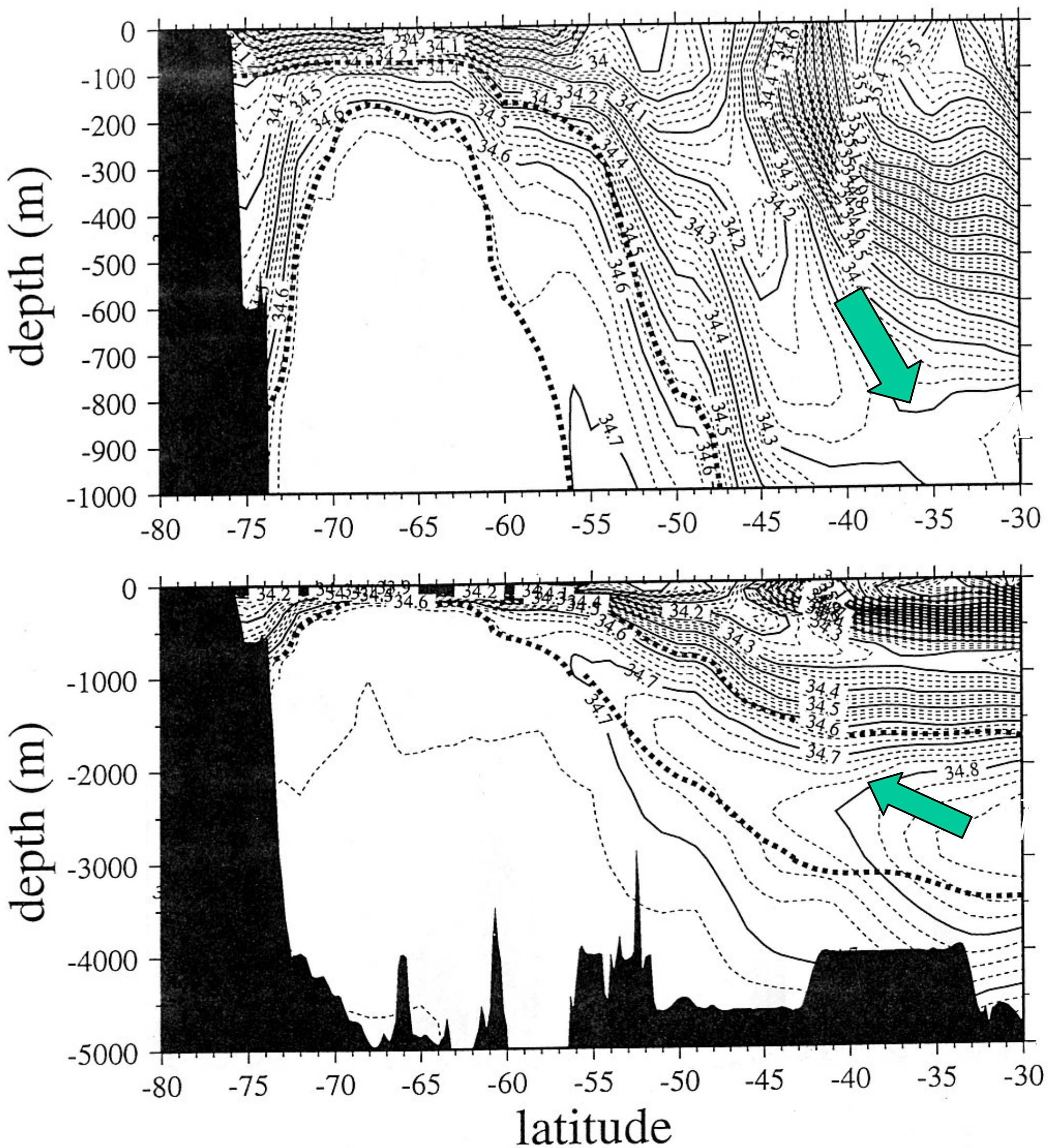

The ACC is the only ocean current with The Problem (how to flow meridionally, given the absolute angular momentum constraint)..yet it has ample topographic bottom slopes to lean on: these clearly balance the zonal wind stress that drives this greatest of all ocean currents

This may be a dominant site of upwelling in the global MOC (with respect z and potential density)

Salinity at 24W longitude

Oceanic meridional overturning strength vs. meridional baroclinic dynamic height gradient in HADCM3

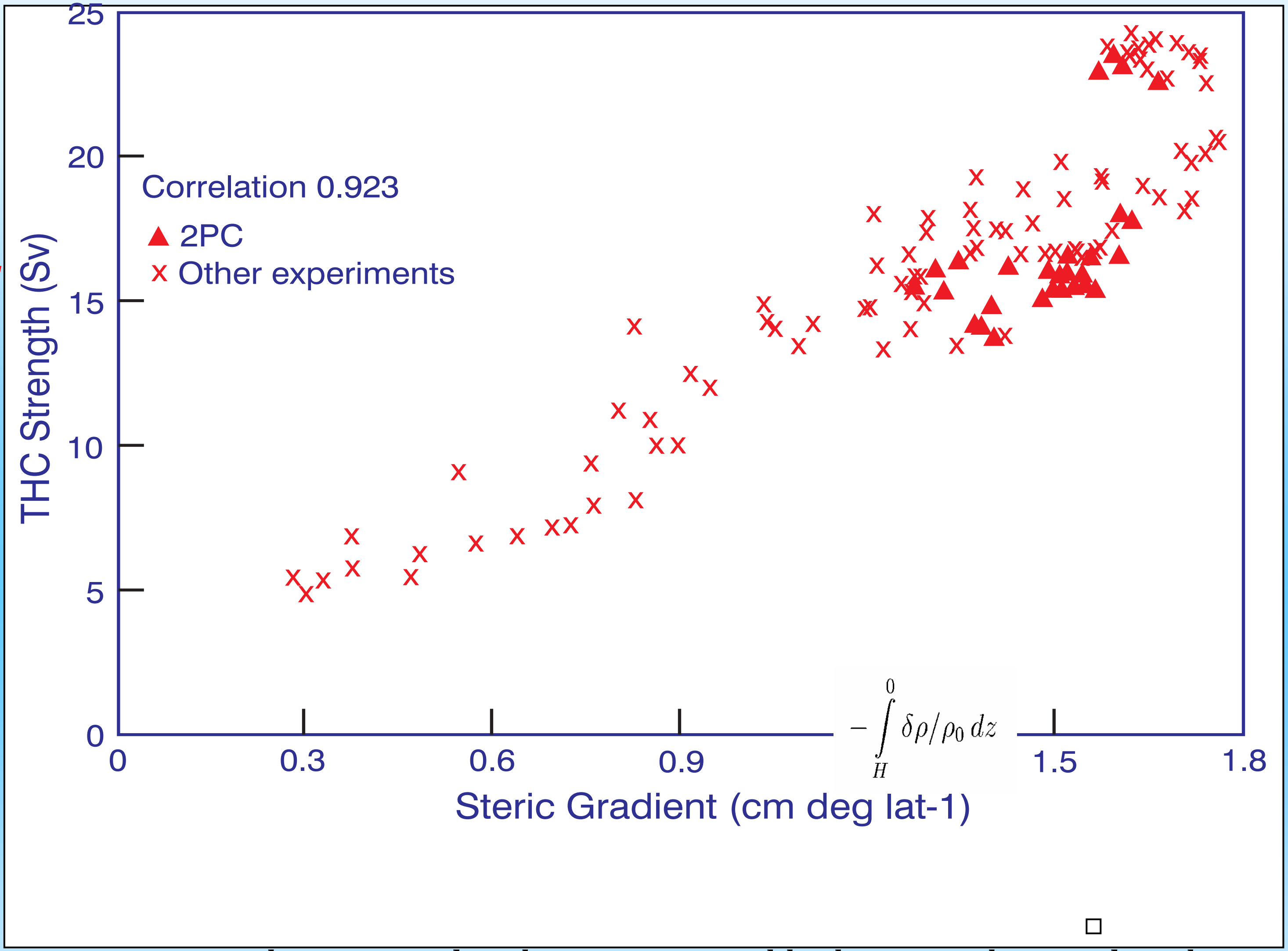

A change in the MOC transport may be associated with some measurable change in the meridional density gradient. HadCM3 finds a very close correlation between Atlantic overturning rate and the S-N gradient of steric height from 30S - 60N through the W Atlantic. But, there is a possible oversensitivity of models to subpolar buoyancy/Labrador Sea.

THE END

An evacuated glass vessel with water in it illustrates the Clausius-Clapyron relation between vapor pressure of water and temperature. The water is pushed from the vessel in my hand to the ‘cold ball’, and the vapor pressure difference between the two ends is close to the hydrostatic pressure measured by the column’s vertical displacement. One can fill out the curve and see the greater sensitivity (to temperature) of water vapor production at high, ‘tropical’ temperature. This all works because we shake the vessel so that a thin film of water lies under my warm hand. It illustrates a key variable in the climate system.

When shaken this water ‘clinks’ like metal,vapor cavities opening up and slamming shut.

- **FDEPS Lectures, November 2007**
- P.B. Rhines, Oceanography and Atmospheric Sciences, University of Washington
- Rhines@ocean.washington.edu
- www.ocean.washington.edu/research/gfd
-
- These lectures will address the dynamics of oceans and atmospheres, as seen through theory, laboratory simulation and field observation. We will look particularly at high latitudes and climate dynamics of the ocean circulation coupled to the atmospheric storm tracks. We will emphasize the dynamics that is difficult to represent in numerical circulation models. We will discuss properties of oceans and atmospheres that are both fundamental, unsolved questions of physics, and are also important, unsolved problems of global environmental change.
- **Lecture 1**:
- Is the ocean circulation important to global climate ? Does dense water drive the global conveyor circulation? Fundamental questions about oceans and atmospheres that are currently under debate.
-
- The field theory for buoyancy and potential vorticity.
- Basic propagators: Rossby waves and geostrophic adjustment.
- Potential vorticity: inversion and flux.
- **Lecture 2**:
- How do waves and eddies shape the general circulation, gyres and jet streams?
- Almost invisible overturning circulations.
- Lessons from Jupiter and Saturn.
- The peculiar role of mountains, seamounts and continental-slope topography.
- **Lecture 3**:
- Dynamics of ocean gyres and their relation with the global conveyor circulation.
- Water-mass transport, transformation and air-sea exchange of heat and fresh water.
- Ocean overflows and their mixing.
- Decadal trends in the global ocean circulation.
- **Lecture 4**:
- Heat, fresh-water, ice: convection in oceans and atmospheres and the texture of geophysical fluids.
- **Lecture 5**:
- Teaching young students about the global environment using the GFD laboratory: science meets energy and environment in the lives of Arctic natives
- **Seminar**:
- *Exploring high-latitude ocean climate with Seagliders and satellites*

Kelvin waves, inertial waves in shallow rotating fluid